SPATIOTEMPORAL ANALYSIS OF LAND AND WATER PRODUCTIVITY USING WAPOR DATA: A CASE OF WONJI SHOA SUGARCANE PLANTATION, ETHIOPIA

DAWIT MILLION ESHETU

A THESIS SUBMITTED TO

THE DEPARTMENT OF WATER RESOURCES ENGINEERING

SCHOOL OF CIVIL ENGINEERING AND ARCHITECTURE

PRESENTED IN PARTIAL FULFILMENT OF THE REQUIREMENT FOR THE DEGREE OF MASTER'S IN

WATER RESOURCES ENGINEERING

(SPECIALIZATION IN HYDRAULIC ENGINEERING)

OFFICE OF GRADUATE STUDIES

ADAMA SCIENCE AND TECHNOLOGY UNIVERSITY

AUGUST, 2023

ADAMA, ETHIOPIA

Spatiotemporal Analysis of Land and Water Productivity Using WaPOR Data: A Case of Wonji Shoa Sugarcane Plantation, Ethiopia

Dawit Million Eshetu (ID: PGR/24753/14)

Advisor: Mesfin Benti Tolera (PhD)

A Thesis Submitted to

The Department of Water Resources Engineering

School of Civil Engineering and Architecture

Presented in Partial Fulfillment of the Requirement for the Degree of Master’s in

Water Resources Engineering

(Specialization in Hydraulic Engineering)

Office of Graduate Studies

Adama Science and Technology University

August 2023

Adama, Ethiopia

DECLARATION

I hereby declare that this Master Thesis entitled **"Spatiotemporal Analysis of Land and Water Productivity Using WaPOR Data: A Case of Wonji Shoa Sugarcane Plantation, Ethiopia"** is my original work. That is, it has not been submitted for the award of any academic degree, diploma or certificate in any other university. All sources of materials used for this thesis have been duly acknowledged through appropriate citations.

Dawit Million Eshetu	________________________	________________
Name of student	Signature	Date

RECOMMENDATION

I, the advisor of this thesis, hereby certify that I have read and revised version of the thesis entitled **"Spatiotemporal Analysis of Land and Water Productivity Using WaPOR Data: A Case of Wonji Shoa Sugarcane Plantation, Ethiopia"** prepared under my guidance by Dawit Million Eshetu submitted in partial fulfillment of the requirements for the degree of masters of science in Water Resources Engineering (Specialization in Hydraulic Engineering).Therefore, I recommend the submission of a revised version of the thesis to the department following the applicable procedures.

Mesfin Benti Tolera (PhD)	____________________	______________
Major advisor	Signature	Date

APPROVAL PAGE

I, the advisor of the thesis entitled "**Spatiotemporal Analysis of Land and Water Productivity Using WaPOR Data: A Case of Wonji Shoa Sugarcane Plantation, Ethiopia**" and developed by Dawit Million Eshetu, hereby certify that the recommendation and suggestions made by the board of examiners are appropriately incorporated into the final version of the thesis.

Mesfin Benti Tolera (PhD)	------------------------	----------------------
Major Advisor	Signature	Date

We, the undersigned members of the Board of Examiners of the thesis by Dawit Million Eshetu, have read and evaluated the thesis entitled "**Spatiotemporal Analysis of Land and Water Productivity Using WaPOR Data: A Case of Wonji Shoa Sugarcane Plantation, Ethiopia**" and examined the candidates during the open defense. This is, therefore, to certify that the thesis is accepted for partial fulfillment of the requirement of the degree of Master of Science in Water Resources Engineering (Specialization in Hydraulic Engineering).

______________________________	______________________	____________________
Chairperson	Signature	Date
______________________________	______________________	____________________
Internal Examiner	Signature	Date
______________________________	______________________	____________________
Eternal Examiner	Signature	Date

Final approval and acceptance of the thesis is contingent upon the submission of its final copy to the Office of Postgraduate Studies (OPGS) through the Department Graduate Council (DGC) and School Graduate Committee (SGC).

______________________________	______________________	____________________
Department Head	Signature	Date
______________________________	______________________	____________________
School Dean	Signature	Date
______________________________	______________________	____________________
Office of Postgraduate Studies, Dean	Signature	Date

ACKNOWLEDGEMENT

First and foremost, I would like to express my heartfelt gratitude to the Almighty God for bestowing upon me the courage, knowledge, enduring strength, and optimism to advance successfully in my academic pursuits. Furthermore, I would like to convey my sincerest appreciation to all those who have provided support, assistance, and guidance in the successful completion of this research work.

I would like to express my deepest gratitude to my advisor, Mesfin Benti Tolera (Ph.D.), for providing constructive and valuable support, advice, and guidance throughout my research. My deepest gratitude and appreciation are extended to Dr. Abebe Chukalla (Lecturer or Analyst in Remote Sensing and Crop Water Productivity, IHE Delft) and Dr. Dereje Birhanu for their remarkable contributions and valuable insights that significantly enriched my work.

I am deeply grateful to Adama Science and Technology University (ASTU) for granting me a scholarship opportunity to pursue my MSc studies in Water Resources Engineering, and for providing the necessary financial support to complete my research work promptly. I also greatly appreciate the cooperation of Wonji Shoa Sugar Plantation, Ethiopian Sugar Corporation (ESC), and Ethiopian Construction Design and Supervision Work Corporation (ECDSWC) during the data collection process. I extend my utmost respect and gratitude to all the staff members of the ASTU Water Resources Engineering Department.

Finally, I would like to express my profound gratitude to my family, particularly Alemaz Shewaye (mother), Welela Lema, Samson Yohannes, Addis Alem Million, Andu Alem Million, Ruhama Yohannes, as well as my best friend Samuel Nigusse.

TABLE OF CONTENTS

LIST OF TABLES

LIST OF FIGURES

LIST OF FIGURES IN THE APPENDIX

ACRONYMS AND ABBREVIATIONS

A	Adequacy
ABWAP	Awash Basin Water Allocation Strategic Plan
AOT	Above Ground over Total biomass
AGBM	Above Ground Biomass
B	Biomass Production
BDA	Basin Development Agency
CV	Coefficient of Variation
CWP	Crop Water Productivity
DEM	Digital Elevation Model
ETc	Crop Evapotranspiration
ETreff	Reference evapotranspiration
ETa,s	Seasonal Actual Evapotranspiration
EOS	End of Season
ESC	Ethiopian Sugar Corporation
ETact	Actual Evapotranspiration
FAO	Food and Agriculture Organization
fc	Light Use Efficiency Factor
GIS	Geographic Information System
GPS	Geographic Positioning System
GBWP	Gross Biomass Water Productivity
GTP	Growth and Transformation Plan
HI	Harvest Index
HVA	Handlers Vereeniging Amsterdam
IHE	The International Institute for Hydraulic and Environmental Engineering
IPCC	Intergovernmental Panel on Climate Change
LCC	Land Cover Classification
fc	Light Use Efficiency Correction Factor

L1, L2 and L3	WaPOR data with a spatial resolution of 250 m (L1), 100 m (L2) and 30 m (L3)
LUE	Light uses efficiency
LCC	Land cover classification
LAI	Leaf Area Index
MC	Moisture Content
NBWP	Net Biomass Water Productivity
NPP	Net Primary Production
NDVI	Normalized Difference Vegetation Index
PCP	Precipitation
P-M	Penman Monteith Equation
PA	Precision Agriculture
R^2	Coefficient of Determination
RS	Remote Sensing
RET	Reference evapotranspiration
SD	Standard deviation
SOS	Start of season
UAS	Unmanned Aerial System
WPb	Biomass water productivity
WaPOR	FAO portal to monitor Water Productivity through Open access of remotely sensed derived data
WaPORWP	Jupyter notebooks on WaPOR based monitoring of Land and water productivity, and irrigation performance indicator

ABSTRACT

As competition for limited land and water resources grows, along with the need to feed a constantly increasing population, innovative methods are required to monitor the performance of irrigation systems and enhance land and water productivity. The Ethiopian government faces the challenge of boosting sugarcane yields in Wonji Shoa while simultaneously reducing water usage. Hence, this research analyzed the spatiotemporal distribution of land productivity, biomass water productivity, and irrigation performance indicators in Wonji Shoa. WaPORWP python library is used for assessing spatiotemporal land and water productivity, as well as other irrigation performance indicators using WaPOR data with 30m resolution from 2009-2022. The analysis covered six indicators: water consumption, uniformity, adequacy, beneficial fraction, land and water productivity, and productivity gaps differentiated by irrigation methods. The WaPOR data were first validated agronomically by examining the biomass response to water, and then the data were used to systematically analyze seasonal indicators for the period 2009-2022 on ~11,000 ha. The yield estimates based on WaPOR were found to be comparable to those measured on estates measured. Consequently, the average difference between WaPOR yield and observed yield was 24.68%, with a standard deviation of 19.52%. The analysis of ETact temporal variation revealed that water consumption increased during cropping seasons, indicating that the goals of the ABWAP for reducing water use have not been met. The highest water consumption rate was found in furrow-irrigated areas, whereas center-pivot irrigated areas had the lowest consumption and demonstrated the best performance in achieving irrigation uniformity. Furrow and sprinkler irrigation methods have a higher beneficial fraction than center pivot methods, and furrow irrigation has the highest adequacy levels compared to other methods. Although there were no noticeable changes in land productivity over time, differences in irrigation methods were observed among the fields. Furrow irrigation achieved the highest biomass production (120.4 tons/ha/year), while center pivot irrigation produced the lowest output (110.5 tons/ha/year). The temporal variation of water productivity decreased over time and the performance in irrigated areas reveals an average WPb of 8.3kg/m^3, with sprinkler-irrigated areas ranking the highest at 8.5kg/m^3. Some areas exhibit both higher and lower WPb values, indicating the potential for improvement in underperforming portions. A 13-year average production gap of 39.0 tons/ha/year was observed in certain areas using furrow and sprinkler irrigation methods, while other areas experienced a gap ranging from 76.2 to 113.2 tons/ha/year. The water productivity gap ranges from 0.014 $kg/m^3/year$ in furrow irrigated areas to 1.26-3.8 $kg/m^3/year$ in areas using sprinkler and center pivot systems. Closing the biomass gap at Wonji Shoa could increase biomass production from 119.9 ton/ha/year to 162.4 tons/ha/year, resulting in an additional 466,947.5 tons/year and closing the WPb raising the WPb from 8.3 kg/m^3 to 8.5 kg/m^3. Zonal analysis from 2009-2022 reveals significant variations in crop yield, water productivity, and yield gap across various zones. Zones 4, 7, and 8 showed high efficiency in water use and better agricultural performance, whereas zones 13 and 18 struggled. This research contributes to a better understanding of RS-based evaluations, providing an economical solution for conducting extensive analyses to pinpoint areas with varying productivity levels and compare irrigation practices across different schemes and cropping seasons. The findings can be useful in identifying opportunities for enhancement by determining the conditions necessary for achieving optimal land and water productivity.

Key Words: Land productivity, Water productivity, WaPOR, Remote Sensing

1. INTRODUCTION

1.1 Background of the Study

Water resources are the lifeline of human civilization, playing a crucial role in sustaining life, promoting economic growth, and preserving the planet's ecosystems. These essential resources support agriculture, industry, and domestic use across the globe, highlighting their importance for social and ecological well-being. However, water resources are facing severe challenges due to unlimited population growth, rapid industrialization, urbanization, expansion of agricultural land, loss of agricultural water, climate change, and competing demands from different sectors, posing a significant threat to food security and environmental sustainability (Mali, 2016). Addressing the critical challenge of ensuring food security for present and future generations requires sustainable use of finite land and water resources. Currently, 820 million people worldwide struggle with hunger (FAO, 2019), whereas approximately four billion individuals face water scarcity for at least one month per year (UNESCO, 2019). Unfortunately, climate change is expected to worsen the situation, as farmers have to deal with increased variability in agricultural water supply, greater unpredictability, and more frequent droughts and floods (FAO, 2011). Competition with the industrial and domestic sectors will further reduce water availability for agricultural production (Bakkes, 2009; Zwart and Bastiaanssen, 2007). To combat this stress, agricultural production must be increased either by expanding agricultural land or by enhancing land and water productivity within existing agricultural areas. However, given the escalating competition and scarcity of limited water and land resources, as well as the environmental and social costs associated with expanding agricultural land (Hess et al., 2016), a more favorable approach is to improve land and water productivity.

Ethiopia is known as Africa's 'water tower' because the headwaters of 12 major rivers flow through the country. The country's population is estimated to be 109 million, growing annually at a rate of 2.4% in 2019, with projections of 190 million by 2050 (UN, 2019). Continued population growth and improvements in living standards will undoubtedly place significant stress on the available water resources (Rijsberman, 2006). In Ethiopia, the agricultural sector is the primary consumer of water, accounting for 85% of the nation's freshwater withdrawals (Karimi et al., 2019). This is significantly higher than the global average, where agriculture uses 70% of total freshwater resources (FAO, 2016). In the Awash River Basin of Ethiopia, there are large-scale commercial sugarcane farms, including Wonji Shoa, Metehara, Kessem, and Tendaho. The Basin Development Agency (BDA), formerly known as the Awash Basin Authority (AwBA), is responsible for ensuring sustainable and equitable water distribution in the basin. However, with increasing users and usage of Awash River, sufficient water struggles to flow downstream, especially during periods of drought. Therefore, downstream users are the first to experience water shortages compared with upstream water users. To address this issue, the BDA, supported by Addis Ababa University, developed an allocation plan for all irrigation schemes in the Awash Basin in 2015. This plan aims to improve transparency regarding natural resource utilization through public sharing and to assist commercial irrigators in managing water for their estates. Despite having an officially fixed water resource distribution in the Awash Basin, allocation plans remain vulnerable to the impact of drought and the growing demand for water downstream, particularly for agricultural expansions. Consequently, all water users must consider that the new allocation plans will provide less water. The Wonji Shoa sugar farm area, particularly the newly developed zones, faces challenges in terms of capturing sufficient water. Therefore, it is crucial to improve irrigation water management, as studied extensively by Dejen (2014), while focusing on increasing land and water productivity in the Wonji Shoa. The growing pressure on the agricultural sector to enhance crop production, especially sugarcane productivity per unit of land and water in existing croplands, must be explored through irrigation performance assessment. This assessment will be vital to ultimately aid irrigation scheme managers and farmers in making informed decisions to boost the land and water productivity of sugarcane, to gain a better picture of high-performing areas (bright spots) and low-performing areas (hot spots) in terms of land and water productivity, subsequently identifying possible solutions for improvements, and ensuring future food security based on the ever-growing demands of the enlarging population.

Monitoring irrigation performance indicators is crucial for assessing overall health, comparing the spatial and temporal performance of the scheme, identifying causes, and implementing corrective actions to enhance service provision and productivity (Bos et al., 2005; Molden et al., 1998). Traditional irrigation performance evaluation focuses on indicators that fall into three categories: (i) water balance, water service, and maintenance,(ii) environmental, and (iii) economic indicators. Water balance, service, and maintenance indicators are based on water flow and production. Key water delivery and production-based indicators include uniformity (even distribution of water within fields), equity (consistent water distribution between fields), adequacy (sufficient irrigation delivery relative to requirement), land productivity (production per unit area), water productivity (production per unit of water use), and efficiency (the proportion of productive water use) (Bos, 1997; Molden et al., 1998; Molden & Gates, 1990). These irrigation performance indicators are evaluated using field data, such as flow (discharge), crop yield, and plot-level water consumption estimates derived from lysimeters or crops (Araya et al., 2011; Dejen, 2015; Edreira et al., 2018).

Recent advancements and enhancements in remote sensing (RS) technology have provided feasible alternatives for irrigation performance assessment (Bastiaanssen et al., 1996; Karimi et al., 2011). The use of RS-derived data has been increasing as a cost-effective method for evaluating irrigation systems. This approach relies on measuring both production and actual water consumption, with the latter considered the net outcome of effective rainfall and irrigation. This allows for hydrological evaluation and quantification of water used by irrigated crops. Moreover, remote sensing provides spatially distributed data, can cover extended periods and vast areas, and allows retrospective analysis (Bastiaanssen et al., 1996; Karimi et al., 2011). In contrast, field data may not accurately represent the spatial variation within an irrigation system and can be expensive to collect (Bastiaanssen et al., 2000). Traditional field-based assessments can complement RS-based assessments, as the former excels in observing horizontal water fluxes, such as discharges, whereas the latter is better at observing high-resolution vertical water fluxes and biomass production. Given the ongoing advancements in remote-sensing data processing capabilities and the availability of real-time, high spatial, and temporal resolution data, RS-based approaches for assessing irrigation performance have become increasingly vital, particularly in data-scarce regions or countries such as the Wonji Shoa.

Generally, remote-sensing-based irrigation performance assessment offers advantages such as spatially distributed data, wide coverage, and retrospective analysis. This study focuses on analyzing the spatiotemporal variation in water and land productivity and other irrigation performance indicators at the Wonji Shoa Sugarcane Estate differentiated by the irrigation application method. Furthermore, the productivity gap was explored. These efforts were aimed at providing insights into better land and water management in the sugarcane industry.

1.2 Statement of the Problem

Wonji-Shoa Sugar Factory needs to increase its production by intensifying production on existing lands without depleting water sources. The allocation plans for water resource distribution in the Awash Basin have been officially fixed, but they remain vulnerable to the impacts of drought, such as a reduced water buffer in Lake Koka and the growing demand for water downstream, particularly for agricultural expansion. Consequently, all water users should be prepared for the possibility of receiving less water under these new allocation plans. In Wonji Shoa, especially in the newly developed areas, challenges arise in securing adequate water resources. This highlights the need for improved irrigation water management, as extensively studied by Dejen (2014), and a significant increase in land and water productivity in Wonji Shoa. However, such efforts should be accompanied by appropriate government incentives to encourage water conservation, such as increasing the cost of water abstraction licenses, as suggested by Girma (2020).

To enhance the efficiency of water usage in agriculture, it is crucial to comprehend the quantity, distribution, and spatiotemporal pattern of water productivity within a specific region. Typically, water productivity is evaluated based on the observed average crop yield and water consumption across a farm along with point-based climatic data. However, this information does not sufficiently depict the spatial variations that occur throughout the irrigation system (Bastiaanssen et al., 2000). Assessments of land and water productivity and irrigation performance based on remote sensing provide practical alternatives to traditional field methods for measuring crop growth and evapotranspiration (Bastiaanssen et al., 1996; Karimi et al., 2011). These RS-based evaluations can serve as an economical approach for conducting large-scale analyses to pinpoint areas with higher or lower water productivity and compare water delivery practices in irrigation systems across multiple cropping seasons. These findings can aid in determining the potential for enhancement by identifying the conditions necessary for achieving high water productivity. One of the primary factors contributing to the variation in water productivity is believed to be farm water management practices. In Wonji Shoa, these practices largely rely on soil and drainage management as well as irrigation application methods. Consequently, an analysis of an estate's productivity in a location such as Wonji should be divided based on (at least) the irrigation method to better understand the factors affecting water productivity and, in turn, identify potential solutions for improvements.

1.3 Objective of the Study

1.3.1 General objective

The general objective of this research was to assess the spatiotemporal variations in land productivity, water productivity, and other irrigation performance indicators at the Wonji Shoa Sugarcane farm.

1.3.2 Specific objectives

- To assess the spatiotemporal variation of land productivity in the Wonji Shoa irrigation scheme.
- To evaluate the spatiotemporal distribution of water productivity in the Wonji Shoa irrigation scheme.
- To assess the irrigation performance in terms of water consumption, uniformity, adequacy, and beneficial fraction.
- To assess the productivity target, identify the bright spot, and productivity gaps in the Wonji Shoa irrigation scheme.

1.4 Research Questions

- To what extent does land productivity vary spatially and temporally in Wonji Shoa, and what factors contribute to these variations?
- How does water productivity vary in terms of its spatiotemporal variability within the Wonji Shoa, and what are the possible explanations for these variations?
- What is the extent of spatiotemporal variability in irrigation scheme performance indicators, including water consumption, uniformity, adequacy, and beneficial fractions?
- To what extent are the productivity target, productivity gap, and bright spots observed in the Wonji Shoa region, and what factors can explain these patterns?

1.5 Significance of the Study

The use of RS-based assessments provides a cost-effective approach for conducting extensive analyses to pinpoint areas with higher or lower water productivity levels and for comparing water delivery practices across different irrigation schemes and crop seasons. This information can be valuable in evaluating potential improvements by identifying the necessary conditions to attain high water productivity. It is believed that one of the primary factors contributing to the differences in land and water productivity is farm water management practices. In Wonji Shoa, these practices largely depend on soil and drainage management as well as irrigation application techniques. Therefore, an analysis of the productivity of an estate such as Wonji Shoa should be segmented according to (at minimum) the irrigation method to gain a better picture of what factors influence land and water productivity and subsequently identify possible solutions for improvements. This study enhances our understanding of the spatiotemporal distribution of land and water productivity in the Wonji Shoa, ultimately aiding irrigation scheme managers and farmers in making informed decisions to boost the land and water productivity of sugarcane in Wonji Shoa. The significance of this study lies in its ability to identify low-performing (hot spots) and high-performing (bright spots) areas, addressing the necessary improvements to bridge productivity gaps within the irrigation scheme.

1.6 Scope and Limitation of the Study

This study aims to assess or provide insight into water and land productivity in the Wonji Shoa sugarcane scheme using remotely sensed data derived from FAO Water Productivity through open-access remotely sensed derived data (WaPOR). The study also focuses on analyzing the spatiotemporal variation of water and land productivity and irrigation performance indicators at the Wonji Shoa sugarcane estate differentiated by the irrigation application method. Furthermore, the productivity gap and the implications of its closure on production are explored.

In our study, remote sensing methods allowed us to observe variability in land and water productivity but could not determine the causes of this variation (Safi et al., 2022). Factors such as farm management, inputs, and stresses caused by waterlogging and salinity may contribute to productivity differences; however, further research is required. To effectively interpret results and develop practical solutions, WaPOR analyses must be combined with observed field data such as water and nutrient input levels, waterlogging, and salinity levels. The integration of these data sources will enable researchers to better understand production settings and explore the existing constraints. Although our findings have limitations, the study procedures may serve as a helpful guide for future research. Socioeconomic performance indicators, such as social water productivity and economic water productivity, could also be considered in future studies, providing valuable insights for policymakers and agricultural stakeholders.

1.7 Thesis Organization

This thesis is organized into five chapters. Chapter one serves as the introduction and includes the background of the study, statement of the problem, objectives of the study, research questions, significance of the study, scope, and limitations. The second chapter, the literature review, provides an overview of the remote sensing approach and its application in precision agriculture, as well as its challenges, limitations, and opportunities. Traditional methods for crop water productivity assessment have also been explored, along with irrigation performance indicators, the Remote Sensing WaPOR database, and its data components. The methodology, standard protocol, and challenges associated with using the WaPOR dataset and protocol are discussed in chapter two. Moreover, in-depth reviews of studies analyzing land and water productivity, particularly for sugarcane irrigation schemes, are included. Chapter three encompasses the materials and methods used in this study. This section describes the study area, including its location, climate, soil, and irrigation application methods. The approach is presented by providing an overview of the data and performance assessment framework used, such as downloading and preprocessing of WaPOR data, seasonal water consumption, net primary production calculations, and performance assessment indicators. This chapter also covers the analysis of land and water productivity, and the identification of bright spots and productivity gaps aimed at meeting the study objective. In Chapter Four, the results and discussion of the study are presented, addressing the research objectives outlined in chapter one. Finally, chapter five offers conclusions and recommendations based on the findings of this study.

2 LITERATURE REVIEW

2.1 Background on Remote Sensing and its Relevance in Agriculture Fields

Digital agriculture and precision agriculture (PA) are terms often used interchangeably to describe the application of advanced crop and environmental analysis tools combined with large data sources to help farmers implement appropriate management practices at the right rates, times, and locations to achieve both economic and environmental objectives. Remote sensing, which is the art and science of gathering data about real-world objects or areas from a distance without directly touching them (Palanisamy et al., 2019), is one of the key technologies used in precision agriculture (PA). Remote sensing (RS) enables farmers to collect, visualize, and assess crop and soil health conditions efficiently and cost-effectively at various stages of production. This technology also serves as an early warning system, allowing for the identification of potential issues and offering opportunities for quick intervention and resolution (Khanal et al., 2020a).

Remote Sensing Applications in Precision Agriculture

2.1.1 Linking RS observations to variables of interest in agriculture

Crop characteristics, soil parameters (such as soil moisture, organic matter, pH, and drainage), topography (such as elevation and slope), and changes in these variables over time and space are all important variables in agriculture (Nock et al., 2016). These characteristics are not directly measurable by remote sensing (RS), they are inferred by fusing spectral observations with ground-truth data using mechanistic, empirical, or a combination of the two methods (Licker et al., 2010).

2.1.2 RS observations to variables of interest in agriculture: a role of resolution

Remote sensing, which has high spatial, spectral, and temporal resolutions, is a crucial tool for supporting agricultural decision-making. The identification of agricultural growth phases, counting of crops, and detection of weeds are all made easier by high-resolution photography. Regular picture access documents seasonal changes in crop water and nutrient demands. Hyperspectral photography, which captures spectral fingerprints in a variety of small bands, improves the characterization and categorization of crop and soil features. Thermal and microwave region photography, which collects crucial information on crop and soil water stress, also detects thermal anomalies in crops and soils (Hong et al., 2019; Möller et al., 2007).

2.1.3 Bridging data gaps

Remote sensing may be very important for filling gaps in data and information. Numerous data components, such as the quantity of irrigated land, precipitation, agricultural output, and crop consumptive water usage, can be derived from or measured using satellites (Bastiaanssen & Bos, 1999; Pareeth et al., 2019; Zwart & Leclert, 2010).

2.1.4 Remote sensing applications in production agriculture

Remote sensing technology also aids in various management activities associated with agricultural production, including pre-season planning, field preparation, planting, real-time monitoring, pest control, harvesting, and post-harvest tasks (Khanal et al., 2020).

Preseason planning

Topographic mapping employing remote sensing data from several platforms facilitates preseason management decisions for field operations, crop selection, and seeding rate during spring planting. Topographic features of a field, such as slope, elevation, and aspect, affect the hydrological balance, which in turn affects soil properties. Field topography data can be collected using digital elevation models (DEMs), survey-grade GPS technology, GPS-equipped agricultural equipment, and remote sensing photography (Renschler et al., 2002; Renschler & Flanagan, 2008).

Subsurface tile drain mapping

A scalable and precise approach utilizing RS technology is used to locate and map drain lines in agricultural areas, enabling improved water management that boosts crop production and lowers nutrient loss to streams (Goswami et al., 2009; Naz et al., 2009).

Filed preparation

Remote sensing from multiple platforms is useful for the evaluation of soil moisture and temperature mapping in fields, which is necessary for management decisions related to planting, fertilizer application, and irrigation. Additionally, RS-based technology assists in analyzing soil compaction by recognizing and measuring soil compaction. Soil compaction has a detrimental effect on soil health and affects crop output by lowering soil porosity, hydraulic conductivity, and nutrient availability. By having a better understanding of the temporal and spatial extent of soil compaction in the field, farmers can minimize in-field compaction and the resulting crop production losses (Kulkarni et al., 2010).

Planting

Crop emergence and density: In agriculture, it is essential to monitor crop populations and densities because they affect yields and harvesting logistics. Unmanned aerial systems (UAS) have been shown in studies by (Fernandez-Ordoñez & Soria-Ruiz, 2017; Jin et al., 2017) to accurately identify crops and assess their density, assisting in mid-season management and replanting decisions.

In-Season Crop Health Monitoring: The use of RS, which offers a rapid and non-destructive tool for locating, quantifying, and mapping crop-related stressors, can help managers make site-specific decisions regarding when to apply nutrients and pesticides rather than treating the entire field. It has been shown that using remote sensing data from diverse platforms is a time- and money-saving alternative to the established approaches for monitoring nitrogen stress in agriculture. According to (López-Granados et al., 2016; Peña et al., 2013), high-resolution photography (both spatial and spectral) also aids in the precise identification and classification of weeds in the field.

Harvest

High-resolution yield maps were created using remote sensing to assess field yield variability. This helps farmers to estimate the potential output of their fields. Crop yields may be accurately predicted by machine learning algorithms and vegetation indices using remote sensing data, especially during mid-seasonal stages. Some have proposed that incorporating crop growth models, seasonal weather predictions, and field management strategies with remote sensing data may further improve yield predictions (Du & Noguchi, 2017; Geipel et al., 2014; Khanal et al., 2018; Lobell et al., 2015).

Grain quality assessment: In agriculture, remote sensing is essential because it helps evaluate grain quality, which has a significant influence on the nutritional value and economic viability of production methods. Research has demonstrated that remote sensing can forecast grain protein by examining imaging data, which is crucial for supporting logistical choices and managing different crops (Jensen et al., 2007; L. Wang et al., 2014; Z. J. Wang et al., 2004).

2.2 RS for Precision Agriculture: Challenges, Limitations, and Opportunities

Due to advancements in the acquisition system technology, the majority of RS technologies are presently accessible and reasonably priced for the agricultural sector. However, the agricultural sector has only recently been able to fully transition from test to production settings using RS technology (Colaço & Bramley, 2018; Higgins et al., 2019). Some of the reasons behind this issue are as follows: (1) there is inadequate knowledge about the efficiency of remote sensing technologies based on sensor and platform types, in addition to the technical and economic advantages of these technologies; (2) there is a lack of remote sensing-based decision-support tools and the training needed to use them; (3) there are challenges in achieving compatibility with data and tools originating from various sources (Khanal et al., 2020); and (4) data quality is sometimes hampered by poor quality measurements. Cloud cover causes remote sensing images to be of poor or absent quality. To fill in the data gaps, interpolated data were used, which increased the noise in the data (Chukalla et al., 2021).

2.3 Traditional Methods for Crop Water Productivity Assessment

2.3.1 Traditional crop yield estimation methods

Methods to evaluate crop yield and biomass include physical assessments, subjective estimates, and micrometeorological techniques. Physical assessments involve complete plot harvesting, crop cutting in smaller plots (Verma et al., 1988), and collection of samples from harvest units, such as sacks, baskets, and bundles. Subjective estimates encompass expert evaluations, farmers' predictions and recollections, and daily log records. Micrometeorological techniques mainly utilize eddy covariance (EC) and chamber methods to measure carbon fluxes.

2.3.1.1 Whole-plot harvest method

The whole-plot harvest method is used to estimate crop yield, primarily in on-farm trials with demonstration plots (Norman, 1995). It involves clear delineation of plot boundaries, harvesting, drying, and weighing of crops (Casley & Kumar, 1988). This method is considered to be the standard for crop yield estimation and provides high accuracy with minimal bias (Sud et al., 2016). However, errors may arise from incorrect area estimations, irregular field shapes, and improper supervision(Murphy et al., 1991). The whole-plot harvest method is most suitable for fields smaller than 0.5 hectares (Casley & Kumar, 1988).

2.3.1.2 Crop-cutting method

The crop-cutting method is used to estimate biomass and crop yield by dividing a plot into smaller sub-plots, collecting samples from each plot, and then estimating the overall production using the ratio of total sub-plot production to the cumulative area of the sub-plots (Simaika, 1982).

2.3.1.3 Farmer surveys

The process of employing farmer surveys to determine crop yields consists of acquiring either retrospective or forecasted estimates from farmers. Retrospective estimates, believed to be more accurate, involve questioning farmers near the postharvest period, with recall durations ranging from a few weeks to three to six seasons. However, forecasted estimates are gathered on a per-plot basis, relying on the knowledge of either the farmer or an expert (Sud et al., 2016).

2.3.1.4 Yield models or predictive algorithms

Yield models are a collection of mathematical equations or computer procedures that predict crop production by considering several variables, such as soil composition, weather, resource utilization, and crop management practices. Another method for estimating yield is to measure carbon fluxes in the field, such as Gross Primary Productivity (GPP) and Net Primary Productivity (NPP), and then translate these numbers into yield using conversion factors that are particular to each crop. The Eddy Covariance (EC) and chamber methods are the primary methods used to quantify these carbon flows (Baldocchi, 2003).

2.3.2 Traditional evapotranspiration estimation method

Traditionally, field observations, meteorological information, changes in soil moisture, plant stress, and empirical formulae have been used to calculate real evapotranspiration (ET) in agriculture (Rana & Katerji, 2000). Several in situ measuring techniques can be used to calculate ETa. These measurement systems are categorized into five groups: plant physiology approaches (such as the Sap flow method and Chambers system), micrometeorological approaches (including energy balance and Bowen ratio, the aerodynamic method, and eddy covariance), analytical approaches (such as the Penman-Monteith model), empirical approaches (using methods based on the crop coefficient approach), and soil water balance modeling-based methods (Rana & Katerji, 2000). According to Rana and Katerji (2000), the traditional methods for estimating ETa are as follows:

2.3.2.1 Hydrological approaches

1. Soil water balance: With this approach, the change in soil moisture content over time was measured, and inputs (precipitation and irrigation) and outputs (evapotranspiration,

runoff, and deep drainage) were taken into consideration. The difference method can be used to determine ETa when the change in soil moisture content is known.

2. Weighing lysimeters: A large container with soil and vegetation inside is called a lysimeter, which enables the monitoring of water intake and output. By keeping track of changes in mass or weight brought on by evapotranspiration, weighing lysimeters can be used to measure ETa directly.
3. Micrometeorological approaches

i. Energy Balance and Bowen Ratio: The net radiation, soil heat flux, and sensible heat flow were all measured as part of the energy balance technique to estimate the latent heat flux, which was then used to determine ETa. The Bowen ratio technique calculates the ratio of sensible heat flux to latent heat flux using measurements of the air temperature and humidity.

ii. Aerodynamic Method: In this method, the turbulent movement of sensible and latent heat between the surface and atmosphere is estimated by monitoring the wind speed and direction, air temperature, and humidity at various heights.

iii. Eddy Covariance: This approach directly calculates the turbulent fluxes of sensible and latent heat using high-frequency observations of the vertical wind speed, air temperature, and humidity.

2.3.2.2 Plant physiology approaches

1. Sap Flow Method: This method measures water flow in plant stems or trunks to calculate transpiration as a part of the ETa.
2. Chamber System: To calculate plant transpiration and ETa, CO_2, and water vapor exchange rates for leaves can be measured in gas exchange chambers.

2.3.2.3 Analytical approach (Penman-Monteith Model)

This model uses meteorological data to determine ETa by fusing principles from the fields of energy balance, aerodynamics, and resistance-based models.

1. Empirical Approach (Crop Coefficient Approach): This approach includes tying reference evapotranspiration estimates acquired from meteorological data to ETa using crop-specific coefficients. These coefficients can be changed depending on the crop development stage and soil moisture level.

2. Soil Water Balance Modeling: This model simulates soil moisture dynamics and estimates ETa using components of soil water balance (precipitation, irrigation, runoff, and deep drainage). The model considers processes, including water absorption by plant roots, evaporation from the soil surface, and capillary rise of water from the groundwater table.

2.4 Comparison Between RS and Traditional CWP Assessment

The advancement of remote sensing technology has revolutionized various fields, including precision agriculture and crop water productivity assessment. Remote sensing offers numerous advantages over traditional methods for crop yield and evapotranspiration estimation, which were time-consuming, labor-intensive, and less accurate. The integration of remote sensing with geographic information systems (GIS) and global positioning systems (GPS) has paved the way for better decision-making and resource management in agriculture (Rana & Katerji., 2000).

Compared to traditional crop yield estimation methods, which relied on in-field sampling, visual observations, and expert knowledge, remote sensing provides a more comprehensive and objective view of crop conditions. Using multispectral and hyperspectral satellite or drone imagery, it is possible to monitor crop health, growth, and water stress at various spatial and temporal resolutions. The use of vegetation indices, such as the normalized difference vegetation index (NDVI), has facilitated the estimation of crop biomass, leaf area index (LAI), and yield potential. Additionally, remote sensing can cover large areas and provide near real-time data, enabling rapid assessment of crop damage due to pests, diseases, and natural disasters (Colaço & Bramley, 2018; Higgins et al., 2019).

In terms of evapotranspiration estimation, traditional methods, such as the combination of pan evaporation measurements and crop coefficients, often lacked accuracy and required site-specific calibration. Remote sensing has overcome these limitations by offering options for direct estimation of evapotranspiration using advanced techniques, such as energy balance models and surface renewal analysis. These methods utilize satellite-derived land surface temperature, albedo, vegetation cover, and other parameters to calculate evapotranspiration rates at different spatial scales (Khanal et al., 2020a). Furthermore, remote sensing-derived evapotranspiration data can be used to evaluate water-use efficiency and crop water productivity, which are essential for sustainable agriculture and water resources management. In conclusion, the advent of remote sensing technology has significantly enhanced our ability to monitor and assess crop conditions and water productivity in agriculture. The availability of accurate, high-resolution spatial and temporal data has made it possible to develop more targeted and efficient management strategies, ultimately contributing to improved agricultural productivity and resource conservation (Palanisamy et al., 2019).

2.5 RS-Based Irrigation Performance Assessment

Monitoring irrigation performance assessment is crucial to evaluate the overall health of the scheme, compare its spatial and temporal performances, pinpoint problems, and take corrective action to improve overall service delivery and productivity (Bos et al., 2005; Molden et al., 1998). Indicators for measuring irrigation performance traditionally fall into three categories: economic, environmental, water balance, water service, and maintenance. The indicators for water balance, water service, and maintenance are based on water flux and production. Uniformity (evenness of water distribution within fields), equity (uniformity of water distribution between fields), adequacy (sufficiency of irrigation delivery compared to the requirement), land productivity (production per unit area), water productivity (production per unit water use), and efficiency (the fraction of productive water use) are water delivery and production-based indicators (Bos, 1997; Molden et al., 1998; Molden & Gates, 1990). These indicators were evaluated using field data from flow (discharge), crop yield, and estimates of plot-level water consumption from lysimeters or crop models (Araya et al., 2011; Dejen, 2015; Edreira et al., 2018).

Recent advancements in remote sensing products provide an effective substitute (Bastiaanssen et al., 1996; Karimi et al., 2011). RS-derived data has been increasingly applied as a cost-effective means of assessing irrigation performance. The RS-derived irrigation performance assessment is based on production and actual water consumption, with the latter regarded as the net outcome and result of efficient irrigation and rainfall. This enables hydrological assessment and quantification of the net water abstracted by irrigated crops. Additionally, it offers spatially distributed data, spans lengthy periods and vast regions, and can be completed retroactively (Bastiaanssen et al., 1996; Karimi et al., 2011). In contrast, field data are difficult to obtain and do not accurately depict the spatial variation within an irrigation system(W. G. Bastiaanssen et al., 2000a). Traditional and RS-based performance assessments can be used in conjunction because the former excels at observing horizontal water fluxes such as discharges, while the latter excels at observing high-resolution vertical water fluxes and biomass production.

2.6 Remote Sensing WaPOR Database

The Food and Agriculture Organization of the United Nations (FAO) has launched the Water Productivity Open-access Portal (WaPOR), a platform that monitors water productivity using open-access data derived from free remote satellite sources. WaPOR is the first comprehensive dataset that combines various aspects of water use (actual evaporation, transpiration, and interception), production (net primary production), land use (land cover classification), phenology, and climate (precipitation and reference evapotranspiration) for Sub-Saharan Africa, the Middle East, and North Africa. The dataset covers information from 2009 to the present and is available in real-time. Users can access WaPOR datasets at the project level (30 m), country and river basin level (100 m), and continental scale (250 m). Table 2.1 shows the spatial resolution and regions of interest of the different datasets covering sub-Saharan Africa and the Middle East and North Africa regions. The latest version of the portal, WaPOR v2.1, was improved based on a quality assessment conducted by IHE Delft and ITC (Mul & Bastiaanssen, 2019a).

Table 2.1 Spatial resolution and regions of interest of different datasets (levels) (FAO 2020).

Dataset	Resolution	Region of Interest
Level 1	250 m (0.00223°)	Africa and Near East (bounding box 30W, 40N, 65E, 40S)
Level 2	100 m (0.000992°)	**Countries:** Tunisia, Morocco, Ghana, Egypt, Niger, Sudan, South-Sudan, Kenya, Mali, Benin, Ethiopia, Rwanda, Burundi, Mozambique, Uganda, Iraq, West Bank and Gaza Strip, Yemen, Jordan, Syrian Arab Republic, and Lebanon.
		River basin: Niger, Nile, Awash and Jordan, and Litani.
Level 3	30 m (0.00268°)	Irrigation scheme and rainfed areas in Egypt, Ethiopia (2 areas), Mali, Lebanon, Kenya, Mozambique, and Sudan.

The WaPOR platform, which tracks water productivity through open access to remotely sensed data, helps governments monitor water productivity, identify gaps in water productivity, and suggest ways to close them, while also boosting agricultural output sustainably. It also considers ecosystems and the equitable use of water resources, which eventually results in a decrease in total water stress. WaPOR opens the door for service providers to help farmers obtain more dependable harvests and improve their standard of living by supplying near real-time pixel information. Simultaneously, government organizations may utilize this information to encourage and boost the effective use of their natural resources. Irrigation authorities have access to information to update their irrigation schemes (Chukalla, Mul, van der Zaag, et al., 2022a; Janssens, 2022).

2.7 WaPOR Data Components

2.7.1 Water productivity

Gross biomass water productivity: The ratio of biomass production to total water consumption during a certain period is known as gross biomass water productivity(FAO, 2019). To provide information on how plant growth influences consumptive water usage and, ultimately, the water balance in a specific area, this indicator links biomass production with total evapotranspiration (which includes soil evaporation, canopy transpiration, and interception)(FAO, 2019).

Net biomass water productivity: The term "net biomass water productivity" describes the ratio of annual biomass production (output) to the quantity of water used by canopy transpiration, excluding soil evaporation. In contrast to gross water productivity, net water productivity is notably useful for determining how effectively vegetation, particularly crops, utilizes water to generate biomass, which eventually contributes to yield (FAO, 2019).

2.7.2 Evaporation, transpiration, and interception

Evapotranspiration is the combined total of soil evaporation (E), canopy transpiration (T), and interception(I). Interception refers to rainfall collected by plant leaves that later evaporates directly from their surface. The sum of these variables, known as actual evapotranspiration and interception (AETI), can be used to determine the amount of water used for agricultural purposes.

(Bastiaanssen et al., 2012) presented a method for calculating evaporation and transpiration based on the ETLook model which employs the Penman-Monteith equation adapted for remote sensing input data. The Penman-Monteith equation predicts the rate of total evapotranspiration and transpiration using commonly measured meteorological data such as air temperature, vapor pressure, solar radiation, and wind speed. This equation has become the standard for the FAO to calculate the actual and reference evapotranspiration. The Penman-Monteith equation is also known as the combination equation because it combines the surface energy balance equation and aerodynamic equation (FAO, 2019).

2.7.3 Precipitation

Daily total precipitation (in mm) was obtained from the CHIRPS18 dataset, an established external data source that integrates satellite observations with global models and local station measurements. Daily precipitation data has a spatial resolution of approximately 5km (0.05°) (FAO, 2019).

2.7.4 Reference ET

Reference evapotranspiration (RET) is the evapotranspiration process that takes place on a well-watered grass surface, which serves as a hypothetical reference crop. By using predetermined crop coefficients, it may be used as a basis for calculating the potential ET for different crops. The spatial resolution of RET, which is offered at Level 1, is 20 km (FAO, 2019).

2.7.5 Land cover classifications

The observed (bio)physical cover of the earth's surface, including plant, bare rock, soil, and man-made structures, is referred to as "land cover." On the other hand, land use might result from land cover being integrated with or connected to human activities or behaviors in their surroundings (Di Gregorio, 2005). The Copernicus Global Land Service with 100m of land cover was used for level 1 and level 2 land cover mapping. Data on agricultural land cover are crucial for assessing current land use practices, because they may be combined with information on water productivity to enable comparisons between various crops grown in one region and the same crop grown in several places (FAO, 2019).

2.7.6 Harvest index

The harvest index is a metric used to distinguish between a proportion of biomass output that can be harvested and one that cannot. It is feasible to calculate agricultural production and water productivity using the harvest index. HI is often used to evaluate the productivity of a particular plant type, reflecting the contribution of biomass production to the crop's harvestable portion (yield). The index has a theoretical maximum value of 1 when all the biomass (TBP) has been collected, ranging from 0 (no harvestable portion) (FAO, 2019).

2.7.7 Phenology

Phenology refers to the seasonal cycle or stage of a crop, including the beginning, peak, and end of the growing season. satellite-based vegetation index time series can be used to obtain information about a crop's phenological development (FAO 2019).

2.8 WaPOR Data Components Per Level

Table 2.2 outlines the data components created for the WaPOR database. All three levels included water productivity, evaporation, transpiration, interception, net primary productivity, above-ground biomass production, and land cover classifications. However, only level-1 data includes reference evapotranspiration and precipitation, with a significantly lower spatial resolution compared to other level-1 data components. Both components were generated daily. Phenology is available for levels 2 and 3, whereas the harvest index (HI) is exclusively produced for level 3, enabling crop yield calculations (FAO, 2020).

Table 2.2 Overview of the WaPOR data components per level, with temporal and spatial.

Data components	Level[1]1 (250m)	Level 2 (100m)	Level 3 (30m)	Remarks
Water productivity (WP)	Annual[2]	Dekadal[3] /Seasonal[4]	Dekadal /Seasonal	Level specific calculations
Evaporation(E)	Dekadal /Annual	Dekadal /Annual	Dekadal /Annual	
Transpiration(T)	Dekadal /Annual	Dekadal /Annual	Dekadal /Annual	
Interception(I)	Dekadal /Annual	Dekadal /Annual	Dekadal /Annual	
Actual evapotranspiration and interception (AETI)	Dekadal /Annual	Dekadal /Annual	Dekadal /Annual	
Net primary production (NPP)	Dekadal	Dekadal	Dekadal	
Total biomass production (TBP)	Annual	Seasonal	Seasonal	
Above-ground biomass production (ABGP)	Annual	Seasonal	Seasonal	
Phenology		Seasonal	Seasonal	
Harvest index (HI)			Seasonal	
Reference evapotranspiration (RET)	Daily			Different resolution:20km
Precipitation (PCP)	Daily			Different resolution:5km
Land cover classification (LCC)	Annual	Annual	Dekadal	Level specific class

1. Level 1: Continental, Level 2: Country/River basin, Level 3: Irrigation scheme/sub-basin.
2. Annual as a standard product, with the possibility of calculating user-defined intervals.
3. Dekadal refers to a period of approximately 10 days. It splits the month into three parts, where the first and second decades consist of 10 days each, and the last decade ranges from 8 to 11 days.
4. Seasonal refers to the growing season. The length and number may vary, with a maximum of 2 growing seasons per year.

2.9 Methodologies and Techniques in Remote Sensing Studies

2.9.1 Standard protocol for the land and water productivity analyses

The protocol was specially designed for the biophysical water productivity of a region (fields and schemes) in similar agro-climatic zones concerning consumed water usage and land productivity. Regardless of the water source (such as precipitation (rainfed), irrigation (augmented by surface water and/or groundwater, or flood/spate), this technique can be used for single water management units and agricultural production. The technique was developed for agricultural regions that grow a single crop throughout a consistent cropping season, which might change from year to year. Implementing the protocol at levels above fields and schemes, such as river basins and entire countries, which may be located in several agroclimatic zones, requires normalization for climate variance, which is outside the scope of the protocol (A. D. Chukalla et al., 2021).

Two open-source libraries (WaPORWP and PySEBAL) are available to evaluate water productivity and related performance indicators based on remote sensing data. PySEBAL is a Python library developed at IHE Delft that calculates water usage and biomass production using a surface energy balance model and then determines seasonal water productivity. On the other hand, WaPORWP is a Python library consisting of scripts designed to implement the standard protocol developed by IHE Delft for assessing spatiotemporal land and water productivity, as well as other irrigation performance indicators using WaPOR data (Chukalla et al., 2021). The WaPORWP Python library was utilized for our Wonji Shoa case study to analyze land and water productivity as well as other performance indicators. The structure of the protocol is outlined and explained in detail in the following sections.

2.9.2 Structure of the protocol

The protocol comprises six modules, accompanied by a Jupyter notebook containing the necessary scripts. Actual water consumption, actual transpiration, reference evapotranspiration (RET), net-primary production, land cover categorization, and precipitation data are all downloaded under Module 0 of the WaPOR portal. Pre-processing the data were preprocessed in Module 1 to align spatial resolution and get rid of non-crop pixels. Module-2 determines the seasonal net primary production and water consumption (actual evapotranspiration, potential evapotranspiration, and transpiration). Various performance indicators were computed in

Module 3. The productivity of land and water was assessed using Module-4. Module-5 also highlights areas of productivity gap and bright spots.

2.9.3 Challenges and limitations of using the WaPOR dataset and protocol

Due to low-quality measurements made from remote sensing images, which can be impacted by factors such as cloud cover, WaPOR data can occasionally have restricted quality. This results in noise and data gaps (Chukalla et al., 2020). Although (Blatchford et al., 2020) validated WaPOR variables, they also reported that ETact (actual evapotranspiration) was frequently overestimated in eastern Africa under dry and hot conditions. This overestimation could be due to poor quality soil moisture content or high vapor pressure deficit. While the error might only be a few mm/days, it could accumulate significantly over a season. Additionally, the varying times and angles of remote sensing images may contribute to low-quality data obtained for actual evapotranspiration. Correction factors are needed to account for these variations; however, they may introduce small errors that can influence ETact values (Chukalla et al., 2020).

According to a study conducted by Chukalla et al. (2020), several factors and elements were identified as potential sources of small deviations in the numerical outputs of WaPOR, which could result in over and under-valuation of the WPb output. These deviations were categorized as statistical noises.

i. Because the Proba-V satellite does not provide the Land Surface Temperature (LST) layer, WaPOR uses the MODIS LST layer at a resolution of 1 km, which affects the accuracy of capturing spatial variability.
ii. Non-agricultural (non-sugarcane) land use within a pixel creates land cover noise, with coarse pixels being more susceptible to this noise than fine pixels, and pixels along the boundaries are particularly prone to it.
iii. The quantity and quality of the RS images (such as cloud cover) used in the analysis and numerical interpolation; the larger the variance in WPb one may anticipate, the fewer the RS images and the worse the quality.
iv. The time of day when the images were collected (which determines when to monitor which section of the daily ET curve and when water stress is most prominent);
v. The angle at which the photograph was taken and how it was corrected.

To keep the sugar factory in operation, sugarcane plantations use a ratooning technique, and harvesting takes place year-round. As a result, each agricultural unit has different start and finish seasons. We assumed the same start and finish of the cropping season for the scheme, which is another source of noise because we lacked comprehensive information regarding the start and end of the season for each plot.

2.10 Remote Sensing in Recent Studies

Several studies have assessed the performance of irrigation schemes that utilize RS-based methodologies. Global research has been conducted to assess the spatial and temporal variability of water and land productivity via their case study. And also, many researchers have tried to estimate water productivity from satellite data. For example (Zwart et al., 2010b), use the WATPRO water productivity model for wheat, using remote sensing data products as input, and came up with the result of water productivity for wheat varies from 0.2-1.8 kg/m^3 of harvestable wheat per cubic meter of water consumed. (Li et al., 2008), also used satellite data to estimate the water productivity of North China Plains and came with maximum and minimum water productivity of 1.67 kgm^{-3} and 0.5 kgm^{-3} respectively. The applications of the remote sensing techniques in sugarcane agriculture have been undertaken with particular emphasis on sugarcane classification and areal extent mapping, thermal age group identification, varietal discrimination, on, yield prediction, and crop health and nutritional status monitoring (Soliman et al., 2008). The sugarcane yield estimated in western Kenya from Moderate Resolution Imaging Spectrometer (MODIS) by using a normalized difference vegetation index (NDVI) shows a root mean square error (RMSE) of less than 5 tons/ha with the historical harvested yield (Mulianga et al., 2013).

2.11 WaPOR Data in Research Studies

WaPOR data have been used in lots of research to study the land and water productivity in different areas (Alemayehu et al., 2020; Bastiaanssen, 2019; Khanal et al., 2020), it does often not include ground-level data for the validation process. This is crucial because it is assumed that solely using remote sensing data can result in wrong conclusions. Not all temporal and spatial differences can be explained properly when solely using remote sensing data. Various studies use the WaPOR data without validating the data themselves because they assume the

WaPOR data is validated by other studies (Barideh & Nasimi, 2022; A. D. Chukalla et al., 2020; Gemechu et al., 2020a).

- **Spatiotemporal Variability of Water Productivity in Ethiopian Sugarcane Estates (Gemechu et al., 2020)**

Gemechu et al. (2020) conducted a study to analyze the spatiotemporal variability of water productivity in Ethiopian sugarcane estates (Wonji, Fincha'a, and Metehara) using open access remotely sensed source with 100 m resolution 10days intervals of Net Primary Production (NPP), AETI, and average fresh weight yields per hectare. The study found that the highest average seasonal AETI was recorded in the Metehara irrigation scheme, followed by Fincha'a and Wonji. However, the largest average seasonal fresh sugarcane yield was observed at the Fincha'a irrigation scheme followed by Wonji, while the smallest yield was observed at the Metehara scheme. The analysis of crop water productivity revealed that the average seasonal water productivity was 7.5 kg/m^3 at Wonji, 7 kg/m^3 at Fincha'a, and 4.3 kg/m^3 at Metahara. High water productivity values ranging from 7.6-9 kg/m^3 were found in Dodota, Sodare, and Wake-Tiyo within the Wonji irrigation scheme, while lower values of 5.7-7 kg/m^3 were observed in the Wonji main sub-irrigation scheme. In the Fincha'a irrigation scheme, high water productivity was found in the northern and southern parts of the sub-schemes showing a high-water productivity range from 7.3-11.2 kg/m^3. High water productivity was observed in the southern part of the Metahara irrigation scheme. Overall, water productivity performance varied spatially and temporally across sub-irrigation schemes ranging from 6.7 to 10.6 kg/m^3. The study only focused on mapping the spatial and seasonal variation in WP of sugarcane crops in three large irrigation schemes in Ethiopia using the WaPOR database without considering ground-level data.

- **Spatial Variation of Crop Production and Water Productivity in Yaqui Valley, Mexico (Zwart & Bastiaanssen, 2007)**

On the other hand, Zwart & Bastiaanssen. (2007) used the Surface Energy Balance Algorithm for Land (SEBAL) with satellite images of variable resolution to examine the spatial variation of crop production, evapotranspiration, and water productivity in Yaqui Valley, Mexico with a high concentration of irrigated wheat to test the validity of their techniques and came up with, the SEBAL based ET predictions were correct with a difference of 8.8% over 110 days. They discovered that the Yaqui Valley's projected average wheat yields of 5.5 tons/ha were in line with the measured yields published in the literature. The SEBAL projected wheat yields were 0.4 tons/ha less than the measured yields in a comparison with 24 farmer fields in the Sirsa region of India. The Yaqui Valley's average water productivity was determined to be 1.37 $\mathrm{kg/m^3}$, which is high when compared to other irrigated systems throughout the world where the same approach was used. The Nile Delta in Egypt (1.52 $\mathrm{kg/m^3}$), Kings County, California, USA (1.44 $\mathrm{kg/m^3}$), and Oldambt, the Netherlands (1.39 $\mathrm{kg/m^3}$) all have higher average water productivity than the rest of the world. Given that water supply in low-productivity systems is unpredictable and farming conditions are not ideal, it was discovered that the spatial variability of water productivity within low-productivity systems (coefficient of variation, CV = 0.33) was higher than that within high-productivity systems (CV = 0.05). The high CV in locations with poor water productivity suggests that substantial advancement is possible. The eight systems had an average improvement potential of 14%, which suggests that it is possible to reduce ET by 14% while keeping the yield the same. In conclusion, Zwart & Bastiaanssen. (2007) the technique was proven to be reliable and to offer insightful information on the spatial variation of water productivity. Implementing localized water conservation measures in irrigation systems for wheat can benefit from this information.

Similarly, Hirwa et al. (2022) Study the water Accounting and productivity analysis to improve water savings in the Nile River Basin, East Africa including from accountability to sustainability aspects using the WaPOR dataset including the ETLook model and Aqua crop model which is built on the WaPOR dataset at which Aqua Crop model used for simulations of major crops in different periods revealed that the CWP and WUE in NRB were influenced by hydrometeorological factors and changed over time and space, the Mann–Kendall (MK) test was conducted and Sen’s slope estimate was used to evaluate the trend of the hydrometeorological time series.

- **Identifying Factors Affecting Yield and Water Productivity in Bekaa Valley, Lebanon (Safi et al., 2022)**

(Safi et al., 2022) conduct a study to evaluate how open-source spatial data products can be used to identify reasons behind low performances and developed a standard procedure (framework) that can be used to utilize open-source remote sensing data for identifying reasons behind WP variations by considering six factors (crop water stress, irrigation uniformity, soil salinity, nitrogen application, crop rotation and soil type) were analyzed to identify their influence on WP and yield in Bekaa Valley in Lebanon considering wheat, potato and table grapes using 30m spatial resolution during the period 2017. The study revealed that four factors have negatively affected yield and WP in the Bekaa Valley (and they are): water stress at the critical crop growth stages; low within-farm irrigation uniformity; low nitrogen application; and improper irrigation schedule based on soil properties. It was also exposed that mono-cropping has reduced yield and WP, but the results are not statistically significant. Whereas topsoil salinity has neither influenced yield nor WP in the Valley. To improve Yield and WP in the Valley investments should target the above four factors.

- **Spatial Variation of Land and Water Productivity in Mozambique Xinavane Sugarcane Estate (Chukalla et al., 2020)**

Chukalla et al. (2020), conducted a study utilizing RS data from the PROBA-V satellite to analyze the spatial variation of land and water productivity, and other irrigation performance indicators over the period 2014-2019 at Mozambique Xinavane sugarcane estate differentiated by irrigation application methods. Additionally, the productivity gap and implications of its closure on production and water use were explored. The analysis of annual water consumption for the period 2014-2015 and 2018-2019 showed that the highest average was from center pivot irrigation (1,505-82 mm/yr) compared to the mix of irrigation (1,343±122 mm/yr) and furrow (1,329±120 mm/yr). The spatial variation of ETa ranged from 777-1,628 mm/yr, and transpiration ranged from 560-1,413 mm/yr, with an average of 1,118±125 mm/yr. The analysis of the uniformity of ETa showed good uniformity with the coefficient of variation of ETa was 9.4 %. However, variations were observed among different irrigation systems. The analysis of the adequacy under irrigation methods showed that areas under furrow irrigation had the highest water deficit (adequacy of 0.69±0.06), while the center pivot had the lowest (adequacy of

0.78±0.04). In terms of land productivity, the study found that center pivot irrigation had the highest average annual B (82±5 ton/ha/year), followed by mixed irrigation (77±7 ton/ha/year), and furrow (76±7 ton/ha/year). This is due to the higher effective water availability for consumptive use by the plant in center pivots, suggesting that better irrigation scheduling is taking place compared with others. The average spatial variation of water productivity revealed that 5.7 ± 0.2 kg/m^3 and it varies from 5-6 kg/m^3 and furrow irrigation has the highest WP with the lowest land productivity, on the other hand, center pivots score high on the land productivity but lower on the water productivity due to the relatively high-water application.

The distribution of land and water productivity revealed a productivity target of 88 tons/ha/year for biomass and 8 kg/m^3 for water productivity. The target varied based on the irrigation method, with the center pivot having the highest B target (84.8 tons/ha/year) and the biomass target for furrow irrigation systems having the lowest. Similarly, the WP target for the center pivot is the lowest at 5.5 kg/m^3, whereas it is 5.6 kg/m^3 for the other systems. The average biomass gaps throughout the five years (2014/2015 to 2018/2019) for the Xinavane sugarcane estate revealed 11.2±6.5 tons/ha/year and 105,860 tons/year for the entire estate. The biomass gap for various irrigation methods revealed that for the center pivot lowest B gap was observed, whereas the WPb gap was the highest, and WPb gaps were the lowest under furrow irrigation. This implies that more water is consumed under pivot irrigation than furrow irrigation to produce the same biomass. The study found that closing biomass gaps could boost output by up to 105,860 tons/year, which is equivalent to harvesting from an additional 1,203 ha of irrigated land. However, this research has a limitation in that it is unable to identify the causes of production fluctuations, including farm management, inputs, and environmental elements, such as salinity and water logging.

- **Spatiotemporal Analysis of Land and Water Productivity in Metehara, Ethiopia (Janssens, 2022)**

Janssens 2022) analyzed spatiotemporal variations in land and water productivity, as well as other irrigation performance indicators, in Metehara, Ethiopia. This study utilized WaPOR data from to 2009-2021 along with ground-level data for verification, focusing on the Merti and Abadir irrigation schemes. The temporal result revealed that water productivity decreased over time and that droughts were explained partly by temporal variations. Furthermore, the biomass did not increase, and the water consumption increased instead of decreasing over time. Due to soil compaction and the related decreased infiltration capacity, more water is applied while not more water reaches the crops. Spatial variations in land and water productivity are related to the influence of Lake Basaka. Fields closer to Lake Basaka had lower productivity. More compact and finer soil textures had higher water consumption, better uniformity, and higher adequacy. Soil texture did not explain spatial land and water productivity variations but did explain temporal variations. Also, fields with a higher water consumption had an overall higher biomass production. Concluding, spatial and temporal distribution in water productivity related to the influence of Lake Basaka, soil texture, and droughts.

- **Spatial Variations in Land and Water Productivity in Wonji Sugarcane Estate, Ethiopia (Alemayehu et al., 2020)**

Alemayehu et al. (2020) conducted a study on the Wonji Shao sugarcane estate to examine spatial variations in land and water productivity, as well as irrigation performance indicators based on different irrigation methods using RS 6-year average (2014/19) data for the level 3 area and 5-year average (2015/19) data for the level 2 area and local information. The analysis of the average annual water consumption showed the highest values for areas irrigated under center pivots (1,622±167 mm/year), followed by sprinkler irrigation, furrow irrigation, and Wake Tio (1,492±258 mm/year). The analysis of uniformity revealed that the overall uniformity of irrigation within the Wonji estate was fair, and sprinkler and hydro flume irrigated areas performed less, which tally with field-level accounts of challenges in operation (electricity outages) and maintenance (high costs). The furrow irrigated areas perform best in terms of uniformity, which considering a large amount of labor input and distribution challenges is remarkable and worth considering for Wonji estate when comparing irrigation scheme performance and trade-offs. The adequacy analysis showed that center pivot irrigated areas showed the highest levels of adequacy (0.83), whereas adequacy in the areas irrigated using hydro flumes was distinctly lower than the rest (0.61), in particular, due to the comparatively lower amounts of water consumed (larger comparative difference between Eta and ETref). An analysis of the average annual biomass production revealed that center pivots irrigated areas attained the highest biomass (112±13 ton/ha/year), followed by sprinkler (109±20 ton/ha/year), and furrow irrigation(103±13 ton/ha/year).

The projected biomass output in Welenchiti was 106±14 tons/ha/year, compared with 104 ± 21 ton/ha/year in Wake Tio. The analysis of average annual biomass water productivity revealed that the highest WPb is observed in areas irrigated by center pivots (6.9±0.2 $\mathrm{kg/m^3}$) followed by sprinkler (6.8±0.2 $\mathrm{kg/m^3}$), and the lowest in furrow irrigation (6.5±0.2 $\mathrm{kg/m^3}$) and level-2 areas of Wake Tio exhibit a WPb of 6.9±0.3 $\mathrm{kg/m^3}$, while For Welenchiti has a higher value of 8.3±0.3 $\mathrm{kg/m^3}$.

The assessment of B and WPb targets reveals that the biomass target of 130 tons/ha/year, WPb target of 7.1 $\mathrm{kg/m^3}$ and the ETa pixel target of 1,831mm/year was achieved in the level-3 area. Similarly, in the level 2 area between 2015/19, the biomass target of 122 ton/ha/year, the WPb target of 8.7 $\mathrm{kg/m^3}$, and the ETa pixel target of 1,402 mm/year was achieved. The eastern part of Wonji Main and Dodota, particularly in surface irrigation and sprinkler-irrigated areas, exhibited the highest performance in meeting the B and WPb targets. The eastern part of Wonji Main showed the majority of the bright spots, with additional bright spots observed in sprinkler-irrigated areas in Dodota. The analysis of the biomass production gap for a 6-year average of 27±13 ton/ha/year. Similarly, the 5-year average biomass gap for Welenchiti was 18±12 ton/ha/year. The 6-year average biomass water productivity gaps were 0.6±0.3 $\mathrm{kg/m^3}$ for Wonji, Dodota, and Ulaga, and 0.4±0.2 $\mathrm{kg/m^3}$ for the 5-year average in Welenchiti. The study concluded that intensification at Wonji by closing the biomass gap can increase production up to 243,008 tons/year, separately for Welenchiti an increase of 13,570 tons/year. However, this would come at an increase in water consumption (ETa) of 23.09 Mm^3/year and 1.03 Mm^3/year, respectively. The total productivity gap in Wonji Main is estimated at 185,520 tons/year, making up for the largest portion of the gap. This study argues that there is a distinct room for improving WPb values in furrow-irrigated areas without actually increasing overall water consumption (ETa). The extent of this 'room for improvement' needs to be determined further. Remote sensing data can be used to evaluate the performance of different areas with different irrigation methods, the spatial variation of water and land productivity, and irrigation performance indicators.

3 MATERIALS AND METHODS

This section describes the methodology used to answer the research question. First, the research area is introduced and the approach is thoroughly explained.

3.1 Description of the Study Area

3.1.1 Location

The Wonji-Shoa Sugar Factory and surrounding sugarcane farming areas are located in the Oromia Region, approximately 80 km southeast of Addis Ababa, and close to the city of Adama (Figure 3.1). The farm lies between the longitudes of 39.21° and 39.40° and the latitudes of 8.33° and 8.62°. The estate is located between altitudes of 1223 and 1553 m above sea level. Sugarcane is the primary crop cultivated in the" Wonji schemes. This study examines sugarcane irrigation schemes, including those managed by growers who farm sugarcane.

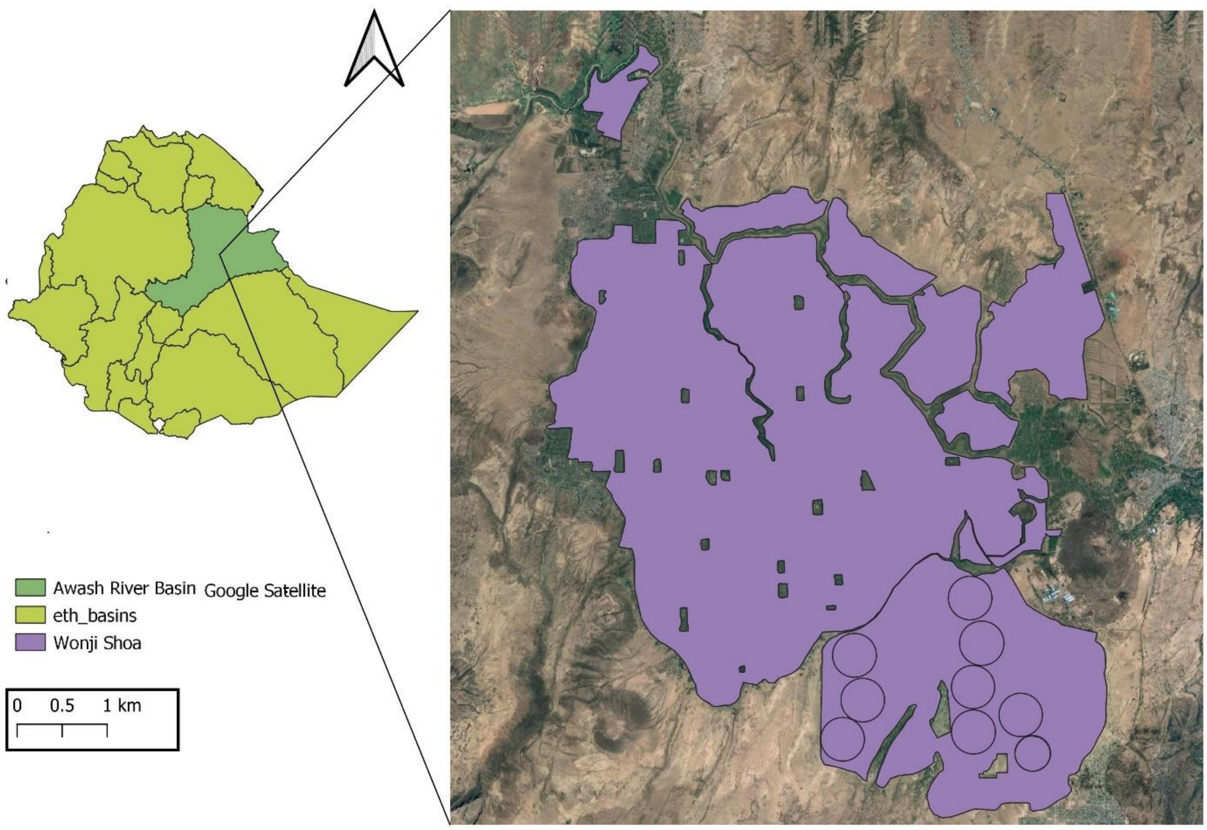

Figure 3.1 Location of Wonji Shoa Irrigation Schemes.

3.1.2 Climate

Rainfall in Wonji is sparse, and with low humidity during the hot and dry seasons, the water demand is high. The short rainy season from March to May leads to the main rainy season that lasts from mid-June to mid-September. Most of the rain was recorded in July and August, whereas the lowest occurred in October and November. The mean annual relative humidity varied between 43.2% and 68.4%. Wonji has a tropical wet climate, characterized by consistent warmth throughout the year. It experiences an average annual rainfall of 831.2 mm and experiences a semi-arid climate, mean annual maximum and minimum temperatures of 27.6°C and 15.2°C respectively, and an average of 9 hours of sunshine during the dry summer and 6.5 hours in August (Girma & Seleshi, 2007a).

3.1.3 Soils

At Wonji Shoa, there are five soil management groups: A1, A2, BA2, B1.4, and C1 (FAO 1998). A1, A2, and BA2 were categorized as heavy black soils, whereas B14 and C1 were classified as light brown soils (Ruffeis et al. 2008). The A1 soil group represents well-drained, deep, and fertile soils that are rich in organic matter, making them suitable for diverse cropping systems. Minimal application of fertilizers and amendments is required to maintain crop growth, and common management practices include crop rotation, cover cropping, and minimum tillage (FAO 2001). A2 soils are similar in drainage and depth, but have moderate fertility levels because of their lower organic matter content. Strategies to maintain crop productivity in these soils include applying organic and inorganic fertilizers and green manure, maintaining a balanced pH, and using crop rotation, minimum tillage, and conservation agriculture practices. BA2 soils have medium to low fertility levels, often facing issues with soil structure, whereas B1.4 soils have poor fertility levels, varying drainage conditions, and possible root development restrictions from soil crusts or compaction layers. Both soil types require management practices aimed at improving soil health, such as adding organic matter, enabling proper nutrient management, and ensuring balanced fertilization (Gonzalez-Rodriguez & Fernandez-Marcos, 2018). C1 soils are poorly drained, have low fertility levels, and are shallow, often resulting in suboptimal crop production potentials. Managing these soils may involve surface drainage, raised beds, and incorporation of organic matter to improve structural properties and waterlogging resistance. Additionally, soil fertility management techniques, such as precision fertilization and integrating leguminous crops into rotation patterns, can help replenish nutrients and improve productivity (FAO, 2001).

3.1.4 Irrigation application methods at Wonji Shoa

Surface irrigation was used to produce Wonji's first regular sugarcane crop in 1954 (Girma and Seleshi, 2007b). Wonji Main, the earliest section of the irrigation system, was created by the Dutch business HVA and is still in operation today. To produce sugarcane utilizing irrigation techniques different from those used at Wonji Main, new out-grower schemes were constructed at Wonji Estate beginning in 2009 (Table 3.1). The recently established sub-schemes include Dodota (featuring center pivots and sprinkler irrigation), Wake Tio expansion (using sprinkler irrigation), Kuriftu, Boku, Adulala, Bishola, Hargitti, WakeMia, and WakeTio (employing furrow irrigation). Table 3.1 provides a summary of each subscheme area, year of establishment, primary crop, irrigation method, and ownership.

Table 3.1 Characteristics of Wonji Shoa Irrigation Scheme.

Sub-schemes	Establishment	Area-ha	Main crop	Irrigation type	Owner
Estate proper	1954	6546.567	Sugarcane	Furrow	Estate proper
Kuriftu	1975	148.824	Sugarcane	Furrow	Out growers
Boku	1975	209.462	Sugarcane	Furrow	Out growers
Adulala	1975	227.800	Sugarcane	Furrow	Out growers
Wake Mia	1975	333.673	Sugarcane	Furrow	Out growers
Wake Tio	2008-2009	154.751	Sugarcane	Furrow	Out growers
WakeTio expansion	2008-2009	666.574	Sugarcane	Sprinkler	Out growers
Hargitti	1975	37.733	Sugarcane	Furrow	Out growers
Bishola	1975	61.091	Sugarcane	Furrow	Out growers
Dodota	2008-2009	2,600	Sugarcane	Centre pivot and Sprinkler	Out growers

Figure 3.2 demonstrate the irrigation methods at Wonji Shoa. The sugarcane schemes analyzed in Wonji have three different irrigation methods. Surface (furrow), Centre Pivot, and Sprinkler. Every scheme has a single specific irrigation method, except for Dodota, where both sprinkler irrigation and center pivot irrigation are applied.

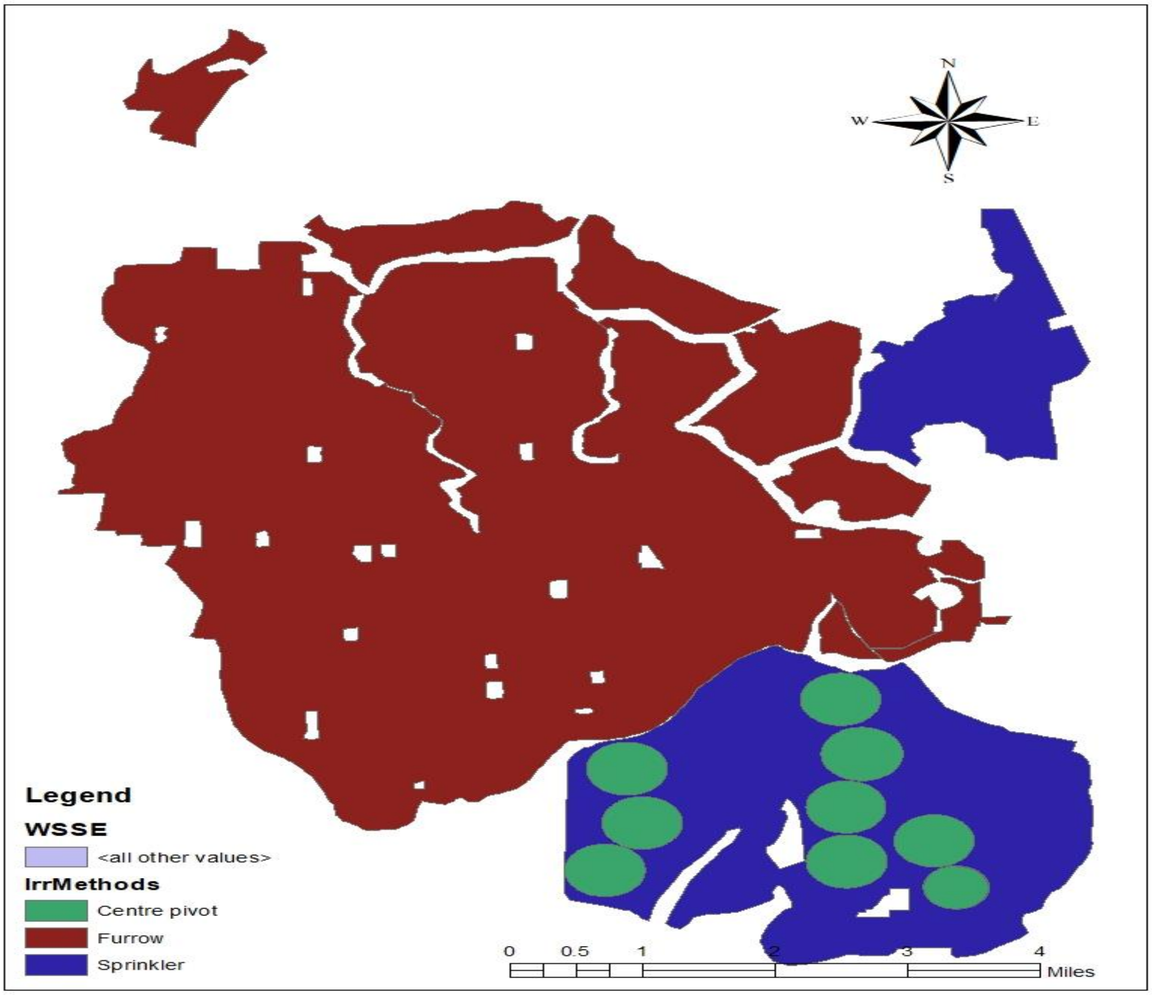

Figure 3.2 Irrigation methods at Wonji Shoa Sugarcane Farm.

3.2 Methodology and Data

In this study, the methodology used is based on the approach established in the waterPIP project, as detailed in (Chukalla et al., 2020a). The research also employs the standard protocol developed by the waterPIP project (Chukalla et al. 2020b). This protocol, specifically designed for land and water productivity analysis using WaPOR datasets and Python Jupyter notebooks, is adapted for biophysical water productivity concerning consumed water use and land productivity at an area (fields & schemes) within a similar agroclimatic zone.

The protocol applies to single water management units and crop production irrespective of the water source (rainfed, irrigation via surface water and/or groundwater, or flood/spate). The protocol is intended for agricultural areas with a single crop and consistent cropping season that may vary between years. To implement the protocol beyond fields or scheme levels, such as at river basin or country levels, which may fall into different agroclimatic zones, climate variation normalization is necessary, but such is not within the scope of the protocol (Chukalla et al., 2021).

The Standardized protocol for land and water productivity analyses using WaPOR is aimed at guiding users to understand the different layers contained in the WaPOR portal which can be used for land and water productivity analyses. The program uses Python scripts for processing and calculating land and water productivity and other performance indicators (Chukalla et al., 2020a). The protocol has six modules (Figure 3.3). A Jupyter notebook containing Python scripts was developed for each module. Module 0 is responsible for downloading WaPOR data related to actual water consumption (ET), actual transpiration, reference evapotranspiration, precipitation, land cover classification, and net primary production. Module 1 involves pre-processing the data to ensure consistent spatial resolution and the removal of non-crop pixels. In Module 2, seasonal water consumption (transpiration, actual evapotranspiration, reference evapotranspiration, and potential evapotranspiration) and seasonal net primary production are calculated. Module 3 focuses on determining different performance indicators. Module 4 computes land and water productivity. Lastly, Module 5 calculates bright spots and productivity gaps (Chukalla et al., 2021).

In this chapter, the approach is presented by first providing a general overview of the data and performance assessment framework used. This study utilized remotely sensed data acquired from FAO Water Productivity through Open access Remotely sensed derived data (WaPOR), which provide spatially and temporally explicit datasets from 2009 to the present. Additionally, ground-level measured data on planting and harvesting dates, as well as sugarcane production per field, were provided by stakeholders. Long-term data on cane and white sugar production were sourced from agricultural data record offices from Wonji Shoa Factory. The data were resampled and aggregated, with analyses conducted at 30 m spatial resolutions, using a seasonal time step of one year.

Performance indicators for productivity and irrigation are used to measure the efficient use of resources and evaluate the quality of irrigation services. In the Wonji Shoa sugarcane farm study, a performance assessment framework is used to evaluate water and land usage and overall irrigation performance. The framework comprises four key stages: First, data on actual water consumption, actual transpiration, reference evapotranspiration, and net primary production are gathered from the FAO Water Productivity through Open access Remotely sensed derived data (WaPOR) and pre-processed to match the spatial resolution while excluding non-crop pixels. Second, seasonal water consumption (including transpiration, actual evapotranspiration, and reference evapotranspiration), as well as seasonal net primary production and biomass, were calculated. Third, the consistency of the WaPOR data is evaluated, following known relationships between biomass (B) vs ETa, and B vs Ta (de Wit, 1958; Steduto et al., 2007) for the entire project area. Fourth, the irrigation performance indicators were examined. Finally, the potential of closing productivity gaps in production is investigated.

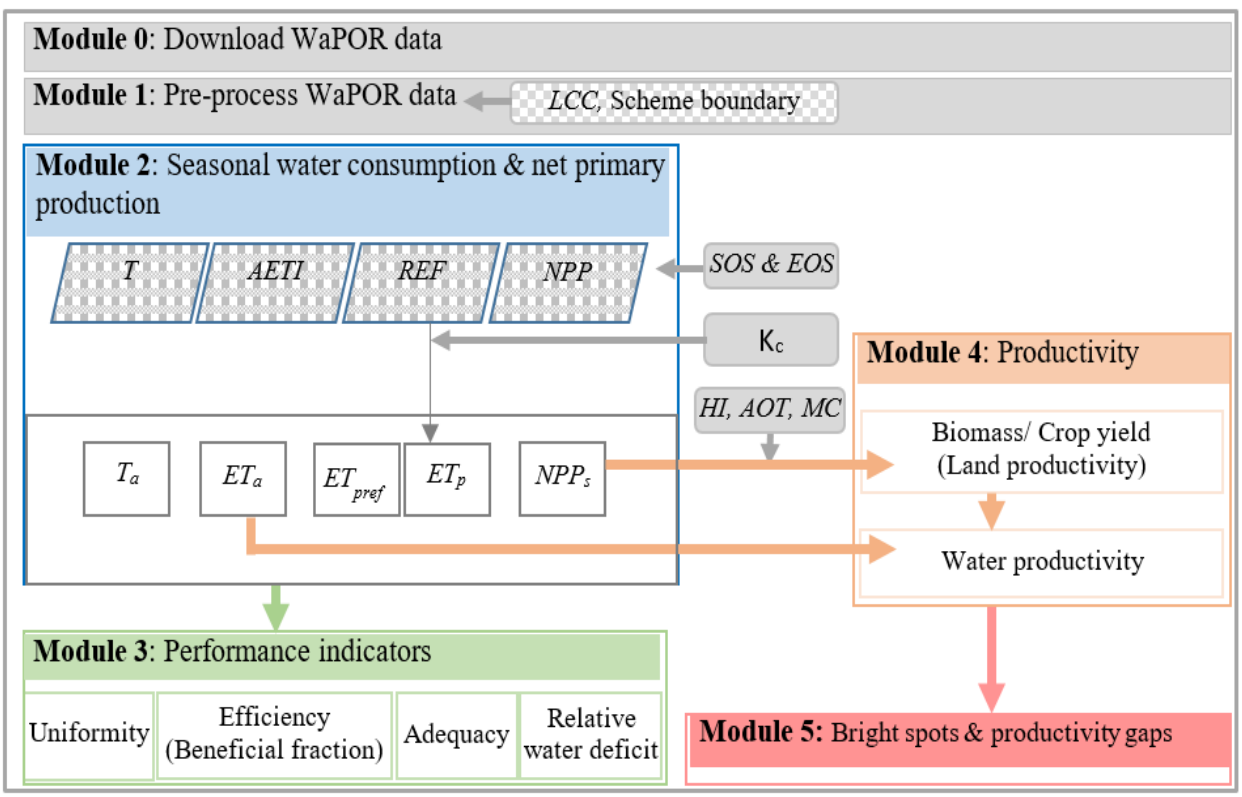

Figure 3.3 Schematic representation of WaPOR-based Irrigation performance assessment framework (Chukalla et al., 2020).

3.3 WaPOR Data

The Water Productivity Open Access Portal, provided by the Food and Agriculture Organization (FAO, 2020a), is an extensive dataset for sub-Saharan Africa, the Middle East, and North Africa regions. It encompasses information on water usage (including actual evaporation, transpiration, and interception), net primary production, land usage (featuring land-cover classification), phenology, climatic factors (such as precipitation and reference evapotranspiration), and water productivity layers. It covers the period from 2009 to the present day and is updated in near real-time. WaPOR datasets are available at various scales, including continental level (Level 1 at 250 m), country and river basin (Level 2 at 100 m), and project level (Level 3 at 30 m). The latest WaPOR portal (WaPOR v2.1), was improved from WaPOR v1.0 following the quality assessment by IHE Delft and ITC (Mul & Bastiaanssen, 2019). The methodology used for compiling the WaPOR database is provided in FAO (FAO, 2020).

WaPOR Level 3 (30m) data are accessible for Awash, making it applicable to our case study area as well. The Level 3 dataset comprises actual evapotranspiration and interception (AETI), net primary production (NPP), and actual transpiration (Ta) at a 10-day (dekadal) timescale, and Level 2 yearly land cover classification (LCC). Additionally, 5 km resolution dekadal precipitation (PCP) and 25 km resolution dekadal reference evapotranspiration (RET) datasets were downscaled to 30m resolution. Figure 3.4 shows locating the study area in the FAO open accesses WaPOR portal to download datasets. A summary of the WaPOR data utilized in this study can be found in Table 3.2.

Table 3.2 WaPOR layers used in the analyses.

Remote sensing products	**Description/Spatial Resolution**	**Temporal resolution (coverage)**
Actual evapotranspiration (ETa)	30 m	Dekadal (2009-2022)
Actual transpiration (Ta)	30 m	
Net primary production (NPP)	30 m	
Precipitation (P)	5 km	
Reference evapotranspiration (RET)	25 km	
Land cover classification (LCC)	100 m	Annual (2009-2022)

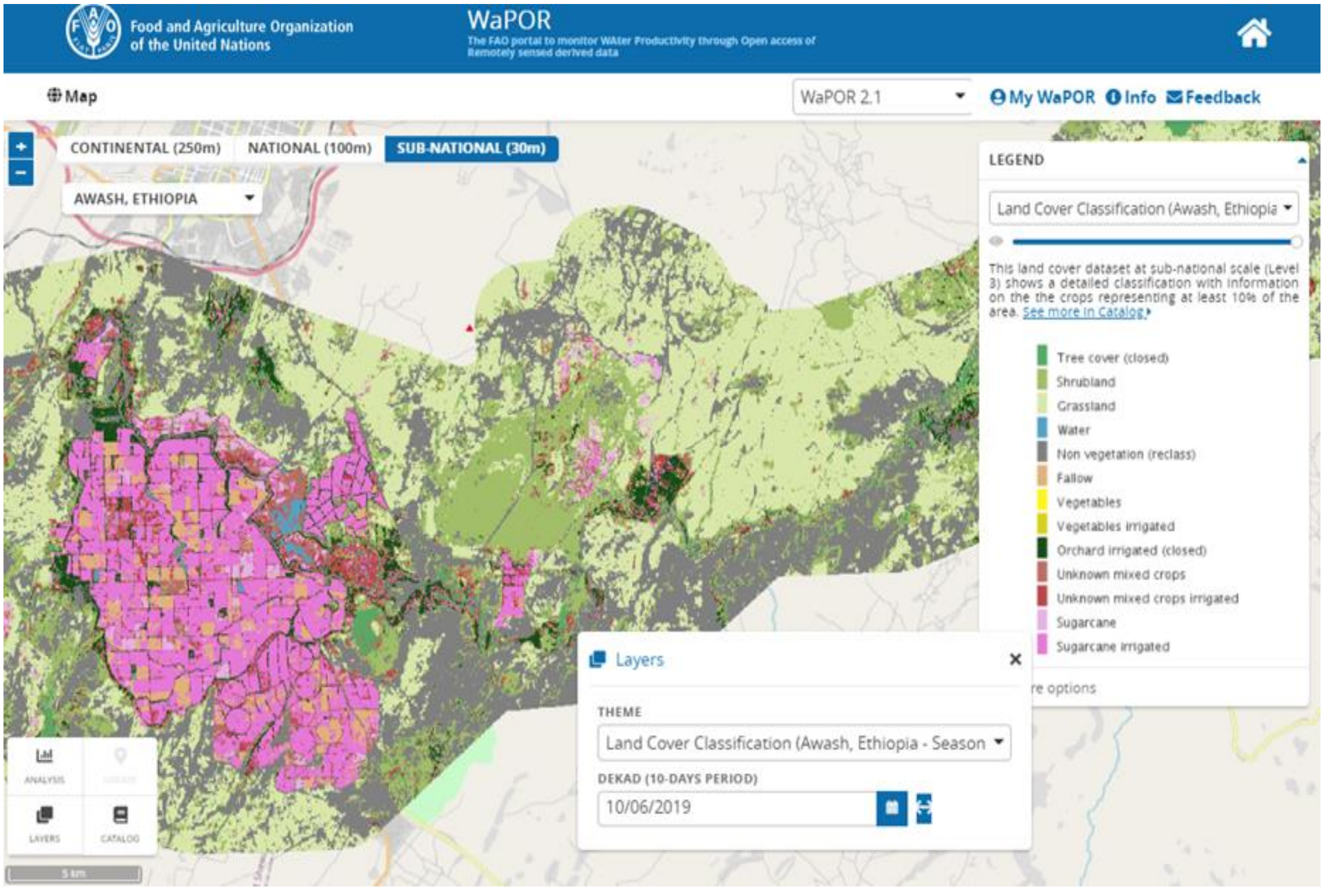

Figure 3.4 Locating the study area in the WaPOR portal to download datasets.

In the standard protocol, the WaPOR data is downloaded under Module-0.In this module, WaPOR data needed for the Water Productivity assessment is downloaded in bulk and corrected to the right unit which follows these steps:

- Step 0a - Import modules/libraries
- Step 0b - Read the geographical extent of the study area
- Step 0c: Bulk-download WaPOR data for the study area.

3.3.1 Preprocessing WaPOR data

Once the WaPOR data has been downloaded in bulk, it needs to be prepared and preprocessed for further analysis. The data preparation process involves several steps, including resampling raster data and filtering non-cropped areas. In the initial stage, selecting the research area from the bulk data. Following that, reference evapotranspiration and precipitation were processed and resampled to a level 3 (30 m) resolution. Finally, filtering out non-cropped areas using a land cover map and the project boundary. This data preparation process ensures that the WaPOR data is ready for subsequent analyses and applications. In the standard protocol, WaPOR data preparation was executed using Module 1. In this module, resampling and masking are undertaken as part of preparing the data for further analyses by following steps:

- Step 1a -Import modules/libraries.
- Step 1b-Resampling raster data (RET and PCP) and save to the output folder 1_WAPOR.v2_dekadal_L1_RET_D_resampled&1_WAPOR.v2_dekadal_L1_PCP_D_resampled respectively.
- Step 1c - Filter the non-cropped area.

3.4 Seasonal Water Consumption and Crop Yield

3.4.1 Growing season

To keep the sugar plant running, the sugarcane estate employs a ratooning process and harvests throughout the year. As a result, each agricultural unit has different start and finish seasons. We used the average yearly biomass output for the period 2009-2022 from July 1 to June 30 for the analysis, because we lacked specific information on the beginning and end of the season for each plot. The inter-annual usage of both land and water resources (i.e., production per unit of land and unit of water utilized) can be compared using a hypothetical annual season. Table 3.4 shows the cropping season at Wonji Shoa irrigation schemes from July-1/2009 to June-30/2022. This study covers 13 growing seasons: season 1(2009/2010) to season 13 (2021/2022)

Table 3.3 Cropping season from July-1/2009 to June-30/ 2022 of Wonji Shoa irrigation schemes.

Seasons	Start of the season (SOS)	End of the season (EOS)
1	2009-07-01	2010-06-30
2	2010-07-01	2011-06-30
3	2011-07-01	2012-06-30
4	2012-07-01	2013-06-30
5	2013-07-01	2014-06-30
6	2014-07-01	2015-06-30
7	2015-07-01	2016-06-30
8	2016-07-01	2017-06-30
9	2017-07-01	2018-06-30
10	2018-07-01	2019-06-30
11	2019-07-01	2020-06-30
12	2020-07-01	2021-06-30
13	2021-07-01	2022-06-30

3.4.2 Calculating seasonal actual water consumption

Total soil evaporation, canopy transpiration, and interception are referred to as evapotranspiration. Seasonal actual evapotranspiration is analyzed from the dekadal WaPOR data by aggregating the seasonal values using Equation 3.1 as shown below.

$$ET_{a,s} = \sum_{SOS}^{EOS} ETa \tag{3.1}$$

Where, ET_a is the actual evapotranspiration that includes evapotranspiration and interception, $ET_{a,s}$ is seasonal actual evapotranspiration in mm/season, SOS and EOS are starting and ending of the crop season.

In WaPOR, evaporation, and transpiration calculations are based on the ETLook model, as described by Bastiaanssen et al. (2012). This model adapts the Penman-Monteith (P-M) equation to remote sensing input data for evaporation and transpiration separately. The differences in the P-M equation for evaporation and transpiration lie in the inputs used to estimate net available radiation, aerodynamic resistance, and surface resistance. For evaporation, the P-M equation utilizes soil heat flux, aerodynamic resistance, and surface resistance at the soil surface, with soil moisture availability influencing these factors. On the other hand, for transpiration, the P-M equation uses aerodynamic and surface resistance at the canopy as influenced by soil moisture availability. Interception is the process of rainfall being intercepted by a plant's canopy and evaporating directly from the leaves and is accounted for by considering the energy not available for transpiration.

3.4.3 Calculating biomass production

The calculation of biomass production is based on the seasonal net primary production (NPP) provided by WaPOR. There are four steps involved in converting NPP to biomass. First, since sugarcane is a C4 crop with a light use efficiency (LUE) of 3.27 MJ/gr biomass, its seasonal NPP needs to be adjusted. This is because WaPOR estimates NPP using a generic LUE of 2.7 MJ/gr biomass for rainfed and irrigated crops under non-stressed growing conditions. To make this adjustment, a light use efficiency correction factor (fc) is applied, which is the ratio of sugarcane's light use efficiency to the light use efficiency used to derive the NPP layer. This factor is set at 1.6, as per (Villalobos & Fereres, 2016a). Secondly, the seasonal NPP of sugarcane is transformed into dry biomass production by multiplying NPP by 22.222. This converts the NPP in gC/m²/day to kg dry biomass/ha/day (FAO, 2020). Thirdly, the total biomass is calculated by adjusting the dry biomass production for the moisture content in the crop (MC). Finally, the above-ground biomass (B) is determined by multiplying the total biomass by the above-ground to total biomass production ratio (AOT) (Equation 3.2).

$$B = AOT \times f_c \times \frac{NPP * 22.222}{(1-m_c)} \tag{3.2}$$

Where, m_c is the moisture content of the fresh biomass, f_c is the light use efficiency (LUE) correction factor, B is the above-ground biomass and AOT is the ratio of the above-ground over total biomass, and NPP is the net primary production.

Due to the lack of field data, literature was utilized as a resource to approximate the mentioned crop parameters. The values and their sources are displayed in Table 3.5 and Table 3.6. To calculate the sugarcane yield, the biomass is multiplied by a harvest index of 1, which is considered a default value as reported by the WaPOR portal (FAO, 2020) (Equation 3.3).

$$Yield = B \times HI \tag{3.3}$$

Table 3.4 Parameters (m_c, fc, AOT, and HI) used in the analyses.

Parameter	Description	Value	Source
MC	Moisture content of fresh crop biomass	59%	Mul and Bastiaanssen. (2019); Yilma. (2017)
fc	Light use efficiency correction factor	1.6	Villalobos and Fereres (2016)
AOT	The ratio of above-ground over total biomass (AOT)	0.8	Smith et al. (2005); Villalobos and Fereres (2016)
HI	Harvest index	1	FAO, (2020a)

The WaPOR NPP statistics are the primary cause of fluctuation in biomass production. The NPP is adjusted for stresses brought on by water, nutrients, pests, and diseases, as stated by Chukalla et al. (2020b), and additional variation may be due to spatial and temporal gap-filling.

In the standard protocol, the computation of seasonal water consumption and net primary production is executed under Module 2 by following steps:

- Step 2a Set up: Import modules/libraries
- Step 2b Defining function and crop season
- Step 2c Calculate seasonal T, ET, RET, ETp, NPP

3.4.4 WaPOR consistency check

Biomass production is known to have a linear relationship with transpiration (de Wit, 1958; Steduto & Albrizio, 2005). The slope of the linear line accounts for the effect of crop variety and soil fertility (Steduto et al., 2007). The biomass was also plotted against two seasonal water consumption variables: actual evapotranspiration and transpiration for the Wonji sugarcane estate. A linear relationship between biomass and water consumption would indicate consistency between the two independently generated datasets.

3.5 Performance Assessment Indicators

Indicators of productivity and irrigation performance provide a means to evaluate resource utilization efficiency and examine an irrigation system. This study utilized the same indicators mentioned in Chukalla et al. (2022a), which include water consumption, equity, beneficial fraction, adequacy, land and water productivity, and productivity gaps. The descriptions and techniques for each indicator presented below are also based on Chukalla et al. (2020a). In the standard protocol the performance indicators scripts are executed under Module 3 by following steps:

- Step 3a - Set up: Import modules/libraries, import data, create output folder
- Step 3b - Calculate uniformity
- Step 3c - Calculate efficiency (beneficial fraction)
- Step 3d - Calculate adequacy
- Step 3e - Calculate the relative water deficit

3.5.1 Water consumption

In this study, seasonal evapotranspiration and seasonal transpiration (beneficial consumption) were considered as the primary indicators for water consumption. Water consumption is defined as the depletion of water from the root zone through the processes of transpiration by crops and direct evaporation from the soil.

3.5.2 Uniformity

The coefficient of variation (CV) of the seasonal actual evapotranspiration, which is equal to the SD divided by the mean (Bastiaanssen et al., 1996; Chukalla et al., 2021) is used to quantify uniformity [%] as a measure of evenness of water supply in the irrigation scheme. There were three levels of uniformity: good, fair, and poor. A CV between 0 and 10% was seen as having high uniformity, between 10% and 25% as having acceptable uniformity, and over 25% as having poor uniformity.

3.5.3 Beneficial fraction (Efficiency)

Beneficial fraction is the ratio of the water that is consumed as transpiration compared to overall field water consumption (ETa). It is a measure of the efficiency of on-farm water and agronomic practices in the use of water for crop growth (Equation 3.4).

$$\text{Beneficial fraction} = \frac{T}{ETa} \tag{3.4}$$

Where T is transpiration and ETa is actual evapotranspiration.

3.5.4 Adequacy

Adequacy (A) is defined as the extent to which the available water in an irrigation system aligns with the water requirements of the crops (Bastiaanssen & Bos, 1999; Clemmens & Molden, 2007). It is calculated by dividing the actual crop evapotranspiration ($ETact$) (mm/season) by the crop water requirement (ETc) (mm/season) (Equation 3.5).

$$A = ET_{act} \ / \ ET_c \tag{3.5}$$

Where A is adequacy, ET_{act} is actual evapotranspiration (mm/season), and ET_c is crop water requirement (mm/season).

Good performance is defined within the range of 0.8 < A ≤ 1, while acceptable performance falls within the range of 0.68 < A ≤ 0.8, and poor performance is characterized by A ≤ 0.68 (Karimi et al., 2019).

The crop water requirement was calculated by multiplying the $ETref$ [mm/season] with the crop coefficient (Kc) (Equation 3.6).

$$ET_c = ET_{ref} \times K_c \tag{3.6}$$

Where ETc is crop water requirement, Kc is cropping coefficient, and ETref is reference evapotranspiration.

The Kc value signifies the features of a crop throughout its growth period, considering the average impact of soil evaporation (FAO, 1998). According to research conducted by Yadeta et al. (2020), the Kc values for sugarcane in Ethiopia show a slight variation when compared to the values recommended by the FAO (refer to Table 3.7). Considering the varying growing and harvesting periods for each farmer's field in Wonji Shoa, utilizing a consistent set of growth stages and their associated Kc values for the entire research area would result in inaccurate ETc estimations. Consequently, this study adopted an average Kc value, which factored in the length of each growing stage while computing the mean.

Table 3.5 Kc values throughout the various stages in a growing season as provided by the FAO and from literature, and the length of the growing stages in days.

	FAO kc	**Yadeta et al. (2020) Kc**	**Length of stage [days]**
Initial Season	0.4	0.42	35
Developing Season	0.83	0.93	60
Mid-Season	1.25	1.26	190
Late Season	0.75	1.05	120
Mean	**0,966**	**1,076**	

3.5.5 Productivity

A measure of productivity is the amount of value produced for each unit of resource utilized. The benefit could be biophysical, economic, or social, and the resource base may be used or given in the form of water or cropland (Bastiaanssen & Steduto, 2017; Hellegers et al., 2009; Karimi et al., 2011; Mutiro et al., 2006; Zwart & Bastiaanssen, 2004). In cases where socioeconomic indicators are not available, studies may concentrate on the biophysical production per unit of land or water resources, which is known as land and water productivity.

Land productivity is defined as the above-ground biomass production or yield in ton/ha/season, which is estimated from the seasonal net primary production (NPP). Crop yield can be estimated by multiplying the land productivity by the harvest index (Equation 3.7).

$$Crop\ yield = B \times H_i \tag{3.7}$$

Biomass and crop water productivity are estimated as the ratio of above-ground biomass or yield over actual evapotranspiration (Equation 3.8):

$$WP_b = \frac{B}{ET_a} \tag{3.8}$$

To obtain WPb in $\mathrm{kg/m^3}$ B in kg/ha/season has to be converted to $\mathrm{kg/m^2/season}$ and ETa in mm/season has to be converted to m/season. It is important to note that this measure of water productivity includes consumed green water (from rainfall) and blue water (from irrigation).

In the standard protocols the productivity scripts are executed under Module 4 on Jupyter Notebook by following steps;

- Step 4a - Set up
- Step 4b - Calculate land productivity: i) biomass and ii) crop yield
- Step 4c - Calculate productivity: i) biomass water productivity and ii) crop water productivity.

3.6 Productivity Gaps

The productivity gaps of land and water provide insights into a field's performance by comparing it to the surrounding area, using a productivity target as the benchmark. The method outlined in this section draws from the research conducted by Chukalla et al. (2020a).

3.6.1 Productivity target

Productivity targets encompass the achievable goals related to biomass and water productivity within a specific agro-climatic zone, considering the varying crop distributions and productivity levels. These targets are essential in gauging productivity disparities and forecasting production improvements, leading to more efficient utilization of land and water resources. While WPb, or water productivity based on biomass, is a relatively stable crop parameter under ideal circumstances across different climates and growing conditions (de Wit, 1958; Steduto et al., 2007), it has been observed to fluctuate when subjected to varying nutrient stress levels (Steduto & Albrizio, 2005).

Biomass (B) and water productivity (WPb) targets, also known as attainable productivities, are determined by applying upper percentiles to the distribution of biomass and productivity values of a specific crop in a particular season and agro-climatic zone. Licker et al. (2010) define the upper percentile for estimating attainable yield within regions of similar climate at the 90th percentile, while Foley et al. (2011) put it at the 95th percentile. Regarding crop water productivity, Zwart & Bastiaanssen (2004) and Zwart et al. (2010) use the 95th percentile to exclude extremes from the productivity distribution of global data.

In this study, we estimate attainable B and WPb of sugarcane at Wonji Shoa for a given year at the 90th percentile of the respective productivity distributions, as shown by the vertical and horizontal dashed grey lines in Figure 3.5 We choose a value from the observed dataset of a similar agro-climatic zone rather than a global target or climate-limited potential because it takes into account the current technology, management techniques, and climatic conditions in the area (and for each season). The upper 10th percentile is used to include highly productive spots resulting from favorable soil and management conditions (Lobell et al., 2002), although their productivity level may not be realistically achievable across all areas. Some may argue that the upper 10th percentile also contains outliers whose productivity is recorded due to noise.

3.6.2 Identifying bright spot

Bright spots are fields that have B and WPb greater than or equal to the target values (Blatchford et al., 2018). The bright spots in Wonji Shoa sugarcane state are identified by tracking the pixels that have both B and WPb equal or greater than the targets for the 13 seasons. Thus, this study employed the 90th percentile threshold for both yield (B) and water Productivity (WP) to categorize areas as bright spots, while fields falling below the 10th percentile were classified as hot spots. Figure 3.5 shows the schematic representation of the productivity target, and disentangled WPb gaps and biomass gaps for a crop plot compared to target productivities. The arrow indicates the path to be followed in closing the productivity gaps in plot A; it links productivity in plot A to the target productivity in plot T. The grey vertical and horizontal dashed lines represent the 90th percentiles of B and WPb, respectively, dividing the plot into four quadrants (Chukalla et al., 2021).

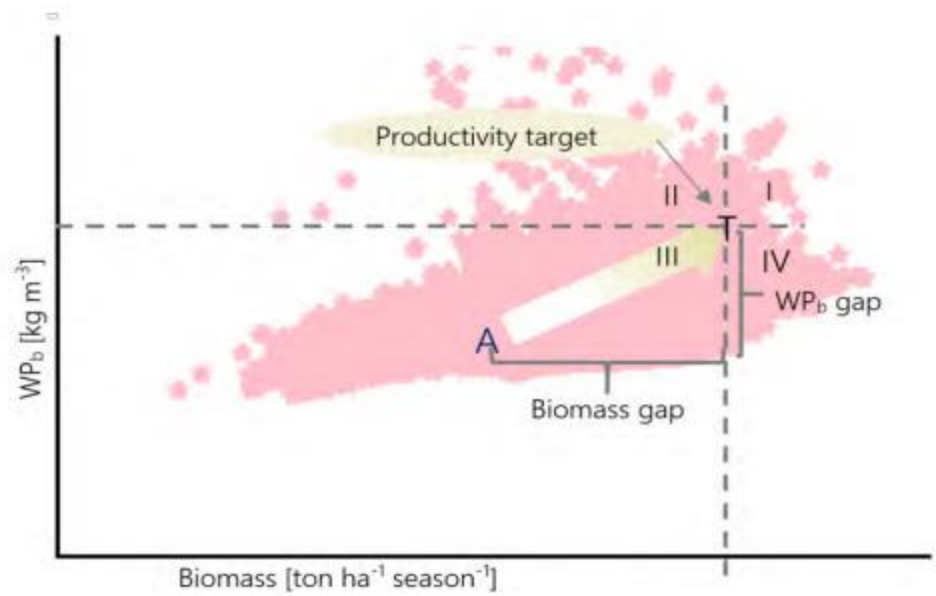

Figure 3.5 Scatter plot that illustrates the Biomass against the water productivity.

3.6.3 Productivity and production gap

The productivity gap is a metric used to evaluate the performance of a specific field by comparing its productivity level to a target value in a particular area. This gap provides insights into how well a field is performing relative to the desired productivity level. To calculate the productivity gap in a given area (Figure 3.5), the productivity value at a specific point (pixel A) from the productivity value at the target point (pixel T) was subtracted. The productivity gap has been broken down into two components: the water productivity gap (vertical) and the land productivity gap (horizontal). These gaps represent the specific differences in productivity levels related to water use and land use, respectively. By analyzing both gaps, the factors contributing to the overall productivity gap and potential areas for improvement were identified.

Referring to the WPb vs B graph (Figure 3.5) and its productivity targets, along with the two 90th percentile target lines, crop plots (represented as pixels) were divided into four distinct sections. I) B > B target and WPb > WPb target, II) B <B target and WPb > WPb target, III) B < B target and WPb < WPb target, and IV) B > B target and WPb < WPb target (Chukalla et al., 2020a). Pixels in the first quadrant (I) exhibit higher B and WPb values, exceeding the target productivity levels. These plots serve as prime examples for identifying bright spots and learning effective practices. On the other hand, the other three quadrants consist of pixels that hold the potential for narrowing the gaps in WPb and B, thus providing opportunities for improvement.

The total production gap, measured in tons, is calculated by adding the land productivity gaps from Quadrants II and III, across the irrigated area as per Equation 3.9. It is important to note that areas where B meets or surpasses its respective target value are excluded from this calculation.

$$B\ gaps\ = \sum_{i}^{n}\ \ (B_i\text{-}B_t)\ \ B_i < B_t$$

$$= 0 \text{ if } \ \ B_i \geq B_t \tag{3.9}$$

Where, B_i and B_t are the biomass of a pixel i and the target biomass in ton/ha/season. The WPb gaps are calculated similarly. Then after appropriate solution will be implemented to close the production and productivity gaps. In the standard protocol, the target productivity and productivity gaps scripts are executed under module-5 by following steps;

- Step 5a - Set up
- Step 5b - Calculate the target productivity
- Step 5c - Identify bright spots
- Step 5d - calculate productivity gaps

3.7 Zonal statistics

Zonal statistics is a method used to summarize the values of a raster dataset (a grid of cells, or pixels-based values) for each feature in a vector dataset (e.g., the 19 zones based on the IDs 1 to 19 of WSSE. It was used to calculate statistics such as the mean, minimum, maximum, and standard deviation of the raster values within each vector feature (IDs based on zones of WSSE).

4 RESULTS AND DISCUSSION

This section describes the results of the spatiotemporal variability in land and water productivity irrigation scheme performance indicators. The maps show the average annual values for the period 2009-2022, and the results for the separate years can be found in Appendix A.3-11. When observing the spatial data, it should be noted that the growing season of one year is hypothetical.

4.1 Consistency of WaPOR Data

The WaPOR consistency serves to demonstrate whether there is a clear and consistent initial outcome for the WaPOR data in Wonji Shoa throughout the entire 2009-2022 period. Figure 4.1 and 4.2 show the average annual biomass plotted against water consumption variables: transpiration, and actual evapotranspiration for the Wonji Sugar Estate area with level 3 data in 2021/22. Figures for the other years are provided in Appendix A.1 and Appendix A.2. Figure 4.1 shows a stronger correlation for B vs T, compared to B vs ETa, the slope is steeper, and the values R^2 are higher for B vs T, which is as expected. Figure 4.1 and 4.2 show a consistent and good correlation between average annual biomass and the different water consumption variable for the Wonji Shoa dataset in the period 2021/22. Therefore, in this analysis, the WaPOR data will be used for the complete period of interest for the different layers during the period 2009-2022.

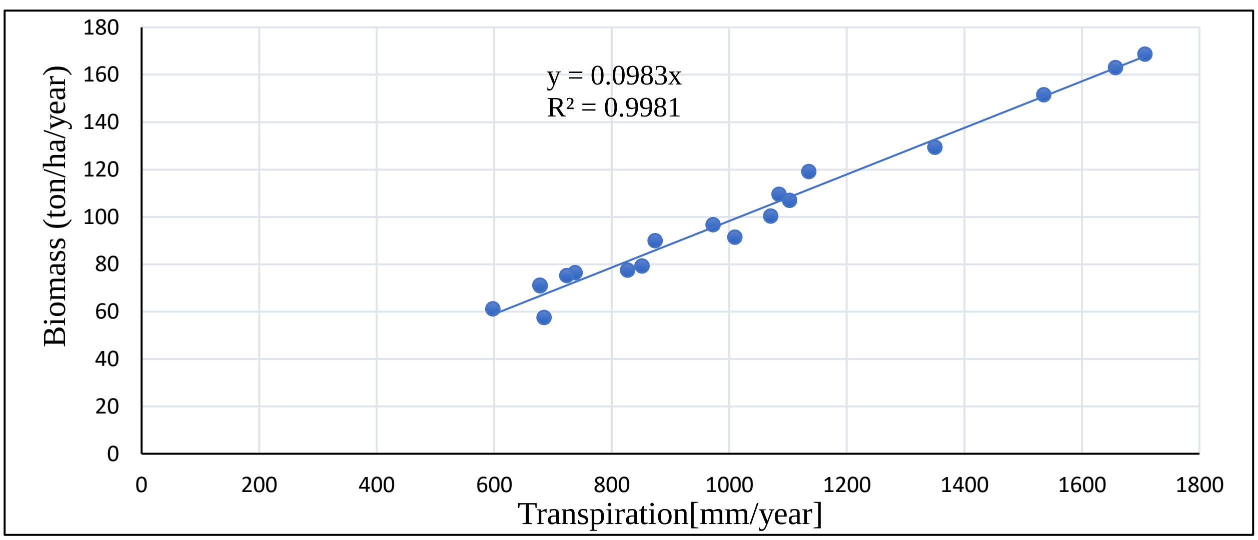

Figure 4.1 The relationship between biomass and transpiration for the Wonji Sugar estate during the period 2021-2022.

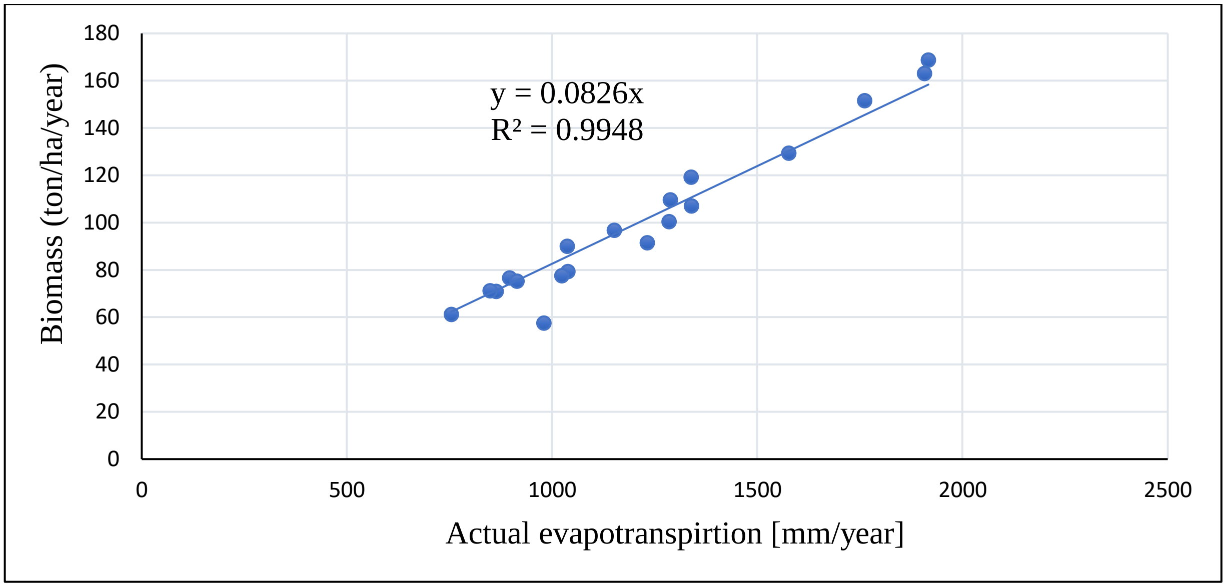

Figure 4.2 The relationship between biomass and actual evapotranspiration for the Wonji sugarcane estate during the period 2021-2022.

Table 4.1 shows the slope, intercept and R^2 for the linear regression lines during the period 2009-2022. The biomass production is directly related to the transpiration therefore, the linear regression line is forced through the origin. The relationship between the biomass and the ETa does not necessarily pass through the origin, the intercept can be attributed to non-beneficial evaporation, such as interception or soil evaporation. In this study, the linear regression line is also forced through the origin of the relationship between biomass and ETa.

Table 4.1 Linear regression parameters for the relationship between biomass Vs Ta, biomass Vs ET_a for the period 2009 to 2022.

R/ship	Regression parameter	Seasonal year						
		2009	2010	2011	2012	2013	2014	2015
B Vs Ta	Slope	0.111	0.107	0.096	0.111	0.109	0.103	0.100
	Intercept	0	0	0	0	0	0	0
	R^2	0.998	0.998	0.998	0.994	0.999	0.999	0.999
B Vs ETa	Slope	0.092	0.09	0.078	0.092	0.096	0.088	0.087
	Intercept	0	0	0	0	0	0	0
	R^2	0.986	0.993	0.995	0.998	0.999	0.999	0.998
		2016	2017	2018	2019	2020	2021	2022
B Vs Ta	Slope	0.096	0.104	0.095	0.111	0.085	0.098	0.998
	Intercept	0	0	0	0	0	0	0
	R^2	0.998	0.997	0.995	0.998	0.990	0.998	0.998
B Vs ETa	Slope	0.080	0.081	0.089	0.096	0.085	0.082	0.083
	Intercept	0	0	0	0	0	0	0
	R^2	0.998	0.992	0.992	0.993	0.990	0.994	0.994

4.2 Water Consumption

Water consumption refers to the amount of water that is depleted from the root zone through the process of transpiration by a crop and direct evaporation from the soil. Figure 4.3 illustrate the temporal variation in AETI over the cropping year from 2009 to 2022. The temporal variation of water consumption in the period of 2009-2022 shows a generally increasing trend. During the study period, the average water consumption at Wonji Shoa sugarcane state is 1,405.73 mm/year with a minimum of 1147.3 mm/year in 2010/2011 and a maximum of 1636.7 mm/year in 2015/2016.

This result is consistent with the findings by Zhang et al. (2015), who used a remote sensing model (METRIC) to estimate the water consumption (ETc) of Hawaiian sugarcane in the USA. They observed an ETc of 2.5-4.5 mm/day (1350 to 2430 mm/season) in the windward area and 2-4.5 mm/day (1080 to 2430 mm/season) in the leeward area. Meanwhile, the average seasonal Actual Evapotranspiration for Irrigation of sugarcane (i.e., water consumption of sugarcane) observed in the Wonji sugarcane scheme was found to be 1,405.73 mm/season. This value is quite close to the maximum seasonal ETc of sugarcane estimated using the METRIC model for Hawaiian sugarcane. (Ferreira et al., 2016), use Energy Balance System (SEBS) model to estimate the Sugarcane water requirement at Minas Gerais State, Brazil, and observed ETc value of 2.89 mm/day to 4.0 mm/day (1560–2160 mm/season) which also very close to the value we observed from WaPOR portal.

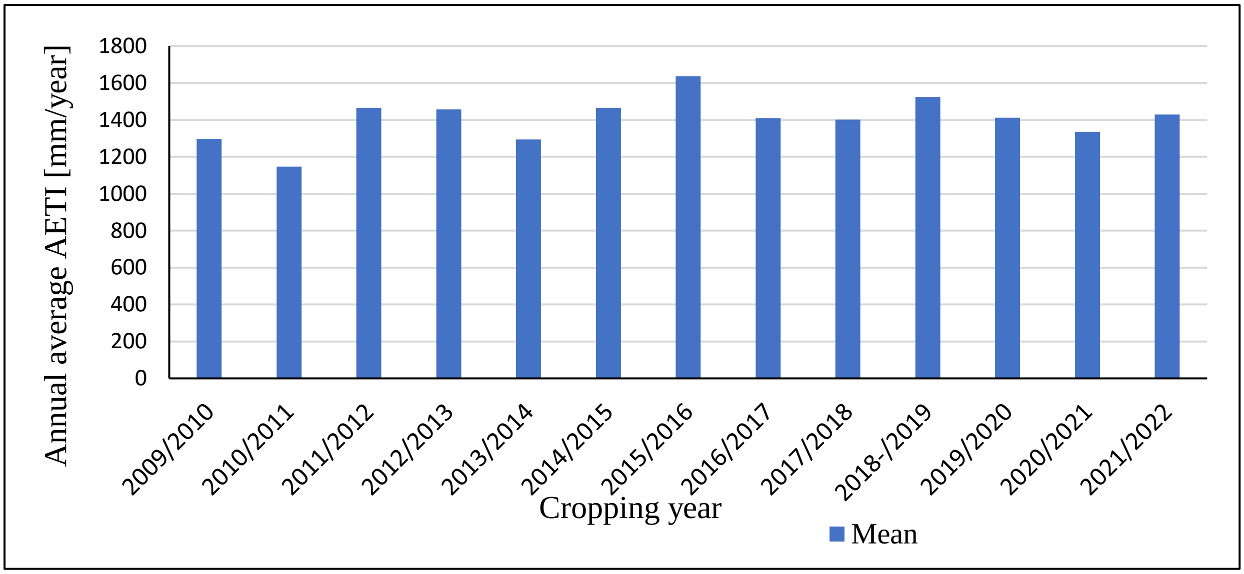

Figure 4.3 Temporal variation of average annual AETI over the cropping year.

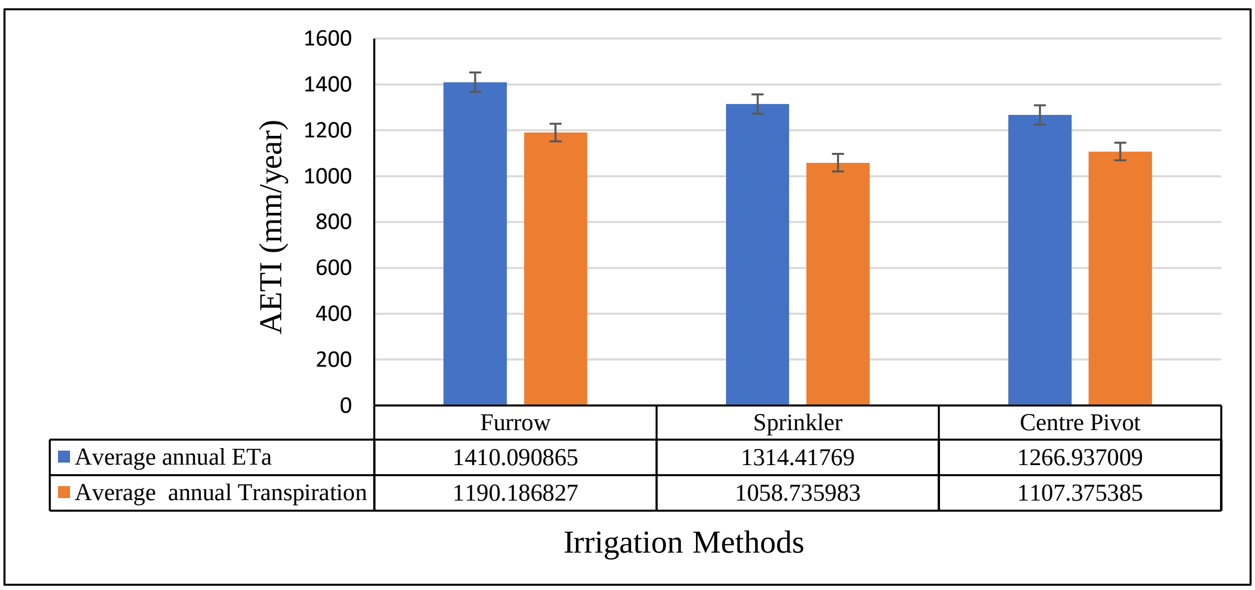

	Furrow	Sprinkler	Centre Pivot
Average annual ETa	1410.090865	1314.41769	1266.937009
Average annual Transpiration	1190.186827	1058.735983	1107.375385

Figure 4.4 The average annual actual evapotranspiration and transpiration are categorized by irrigation methods.

Figure 4.4 shows the average annual ETa and Ta over the period 2009-2022 for different irrigation methods. The land irrigated by furrow has the highest average ETa (1,410 mm/year) compared to the land irrigated by sprinkler irrigation (1,314.41mm/year), and center pivot irrigation (1,266.937 mm/year). The transpiration for the whole area has a mean value of 1,185.03 mm/year. The transpiration is also highest for furrow irrigation (1,190.18 mm/year), followed by center pivots (1,107.37 mm/year) and sprinkler irrigation (1,058.73 mm/year). The spatial distribution annual average of ETa and Ta across the Wonji Shoa sugarcane estate is shown in Figure 4.5 (annual maps from 2009-2022 are provided in Appendix A.3). Figure 4.5 shows the spatial variability of the average annual ETa, which varies between 720.46 and 1612.12 mm/year. The spatial distribution of the average annual transpiration is shown in Figure 4.6. The transpiration varies between 566.52 and 1,407 mm/year with an average of 1,185.03 mm/year.

The variation in water consumption between different irrigation methods can be attributed to several factors. Furrow irrigation, which involves flooding fields with water, tends to have higher evapotranspiration rates due to increased surface area exposure and potential runoff. In contrast, sprinkler and center pivot irrigation systems provide controlled and targeted water application, minimizing water loss through evaporation and runoff. Furrow irrigation may also have lower water distribution uniformity, leading to uneven wetting patterns and potential overwatering. Additionally, furrow irrigation is more susceptible to evaporation losses and wind drift, while sprinkler and center pivot systems mitigate these losses by applying water closer to the ground. Different soil characteristics, as well as management practices, can also influence water consumption. The type of crops grown on furrow-irrigated land and differences in irrigation scheduling, timing, and overall management practices can contribute to the observed variation in water consumption.

This result is inconsistent with the findings by Chukalla et al. (2020) evaluating annual average ETa for the period 2014/2015-2018/2019 for the different irrigation methods on the Xinavane sugarcane estate, where center pivot irrigation had the highest annual average ETa (1,505±82 mm/year), followed by a mix of irrigation systems (1,343±122 mm/year) and furrow irrigation (1,329±120 mm/year). Several factors could lead to the variation in the results such as factors of hydroclimatic factors, crop types, soil types, other environmental factors, and irrigation management practices. The methodology used in this study appears to be reliable as studied by previous researchers to assess remote sensing-based water consumption. (Janssens, 2022) conducted a study to examine the water consumption of Merti and Abadir Sub schemes in Metehara, Ethiopia, using remote sensing WaPOR data covering 2009-2021. Chukalla et al. (2021) used open-source libraries (WaPORWP) for assessing RS-based water consumption (ETa) in the Xinavane sugarcane estate for the period 2014-2019, yielding different average values for different irrigation methods. Zhang et al. (2015) utilized remote sensing models to estimate the water consumption of Hawaiian sugarcane in the USA. Moreover, the study by (Ferreira et al., 2016) employed the remote sensing model to estimate sugarcane water requirements in Minas Gerais State, Brazil. The methodology used in this study appears to be reliable as previous studies assess the spatial distribution of average annual ETa and Ta. Chukalla et al. (2020) reported that the average annual ETa varies between 777 and 1,628 mm/year. Additionally, the average annual transpiration fluctuates between 560 and 1,413 mm/year, averaging 1,118±125 mm/year in the Xinavane sugarcane estate.

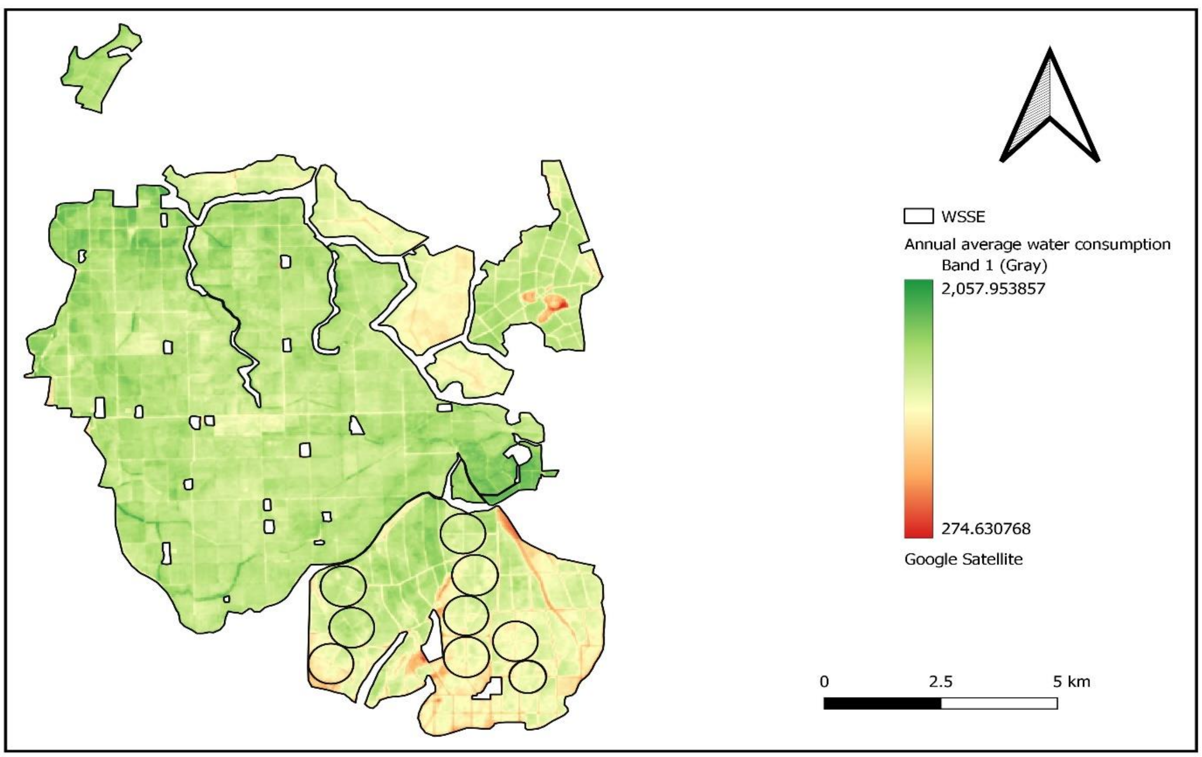

Figure 4.5 Spatial distribution of the average annual ETa over the period 2009-2022 for Wonji Shoa sugarcane estates.

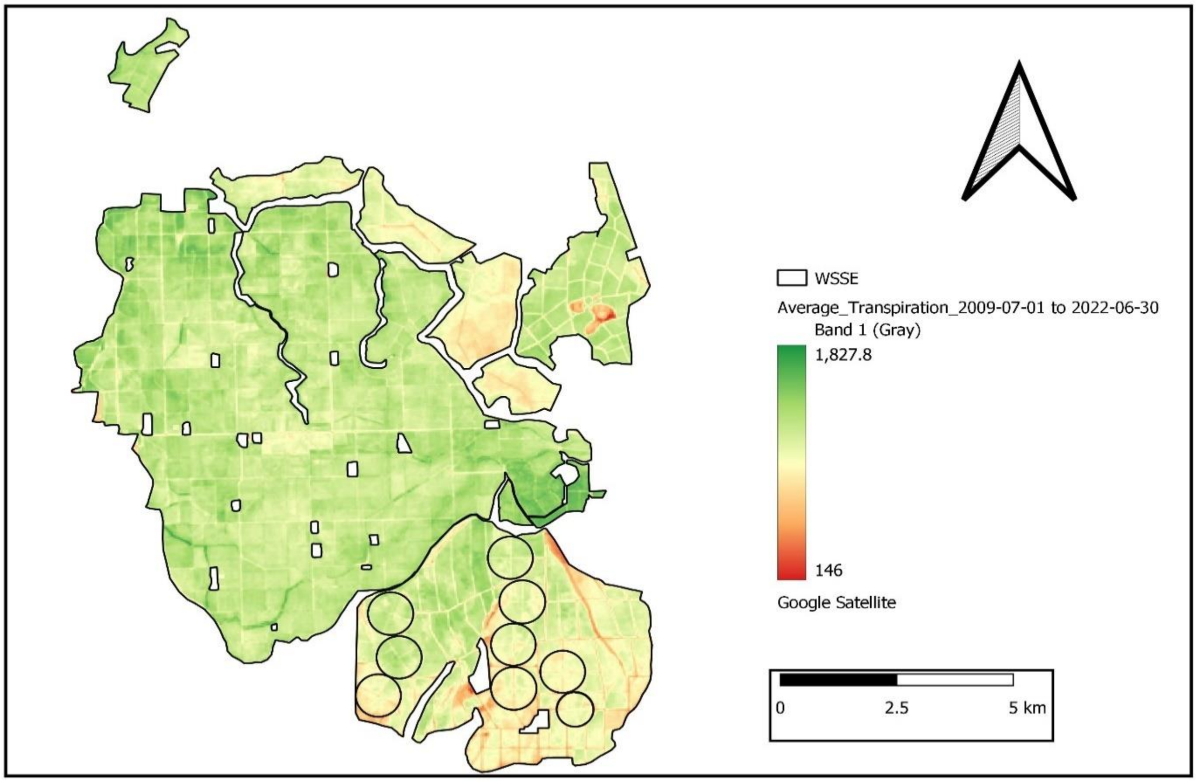

Figure 4.6 Spatial distribution of the average annual Ta over the period 2009/22 for Wonji Shoa sugarcane estates.

4.3 Uniformity

The uniformity of the water supply in an irrigation system, also known as evenness, can be evaluated using the coefficient of variation (CV) of the actual evapotranspiration (ETa). Table 4.2 shows the coefficient of variation of ETa, between pixels at the Wonji sugarcane scheme using the data from 2009-2022. The uniformity of water consumption at Wonji Shoa is 24 % which shows fair uniformity; thus, the water is fairly distributed over the area. The coefficient of variation of ETa for the areas which was irrigated under furrow, center pivot, and sprinkler irrigation system are 15.9, 9.3, and 24%, respectively. Thus, the Wonji Shoa sugarcane estate has fair uniformity for all irrigation methods, with good uniformity for the center pivot irrigated area. The reason sprinkler irrigated areas perform less, which tally with field-level accounts of challenges in operation (electricity outages) and maintenance (high costs), and furrow irrigation generally exhibits lower uniformity due to uneven water distribution. The coefficient of variation (CV) for furrow irrigation systems can vary depending on factors such as field topography, furrow design, and management practices.

This result is consistent with the findings by Chukalla et al. (2021), which found that the Xinavane sugarcane estate has good uniformity of water consumption at 9.4%, with higher uniformity for center pivots. The coefficient of variation of ETa for center pivot, furrow, and mixed irrigation systems are 9%, 5.5%, and 9%, respectively. These results indicate that both sugarcane estates have good uniformity in their irrigation methods, ensuring efficient water usage for crop production. These findings are also supported by a study conducted by Alemayehu et al. (2020), which reported that for the areas under surface irrigation (furrow), center pivot irrigation, and sprinkler irrigation the CV of ETa is respectively 9.8%, 10.3%, and 15.9% further confirming their fair uniformity.

The study conducted for the Wonji Shoa sugarcane estate used open-source libraries (WaPORWP) for assessing remote sensing (RS) based coefficient of variation of ETa (uniformity). Studies provide supportive evidence for the methodology used. (Janssens, 2022) conducted a study to examine the coefficient of variation of the ETact for each irrigation season from 2009-2021 in Abadir and Merti using remote sensing WaPOR data. Chukalla et al. (2021), evaluated the uniformity of the Xinavane sugarcane estate during the period 2014/2019 using open-source (WaPOR) for the coefficient of variation of AETI assessments in different irrigation methods.

Table 4.2 shows the coefficient of variation of ETa at the Wonji sugarcane scheme from 2009/2022.

Cropping Seasons	CV of AETI (%)	Uniformity
2009-07-01/2010-06-30	39.4	Poor
2010-07-01/2011-06-30	43.2	Poor
2011-07-01/2012-06-30	27.3	Poor
2012-07-01/2013-06-30	17.2	Fair
2013-07-01/2014-06-30	22.9	Fair
2014-07-01/2015-06-30	19.3	Fair
2015-07-01/2016-06-30	19.6	Fair
2016-07-01/2017-06-30	22.6	Fair
2017-07-01/2018-06-30	22.4	Fair
2018-07-01/2019-06-30	26.4	Poor
2019-07-01/2020-06-30	21.3	Fair
2020-07-01/2021-06-30	25.0	Poor
2021-07-01/2022-06-30	26.2	Poor

4.4 Efficiency (Beneficial fraction)

The beneficial fraction is a measure of the proportion of water used for transpiration to the total water consumption in a field (ETa). This ratio indicates the effectiveness of on-farm water management and agricultural practices in utilizing water for crop growth. Figure 4.7 shows the spatial distribution of the average beneficial fraction from 2009 to 2022 (annual maps from 2009-2022 are provided in Appendix A.4). The beneficial fraction (efficiency) for the areas irrigated under furrow, center pivot, and sprinkler irrigation system are 0.8289, 0.8033, and 0.8203, respectively. A higher beneficial fraction was observed in the fields of Wonji main (section B), Boku (section G), WakeTio expansion (section E), Kuriftu (section F), and Adulala (section H) meaning a larger fraction of the water applied to the crop is being used for transpiration and therefore for crop growth and lower beneficial fraction observed in the fields of WakeMia (section D), WakeTio (section C) and parts of Dodota (section A), indicates that more water is being lost to non-beneficial processes such as evaporation from the soil surface and deep drainage below the root zone.

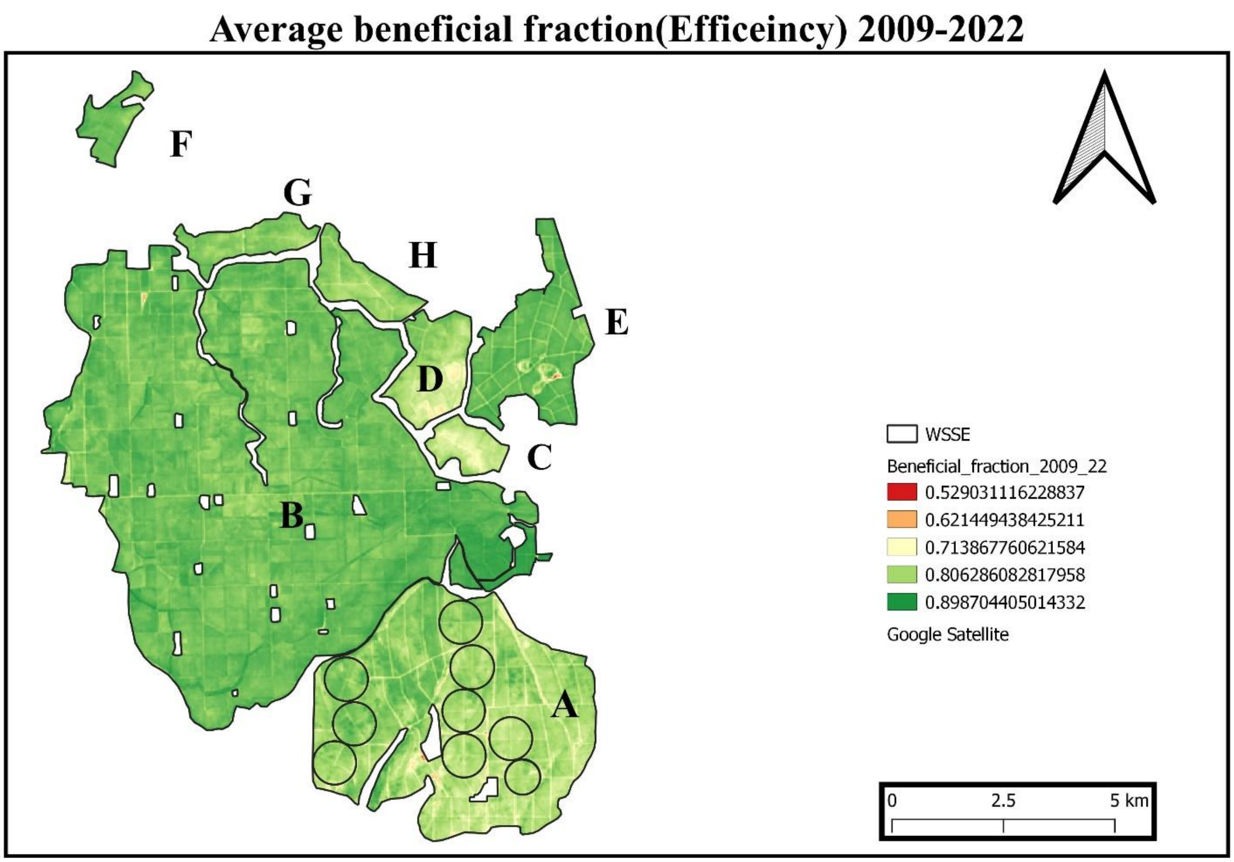

Figure 4.7 Average beneficial fraction during the period 2009-07-01 to 2022-06-30.

4.5 Adequacy

Adequacy refers to the extent to which the water supplied for irrigation meets the necessary water consumption for crop growth. In the Wonji sugarcane estate, the adequacy of irrigation water delivery is illustrated in Figure 4.8. The level of adequacy can vary depending on the irrigation technique used. For the period analyzed (2009 to 2022), the results show that the highest adequacy for the areas with furrow irrigation (adequacy of 0.70), followed by the sprinkler irrigated area (0.65), and lowest for the center pivot irrigated area (0.64). Furrow irrigation has an acceptable range of adequacy ($0.68< A \leq 0.8$), and sprinkler and center pivot had poor performance (Karimi et al., 2019).

The reason for low adequacy of sprinkler and center pivot irrigation methods can be attributed to several factors. These include issues related to water distribution uniformity, such as nozzle clogging, uneven pressure distribution, and inadequate sprinkler spacing, resulting in uneven water distribution and areas of overwatering or underwatering. Wind drift and evaporation losses also impact performance, as high wind speeds can carry water droplets away from the target area, reducing coverage, while evaporation further diminishes water reaching the crops. Proper system design and operation, regular maintenance and adjustments, and effective management practices are essential for improving adequacy by addressing issues such as system design flaws, maintenance neglect, and inadequate scheduling or monitoring (Waller & Yitayew., 2016).

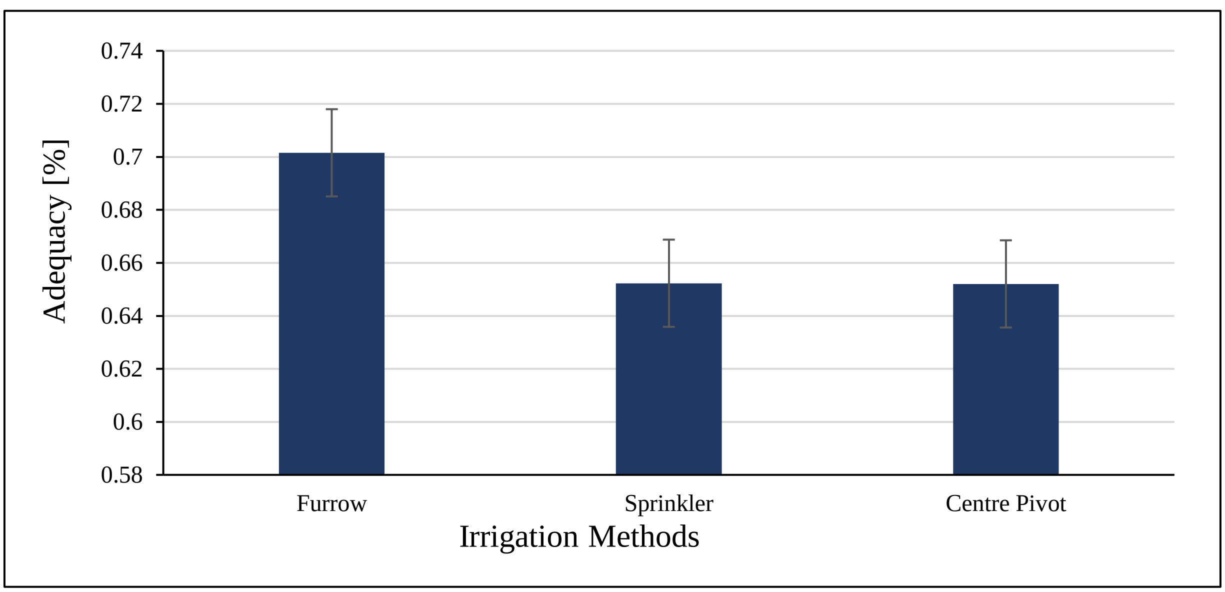

Figure 4.8 Adequacy of the average annual water consumption at Wonji sugarcane estate categorized by irrigation methods.

The spatial distribution of the adequacy (2009-2022) for the Wonji sugarcane area is provided in Figure 4.9, and seasonal maps are provided in Appendix A.5. Higher adequacy was observed in areas such as Wonji Main, Hargitti, Bishola, the northwest parts of Dodota, Kuriftu, and Wake Tio expansion site, with values ranging from 0.78 to 1; thus, the crop water requirements were also quite well met, while the adequacy was mostly above 0.7. Moderate adequacy (values between 0.56 and 0.78) was noticed in the northeast and southeast parts of the Dodota site and Boku. Lower adequacy levels were found in Adulala, Wake Mia, and WakeTio, with values ranging between 0.34 and 0.56.

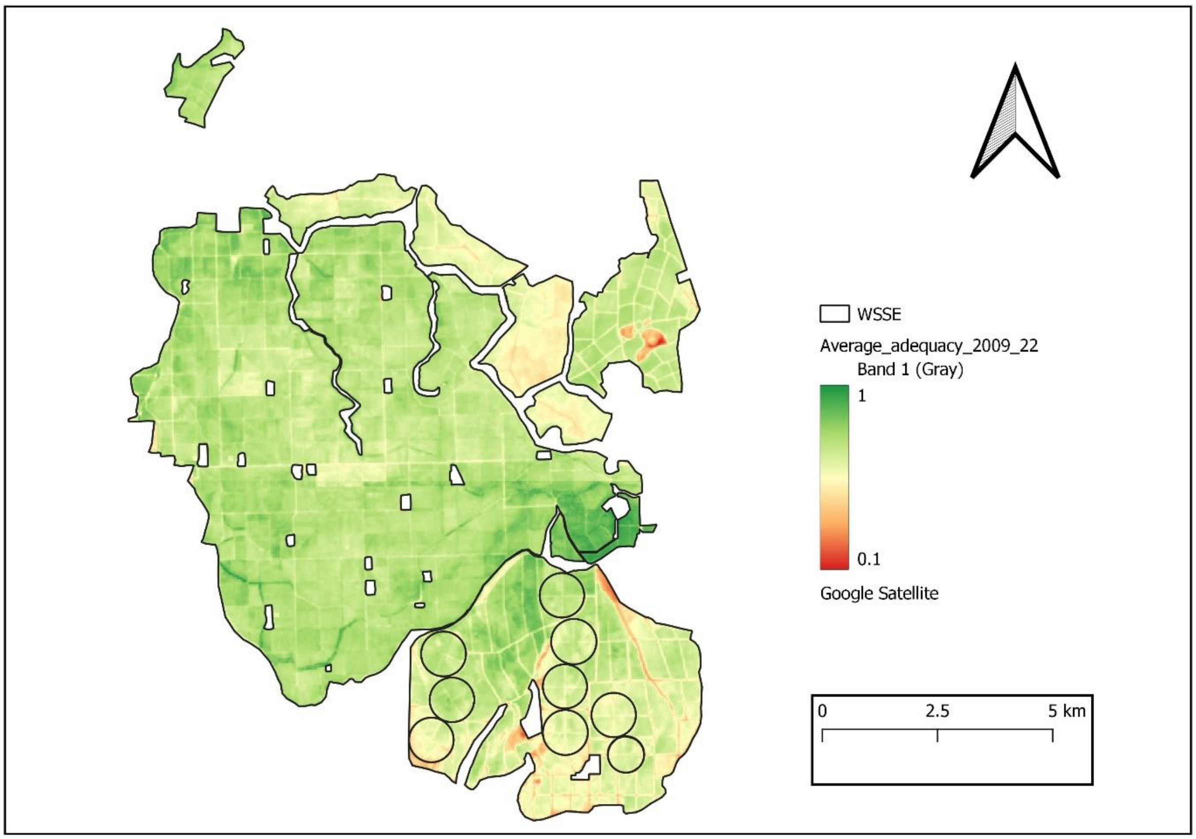

Figure 4.9 Spatial distribution of the adequacy of the Wonji Shoa irrigation scheme from 2009 to 2022.

Adequacy is the ratio of actual evapotranspiration (ETa) to the required evapotranspiration (ETrequired). For this study, it has been simplified as the ratio of ETa to the reference evapotranspiration (ETreff) as shown in equation (3). However, this simplification is not agronomically accurate, since the required evapotranspiration varies depending on the irrigation method, frequency, and soil type as per (Allen et al., 1998) (referencing equation 59, table 20, figure 29, and figure 30). To perform a meaningful adequacy assessment, one thus needs to be able to assess the differential ETrequired per irrigation method. But this requires a more detailed information base on soil type, irrigation frequency and application rates, crop growth stages as well as climatic conditions – all of which (except climate) are beyond the scope of WaPOR to determine on the basis of its RS images.

The methodology used in this study appears to be reliable as studied by previous researchers to assess remote sensing-based adequacy. Chukalla et al. (2021) evaluated the adequacy of the Xinavane sugarcane estate for the period 2014/2019 using open-source libraries (WaPORWP) for remotely sensed-based adequacy assessments for different irrigation methods. (Janssens, 2022), also conducted a study to examine spatial variations in the adequacy of Merti and Abadir Sub schemes in Metehara, Ethiopia, using remote sensing WaPOR data covering 2009-2021.

4.6 Land and Water Productivity

Table 4.3 shows the biomass obtained from WaPOR data according to the hydrological season in the study area, as well as the recorded yield (Wonji-Shoa Sugar Factory, 2022). From the seasonal data first, the annual production was calculated with the use of the average growing season. This can then be compared with the yield estimated with WaPOR biomass and a literature-based harvest index. The differences between the observed yield and the estimated yield from WaPOR biomass could be explained by the use of the calculated inter-seasonal average biomass for the comparison, as well as by the estimates made, such as the exact season length per irrigation scheme and the harvest index set at one value for all areas. The estimated sugarcane yield production is fairly comparable to the observed yield for the Wonji Shoa sugarcane estate.

Table 4.3 Average observed yield and WaPOR yield.

Seasons	**WaPOR yield (ton/ha)**	**Average observed yield(ton/ha)** (Wonji-Shoa Sugar Factory, 2022)
2009-07-01/2010-06-30	118.8	133.4
2010-07-01/2011-06-30	100.7	155.3
2011-07-01/2012-06-30	115.5	129.5
2012-07-01/2013-06-30	129.1	149.8
2013-07-01/2014-06-30	121.2	174.19
2014-07-01/2015-06-30	125.9	164.1
2015-07-01/2016-06-30	138.6	149.1
2016-07-01/2017-06-30	110.4	109.7
2017-07-01/2018-06-30	121.2	90.1
2018-07-01/2019-06-30	118.9	107.9
2019-07-01/2020-06-30	131.5	110
2020-07-01/2021-06-30	109.9	83.7
2021-07-01/2022-06-30	117.3	64.14

Note: Data for sugarcane production per season from Wonji-Shoa Sugar Factory (2022).In WaPOR, the yield is calculated by multiplying the biomass by a harvest index of 1, which is the default harvest index for sugarcane in the WaPOR portal (FAO, 2020a).

Figure 4.10 shows the comparison of WaPOR data and observed yield data during the period 2009 to 2022. In this study, a comparison between WaPOR data and ground-level data showed inconsistencies in the WaPOR data. Consequently, the average difference between the WaPOR yield and the observed yield was 24.68%, with a standard deviation of 19.52%. The WaPOR quality assessment report indicates that the calculated B in WaPOR data is consistently underestimated by 58% (FAO and IHE Delft, 2019). Blatchford et al. (2019) also suggest that comparing remote sensing data with ground-level data can be challenging due to several factors. Firstly, ground-level data is often collected on local and point scales, while remote-sensing data is continuous in both space and time (Blatchford et al., 2019). Secondly, remote sensing data often contain systematic errors due to variations in energy balance components across space and time (Foken, 2008). Finally, remote sensing assumes that there is vegetation heterogeneity within a pixel, which may not always be accurate and can lead to incorrect conclusions (Blatchford et al., 2019; Conrad et al., 2020). This result is consistent with the findings by (Chukalla, Mul, van der Zaag, et al., 2022b) showed that WaPOR-based yield estimates were found to be comparable to the estate-measured yields with ±20 % difference, a root mean square error of 19±2.5 t ha^{-1} and a mean absolute error of 15±1.6 t ha^{-1} at the Xinavane sugarcane estate, Mozambique.

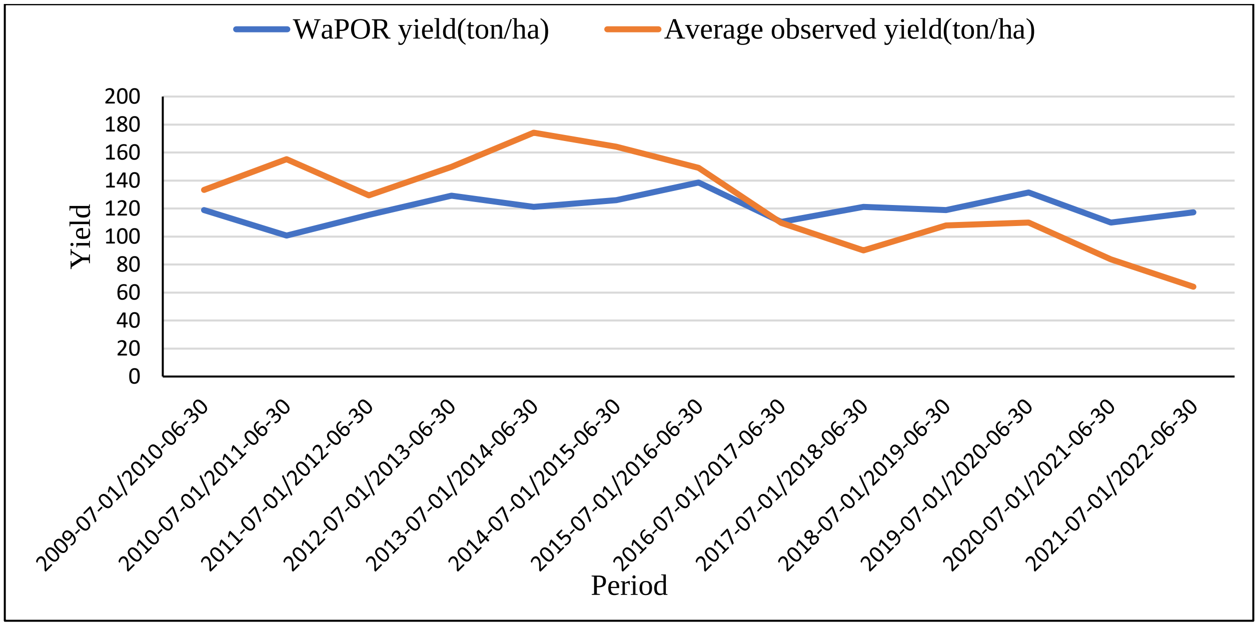

Figure 4.10 Comparison of WaPOR data and observed yield data during the period 2009 to 2022.

From the above figure, it can be observed that in the initial years, the WaPOR yield was lower than the average observed yield. However, this pattern began to change around 2016-07-01/2017-06-30. After this date, the WaPOR yield is generally higher than the observed yield. A few possible explanations of the pattern change could be: The conditions captured by WaPOR (which includes satellite data on actual evapotranspiration and biomass production) have changed over time, possibly due to factors like climate change or improvements in agriculture technology or practices. The methodology of collecting or calculating the average observed yield has changed, causing a discrepancy between the two data sets. There may be other variables in play that are influencing the yields. For example, factors like pests, disease, or weather events that are not accounted for in the WaPOR data could be impacting the observed yield and the WaPOR data might have been more accurately capturing the actual yield potential compared to the observed yield, which could be influenced by on-ground challenges in farming operations.

4.6.1 Land productivity

Land productivity is defined as the biomass production or yield in ton/ha/season. Figure 4.11 illustrates the temporal variation of land productivity in the period of 2009 to 2022. The temporal findings revealed that biomass did not decrease nor increase over time. However, there was a drop in B in the season of 2010-11. The highest and lowest mean biomass was observed in the year 2015-2016 with values of 138.6 ton/ha/season and 2010-2011 with values of 100.7 ton/ha/season respectively.

This result is consistent with the findings by Morel et al. (2014), estimated the value of the sugarcane yield of Reunion Island based on remote sensing data and came up with the annual average sugarcane yield result of 80 ton/ha to 160 ton/ha which is closer to the value we estimated at Wonji Shoa irrigation schemes (119.9 ton/ha/year.). Gemechu et al. (2020), use the remote sensing-derived dataset to estimate the agricultural land productivity in three large irrigation schemes of Ethiopia (Wonji, Fincha, and Metehara) and come with the average sugarcane yield at three schemes of 146.7 ton/ha/year for Wonji, 107.0 ton/ha/year for Metehara, 151.4 ton/ha/year for Fincha'a irrigation scheme. Since the growing season of sugarcane at the selected three schemes is more than a year (18 months) the higher value observed is expected.

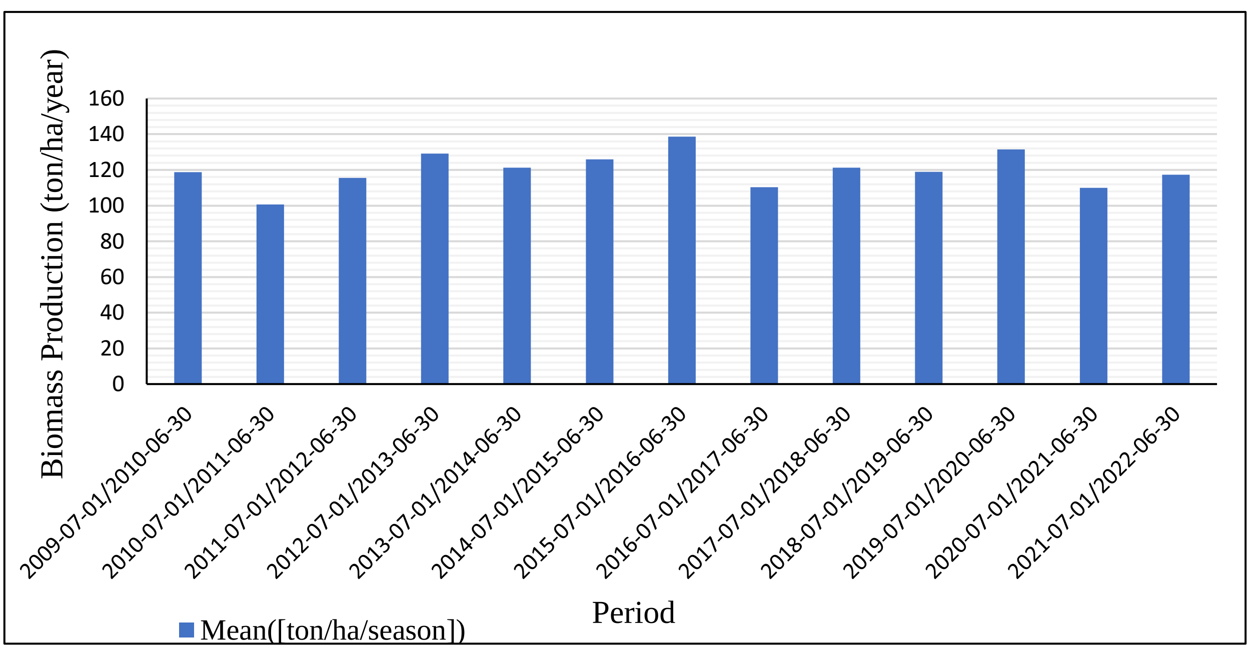

Figure 4.11 The temporal variation of biomass production at Wonji Shoa from 2009-2022.

The average annual biomass production per irrigation method for the period 2009-2022 is shown in Figure 4.12. Land productivity varies between irrigation methods. The average annual above-ground biomass production (ton/ha/year) over the period 2009-2022 for the Wonji sugarcane estate is 119.9 tons/ha/year. Irrigated areas under furrow have the highest average annual land productivity (120.4 ton/ha/year) followed by areas irrigated under sprinkler irrigation system (115.8 ton/ha/year), and center pivot (110.5 ton/ha/year). The result shows that different irrigation methods can impact land productivity, with furrow irrigation having the highest average annual land productivity in the Wonji Shoa sugarcane estate. During a field visit, it was observed that the underperformance of center pivot and sprinkler irrigation systems was primarily due to the usage of light soil types (B_{14} and C_1 soil management group), which have low water retention capacity. As a result, plants grown in these soils require more frequent watering compared to those grown in black or mixed soils. In addition, pipe leakage and faulty electric pumps need immediate attention to improve the performance of irrigation systems. Furthermore, frequent interruptions in the power supply hurt the proper functioning of these pumps, leading to reduced efficiency of the irrigation systems which result low performing areas in production.

These results contrary with the study conducted by Chukalla et al. (2021) due to different hydroclimatic condition, soil type, management practice and other factors, which demonstrated that, center pivot irrigation method had the highest average annual land productivity (82±5 ton/ha/year), followed by a mixed irrigation system (77±7 ton/ha/year), and furrow irrigation (76±7 ton/ha/year).

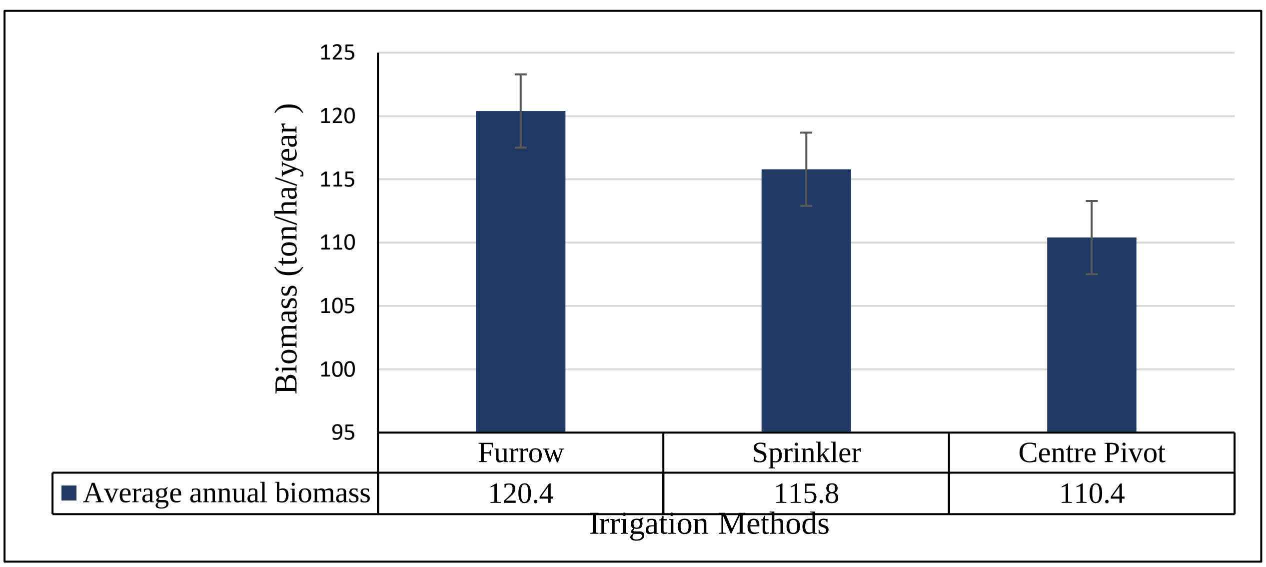

Figure 4.12 Average annual biomass production [ton/ha/year] for the period 2009-2022, categorized by irrigation method.

Figure 4.13 shows the spatial distribution of the average annual biomass production [ton/ha/year] over the period 2009-2022 (annual maps from 2009-2022 are provided in Appendix A.6). Some locations exhibiting a lower average B, such as Boku, Adulala, Wake Mia, Wake Tio, and the southeastern parts of Dodota fields with a range of 54-96 tons/ha/year. Conversely, areas with the highest average annual land productivity (B) were found in Bishola and Hargitti, Wonji main, Kuriftu, and Wake Tio expansion, with a range of 139-181 tons/ha/year. The spatial distribution of B from 2009 to 2022 is comprehensively discussed and analyzed by classifying it into distinct zones to underscore the site disparities in land productivity. This in-depth examination utilizes zonal statistics as outlined in Section 4.8 of the forward pages, which provides a detailed and systematic approach to understanding the variations in productivity across different zones.

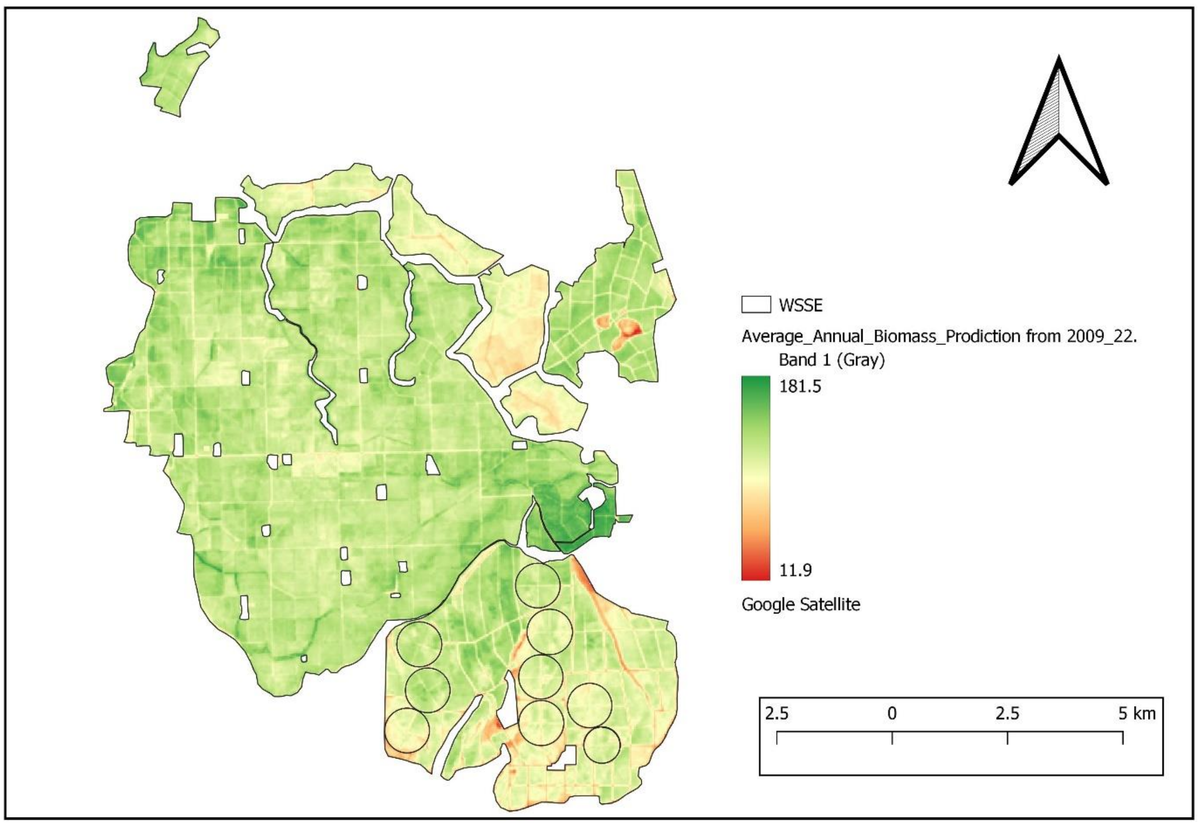

Figure 4.13: Spatial distribution of the average annual biomass production [ton/ha/year] over the period 2009-2022.

The methodology used in this study appears to be reliable as studied by previous researchers to assess remote sensing (RS) based land productivity which gives reasonable results. Morel et al. (2014) estimated the sugarcane yield of Reunion Island using remote sensing data and obtained an annual average sugarcane yield of 80 to 160 ton/ha. Gemechu et al. (2020), also used remote sensing-derived datasets to estimate the seasonal and spatial variability of agricultural land productivity in three large irrigation schemes of Ethiopia, including Wonji. Their results showed an average sugarcane yield of 146.7 ton/ha/year for Wonji. (Janssens, 2022) conducted a study to examine spatial variations in land productivity of Merti and Abadir Sub schemes in Metehara, Ethiopia, using remote sensing WaPOR data covering 2009-2021. Another relevant study conducted by Chukalla et al. (2021) evaluated land productivity on the Xinavane sugarcane estate for the period 2014/2019 using open-source libraries (WaPORWP) for remotely sensed land productivity assessments for different irrigation methods.

4.6.2 Water productivity

The term water productivity, also known as biomass water productivity (WPb), is defined as the proportion of biomass produced with the actual evapotranspiration (ETa). Figure 4.14 shows the temporal variation of biomass water productivity over the period 2009-2022 for the Wonji Shoa sugarcane estate. The temporal findings revealed that the average WPb decreased over time, meaning that over time more water was needed to produce the same amount of biomass. The peak biomass water productivity value of 9.3 kg/m^3 occurred during the 2013-07-01/2014-06-30 season, while the lowest value of 5.7 kg/m^3 was recorded in 2021-2022.

This result is consistent with the findings conducted by Gemechu et al. (2020), using remote sensing data to determine the average water productivity at Wonji, Metehara, and Fincha'a. The results showed that between 2009-2019, the average water productivity was 7.5 kg/m^3 for Wonji, 4.3 kg/m^3 for Metehara, and 7.0 kg/m^3 for Fincha'a which is closer to the value we estimated. (Yilma, 2017b), estimated the sugarcane water productivity at Wonji Ethiopia by applying an automated version of the SEBAL (PySEBAL) model, and the result ranged between 2.57 to 11.95 kg/m^3 with a mean value of 5.12 kg/m^3. Therefore, the average sugarcane water productivity we observed at Wonji from WaPOR portal (7.5 kg/m^3) was closer to the value observed by SEBAL model.

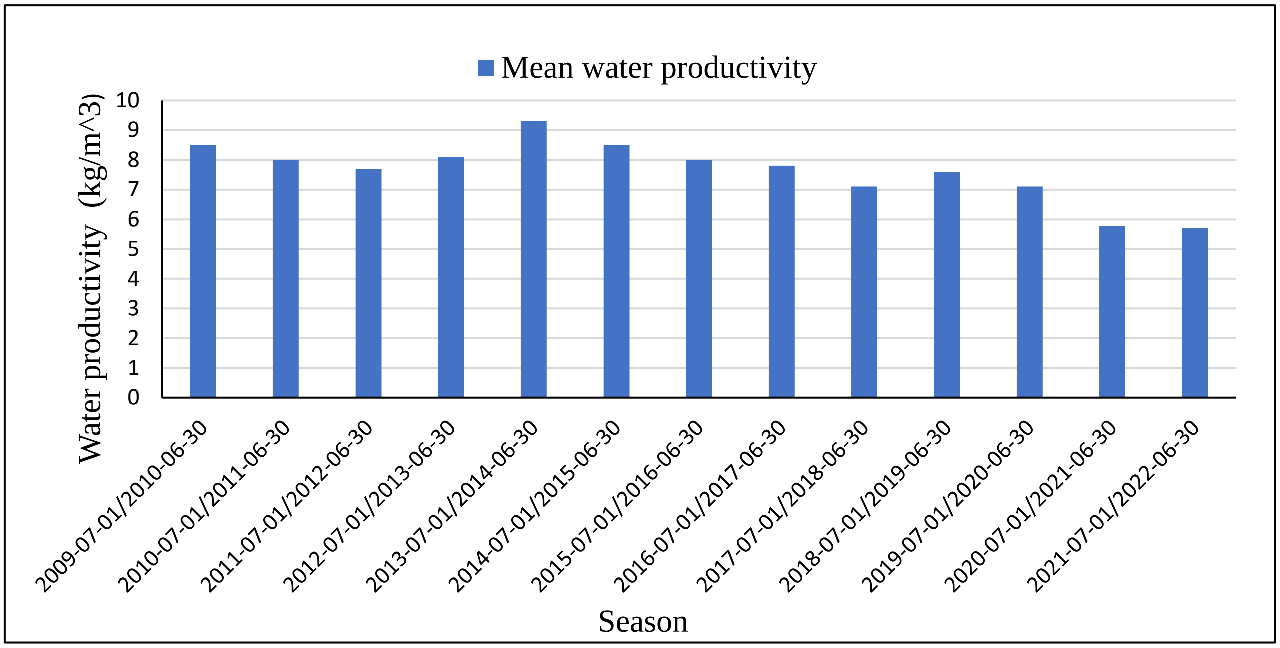

Figure 4.14 Temporal variation of average annual water productivity from 2009 to 2022 in the Wonji Shoa irrigation scheme.

Figure 4.15 shows the average annual water productivity (WPb) for the period 2009 to 2022, categorized by irrigation methods. The highest WPb is observed for the areas irrigated by sprinklers with an average annual value of 8.5 kg/m^3, followed by the areas irrigated with center pivot, and furrow irrigation have almost the same water productivity value of 8.3 kg/m^3.

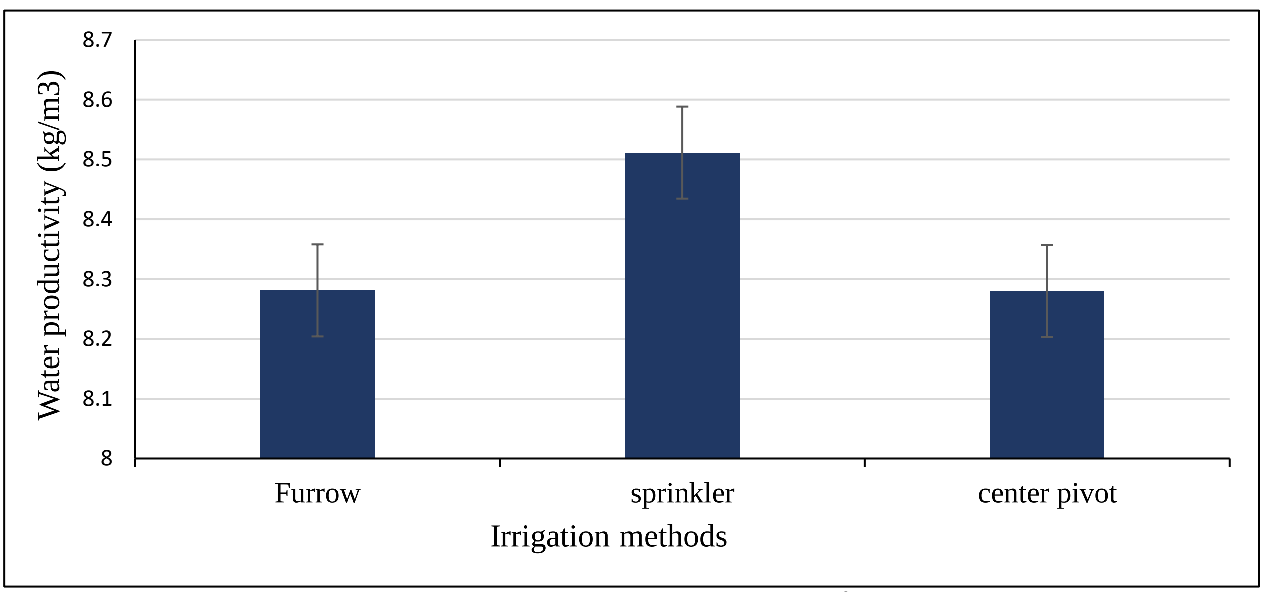

Figure 4.15 Average annual biomass water productivity (kg/m^3) for the period 2009-2022, categorized by irrigation methods.

These findings are contrary to the result reported by Chukalla et al. (2022), which examined the water productivity at Xinavane from 2014-2018. In that study, it was found that furrow-irrigated fields had the highest average water productivity (6.9 kg/m^3) compared to sprinkler-irrigated fields (6.7 kg/m^3) and centre pivot-irrigated fields (6.6 kg/m^3). And also Chukalla et al. (2021) conclude that the average WPb at Xinavane is 5.7±0.2 kg/m^3 and it varies from 5 to 6 kg/m^3 from 2014/2015 to 2018/2019. The variability in water productivity in the irrigation methods results due to variation of hydroclimatic, soil properties, and irrigation management practices and local condition.

Figure 4.16 shows the spatial distribution of the average annual biomass water productivity over the period 2009-2022. The seasonal spatial variation is provided in Appendix A.7. Although WPb was quite evenly distributed over the research area, there were some locations with a lower mean WPb (Figure 4.16): parts of Wake Mia, parts of Wake Tio, and the northeastern Dodota fields which ranges from 8-5.7 kg/m^3. The areas with the highest average biomass water productivity were in the Hargitti, Bishola, Wonji main, Kuriftu, Wake Tio expansion, parts of Boku and Adulala schemes which range from 8.6-10 kg/m^3. The spatial distribution of biomass water productivity from 2009 to 2022 is comprehensively discussed and analyzed by classifying it into distinct zones to underscore the regional disparities in biomass water productivity. This in-depth examination utilizes zonal statistics as outlined in Section 4.8 of the forward pages, which provides a detailed and systematic approach to understanding the variations in productivity across different zones.

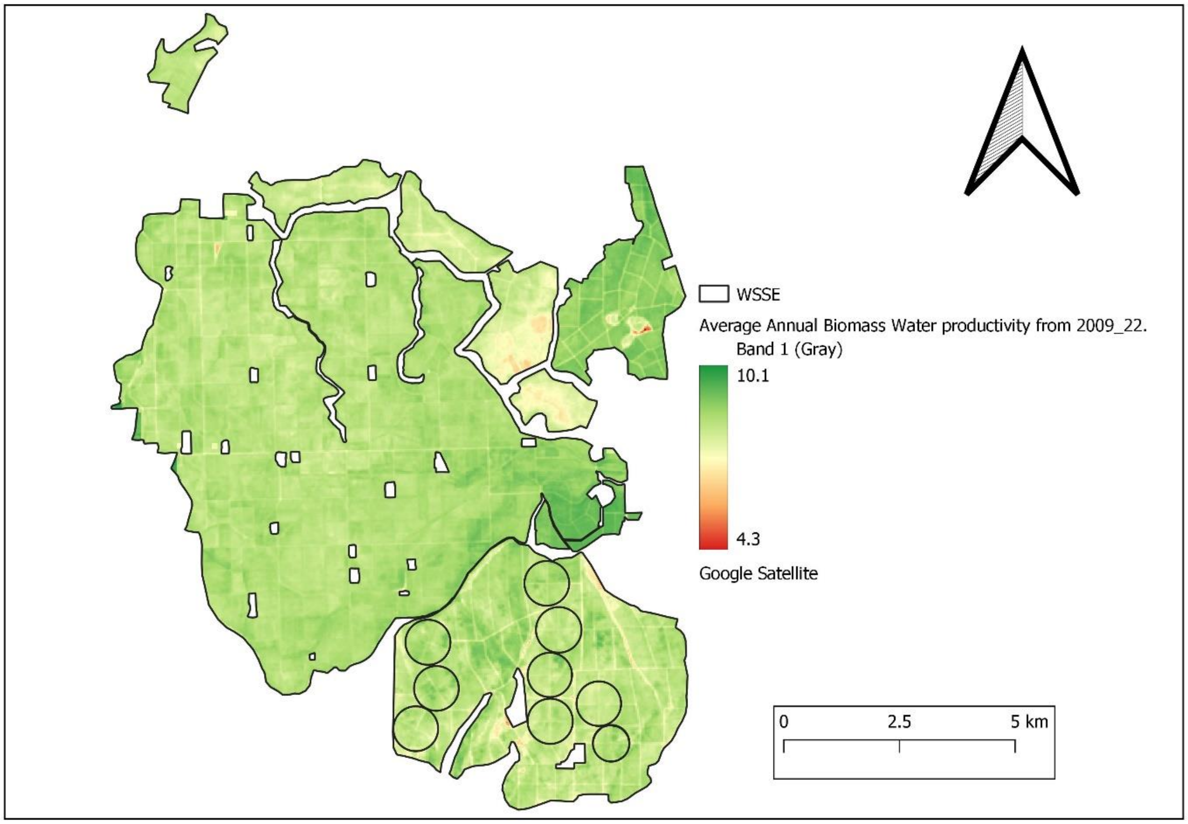

Figure 4.16 Spatial distribution of the average annual biomass water productivity over the period 2009-2022.

The methodology used in this study appears to be reliable as studied by previous researchers for assessing remote sensing (RS) based water productivity which yields reasonable results. Gemechu et al. (2020), use remote sensing data to estimate the average water productivity and the spatial variation of crop water productivity for the Wonji, Metehara, and Fincha'a irrigation scheme from January 1/2009 to June 30/2019, and concluded that the water productivity of the Wonji irrigation scheme showed variations in at different sites. (Janssens, 2022) conducted a study to demonstrate the mean irrigation seasonal spatial variation in WPb in Merti and Abadir, using remote sensing WaPOR data and identify the higher and lower performing sections in biomass water productivity in both Abadir and Merti sub-schemes. Chukalla et al. (2021) evaluated water productivity on the Xinavane sugarcane estate for the period 2014/2019 using open-source libraries (WaPORWP) for remotely sensed land productivity assessments for different irrigation methods.

4.7 Productivity gaps

4.7.1 Calculate target biomass(B) and target biomass water productivity (WPb)

The land and water productivity distributions and the productivity targets based on the 90th percentile of sugarcane at Wonji scheme for the years (2009/2010 and 2021/2022) are shown in Figure 4.17 (annual maps from 2009/2010-2021/2022 are provided in Appendix A.8). The productivity of land and water for sugarcane in Wonji appears to adhere to a normal distribution. As a result, statistical parameters like average, standard deviation, and percentiles can effectively depict the productivity distribution's characteristics. This normal distribution pattern can be observed in the studies conducted by (Sawasawa, 2003) for yield and Zwart & Bastiaanssen (2007) for water productivity. However, some researchers, such as (Ramirez et al., 2003), have discovered that crop yields do not always follow a normal distribution.

The seasonal land and water productivity targets in the Wonji scheme are determined by analyzing the productivity distributions across pixels. These targets are deemed achievable using existing technology and best management practices, as the area falls under the same agro-climatic zone. Table 4.4 shows the target biomass(B) and target biomass water productivity (WPb) fluctuate across different seasons. For instance, the 2009-2010 season saw the highest target biomass at 179.0 ton/ha/season, whereas the lowest was in the 2016-2017 season at 146.0 ton/ha/season. In a similar vein, the highest target biomass water productivity (WPb) was recorded in the 2019-2020 and 2013-2014 seasons at 10.0 kg/m^3, while the lowest occurred in the 2011-2012 season at 8.5 kg/m^3. The intended target land productivity (biomass) for the Wonji sugarcane farm between 2009 and 2022 is an annual average of 162.4 ton/ha/year, while the target biomass water productivity (WPb) is 8.5 kg/m^3.

Table 4.4 Distribution of the B target and WPb targets for the individual years from 2009-22.

Seasons	Target biomass	Target biomass WP(WPb)
2009-07-01/2010-06-30	179.0	9.9
2010-07-01/2011-06-30	153.0	9.4
2011-07-01/2012-06-30	157.0	8.5
2012-07-01/2013-06-30	161.0	9.5
2013-07-01/2014-06-30	163.0	10.0
2014-07-01/2015-06-30	161.0	9.1
2015-07-01/2016-06-30	177.0	9.1
2016-07-01/2017-06-30	146.0	8.5
2017-07-01/2018-06-30	165.0	9.6
2018-07-01/2019-06-30	163.0	8.6
2019-07-01/2020-06-30	172.0	10.0
2020-07-01/2021-06-30	149.0	8.9
2021-07-01/2022-06-30	165.0	8.8

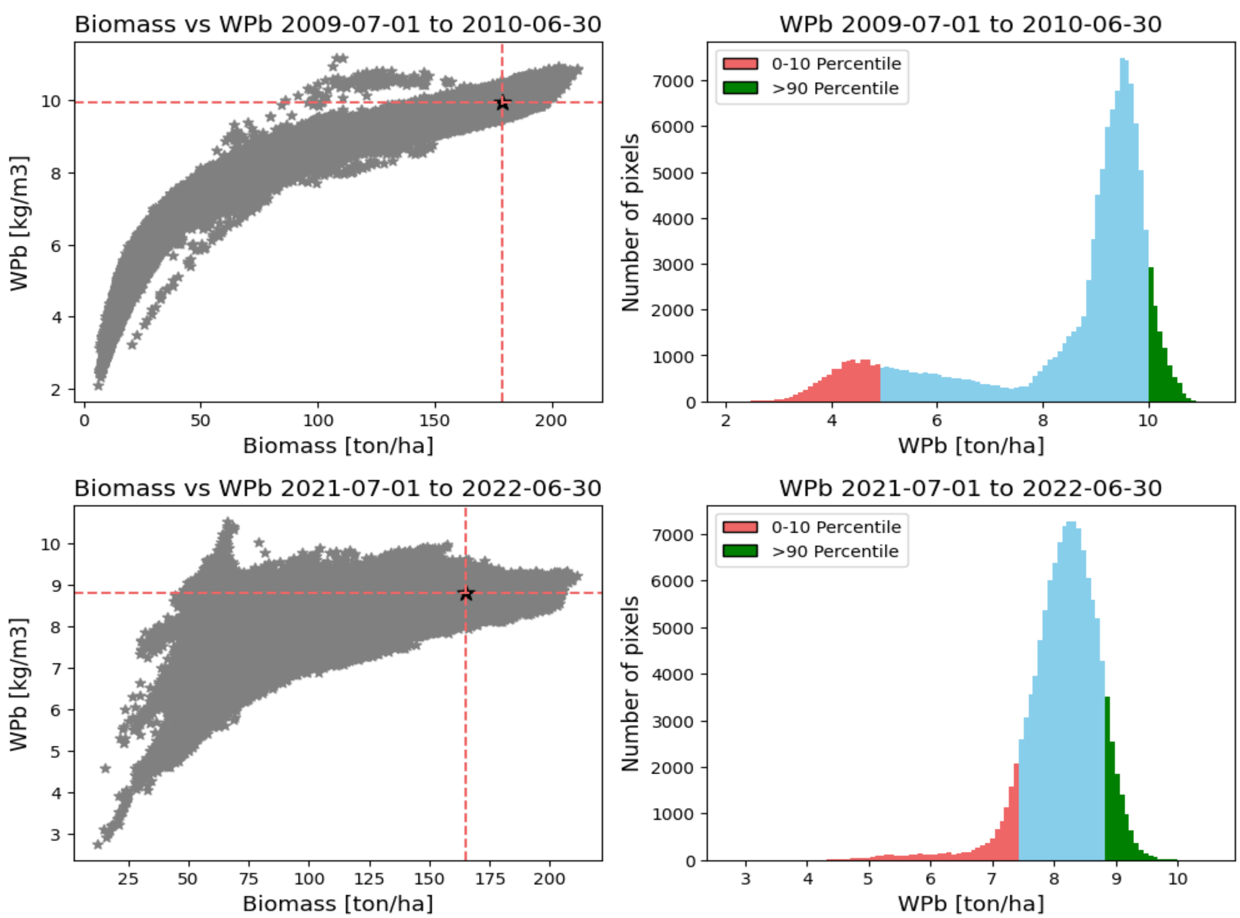

Figure 4.17 The biomass target and biomass water productivity target at Wonji Shoa for the year 2009/10 and 2021/22.

The dashed lines present the land and water productivity targets (a). The right figure presents the distribution of the average annual biomass production and biomass water productivity (b), the top 10%, and the bottom 10% in a normally distributed histogram.

The biomass target productivity and biomass water productivity target (WPb) at the 90 percentiles are indicated in green and by the red dashed lines as shown the Figure 4.17. The green highlighted cells were the locations that meet or exceed the target WPb and B, which were perceived as the bright spots. Figure 4.17a illustrates a scatterplot of the land and water productivity in which each grid cell is plotted together with the target productivities and Figure 4.17b exhibits the normal distribution of the WPb. Figure 4.17a illustrates that for the majority of cells in the study area to achieve the desired targets, they must either boost their biomass (B) or enhance both their biomass and biomass water productivity (WPb).

These results are consistent with the study conducted by Chukalla et al. (2020), who investigated the land and water productivity targets for sugarcane farms focused on the Xinavane scheme and found that the biomass target for 2014/2015-2018/2019 was 88 tons/ha/year, while the biomass water productivity (WPb) target was 6 kg/m^3. Comparing the result to their findings, it is evident that the intended land productivity for the Wonji sugarcane farm between 2009-2022 has a higher annual average of 162.4 tons/ha/year and a higher biomass water productivity target of 8.5 kg/m^3.

The consistency of findings across various studies supports the methodology employed in assessing land and water productivity targets for the Wonji Shoa sugarcane estate using remote sensing (RS) data. (Janssens, 2022) conducted research on the Metehara region, including Merti and Abadir sub-schemes, utilizing remote sensing WaPOR data from 2009-2021. The study determined a WPb target of 4.4 kg/m^3 and biomass (B) targets 77.0 ton/ha/season for Merti and 78.0 ton/ha/season for Abadir, noting a normal distribution and small standard deviation. Similarly, Chukalla et al. (2021) assessed sugarcane farm productivity in the Xinavane scheme for 2014/2015-2018/2019 using remotely-sensed data and open-source libraries (WaPORWP). They found a biomass target of 88 tons/ha/year and a WPb target of 6 kg/m^3.

4.7.2 Identify the bright spots

The bright spots are identified based on the target biomass and target biomass water productivity (WPb). The identification of bright spots is crucial for determining the most effective practices and for adapting lessons to suit the unique conditions of each area. Thus, we employed the 90th percentile threshold for both yield and Water Productivity (WP) to categorize areas as bright spots, while fields falling below the 10th percentile were classified as hot spots. Figure 4.16 demonstrates the locations that reach the target levels in B (green), WPb (red), and the bright spots (blue). Figure 4.18 shows the annual maps of the bright spot for 2009/2010 and 2021/2022 (annual maps from 2009/2010 to 2011/2012 are provided in Appendix A.9). The majority of the areas that meet the land productivity target and the biomass water productivity are located in the Wonji main (surface irrigation), the eastern section of Boku (furrow irrigation), most parts of Adulala (furrow irrigation), the northern section of WakeMia(furrow), northeastern of WakeTio(furrow) and the most parts of WakeTio (sprinkler irrigation) expansion during 2009/10. Between 2021 and 2022, most of the bright spots are located below the center in Wonji main and Dodota.

During 2010-2011, fields achieving targets B and WPb were primarily located in certain areas of Wonji main, Adulala, Wake Mia, Wake Tio, Wake Tio expansion, Hargitti, and Bishola site. In 2011-2012, the same bright spots were observed, but with increased targets B and WPb in the Wonji main site. In 2012-2013, most of the Wake Tio expansion, Hargitti, Bishola, and several parts of Dodota reached their goals. In the 2013-2014 period, parts of Adulala, Wake Mia, Wake Tio, Dodota especially in sprinkler-irrigated areas, and Bishola site met their targets. During 2014-2015, sections of Boku, Wake Mia, northeastern parts of Wake Tio expansion, and areas below the center of Dodota also achieved their targets. In 2015-2016, parts of Adulala, Boku, Wonji main, Wake Mia, Wake Tio, northeastern Wake Tio expansion, Hargitti, Bishola, and areas above the center of Dodota reached their targets. During 2016-2017, a small section of Wake Tio expansion, areas below the center of the Dodota, Bishola, and Hargitti sites achieved their goals. In 2017-2018, similar patterns of bright spots were observed as in 2016-2017, but with an increasing number of target spots at Wake Tio expansion, Hargitti, Bishola, and Dodota sites. In the 2018-2019 period, sections of the northeastern edge of Wonji main, Dodota, Hargitti, Bishola, and a small portion of Wake Tio expansion achieved their targets.

During 2019-2020, the center of Wonji main, Hargitti, Bishola, and most of the Dodota site reached their goals. In the 2020-2021 period, parts of Wake Tio expansion, most sections of Hargitti and Bishola, and the majority of Dodota achieved their targets.

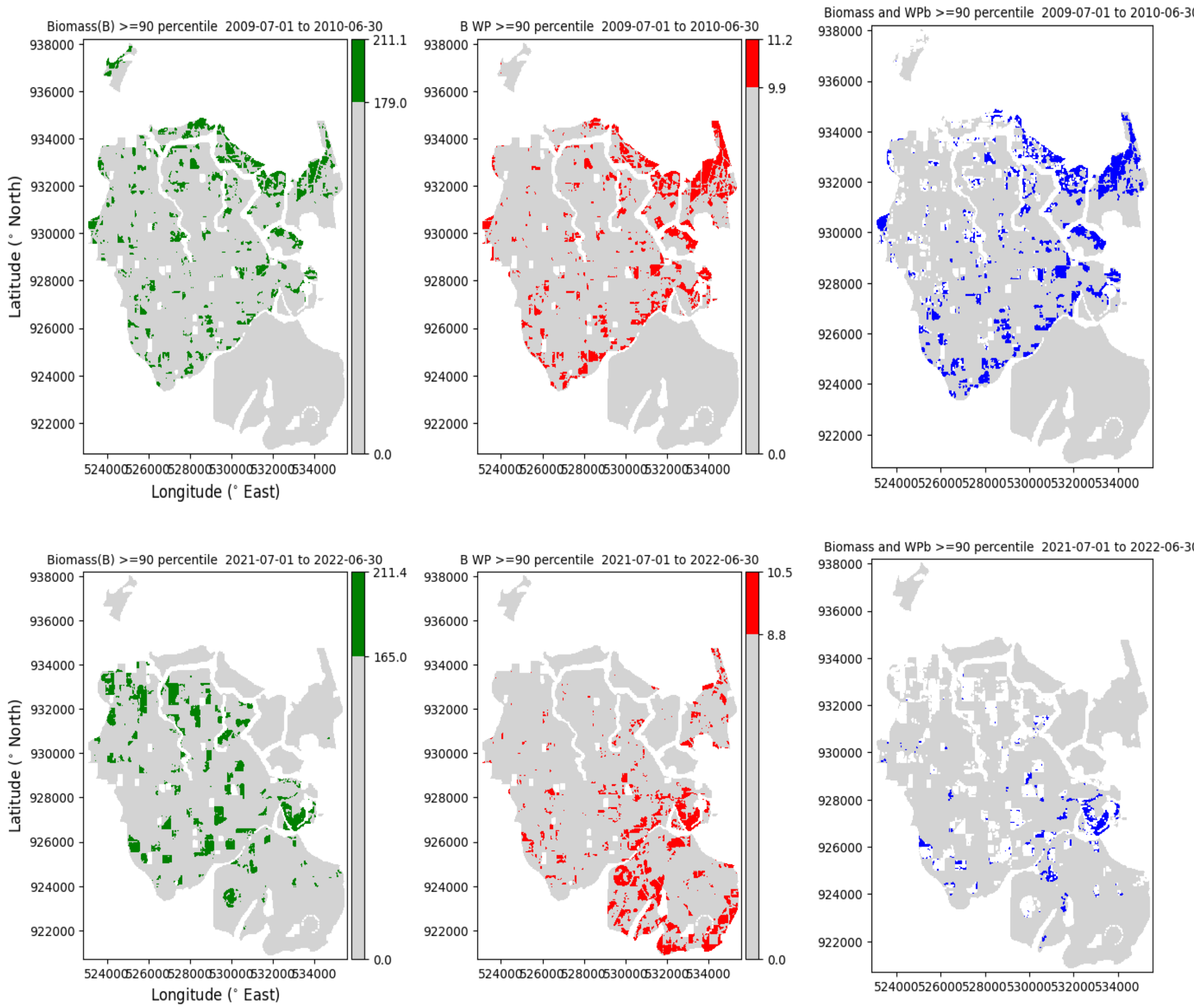

Figure 4.18 Spatial distribution of the bright spots, spots where biomass is beyond the target (a), spots where WPb are beyond the target (b), Spatial distribution of the bright spots, spots where biomass is beyond the target (a), spots where WPb are beyond the target (b), and spots where both biomass and WPb are beyond the target productivities (c) for the year of (2009-2010 and 2021-2022).

The methodology used in this study appears to be reliable as studied by previous researchers to assess remote sensing based on the spatial distribution of bright spots, spots where biomass is beyond the target, spots where WPb are beyond the target, and spots where both biomass and

WPb are beyond the target productivities for the Wonji Shoa sugarcane estate using remote sensing (RS) data. (Janssens, 2022) conducted research on the Metehara region, including Merti and Abadir sub-schemes, utilizing remote sensing WaPOR data from 2009-2021. The study determined a spatial distribution of the bright spots, demonstrating the locations that reach the target levels in B (green), WPb (red), and the bright spots (blue). Chukalla et al. (2021) similarly identified bright spots where both biomass and WPb are beyond the target productivities for the average season based on a five-year average (2014/2015 to 2018/2019). Their research revealed that the bright spots are located within the area classified as a mixed irrigation system, rather than the center pivot and furrow irrigation methods.

4.7.3 Productivity gaps

The productivity gaps were demarcated as the difference between the actual and target productivity of a certain field. The gaps were calculated for biomass and biomass water productivity separately. For each grid cell, the gap between the actual value and the target value in B and WPb was calculated and plotted in Figure 4.19. The annual maps providing the spatial distribution of each year's biomass gaps of sugarcane at Wonji Shoa from 2009 to 2022 are provided in Appendix A.10 and the biomass water productivity gaps are provided in Appendix A.11.

Under the furrow irrigation method implemented in the regions of Wonji main, Kuriftu, Hargitti, and Bishola, as well as the sprinkler irrigation methods employed in the WakeTio expansion, an average production gap of 39.0 ton/ha/year was observed during the period 2009-2022. Meanwhile, under the furrow irrigation method implemented in the areas of Boku, Adulala, WakeMia, and WakeTio, as well as the sprinkler irrigation method employed in the center of WakeTio expansion, and Dodota (both sprinkler and center pivot), the 13-year average production gap ranged from 76.2 to 113.2 ton/ha/year during the same period. Under the furrow irrigation method implemented in the region of Wonji main, Hargitti, Bishola, and Kuriftu, the average water productivity gap for 13 years (WPb) is 0.014 kg/m^3 /year. Meanwhile, in the areas of Boku, Adulala, WakeMia, WakeTio, and Dodota (both sprinkler and center pivot), the water productivity gap ranges between 1.26 and 3.8 kg/m^3 /year.

The spatial distribution of the productivity gap from 2009 to 2022 is comprehensively discussed and analyzed by classifying it into distinct zones to underscore the regional disparities in the productivity gap. This in-depth examination utilizes zonal statistics as outlined in Section 4.8 of the forward pages, which provides a detailed and systematic approach to understanding the variations in productivity across different zones.

The methodology used in this study appears to be reliable as studied by previous researchers to assess remote sensing-based productivity gaps. (Janssens, 2022) conducted research on the Metehara region, including Merti and Abadir sub-schemes, utilizing remote sensing WaPOR data from 2009-2021 for the spatial distribution of the gap between the actual value and the target value in B and WPb. Overall, the results suggest the need for improvements in irrigation techniques to bridge the production gap as well as to enhance land and water productivity in these regions.

Closing the biomass gaps at Wonji Shoa would raise the 13-season average biomass production from 119.9 ton/ha/year over 10,987 ha to the target biomass of 162.4 ton/ha/year, this could increase the biomass production by 466,947.5 tons/year. And also closing the biomass water productivity gap at Wonji Shoa raise the 13-year average biomass water productivity from 8.3 $\mathrm{kg/m^3}$ to the target biomass water productivity 8.5 $\mathrm{kg/m^3}$. Thus, such an increase in production from the existing irrigation scheme helps to limit agricultural land expansion which otherwise would compete with the land use by other crops or biodiversity. This result is supported by research conducted by Chukalla et al. (2020), who found a similar effect when closing the biomass gaps at Xinavane would raise the five-season average biomass production from 77±7 ton/ha/year over 9,453 ha to the target biomass 88±6 ton/ha/year. This could increase the biomass production by 105,860 tons/year, which is equivalent to expanding the cultivation by ~1,203 ha (based on the target productivity: 78 ton/ha and 5.5$\mathrm{kg/m^3}$) to ~1,375 ha (based on the current productivity: 77 ton/ha).

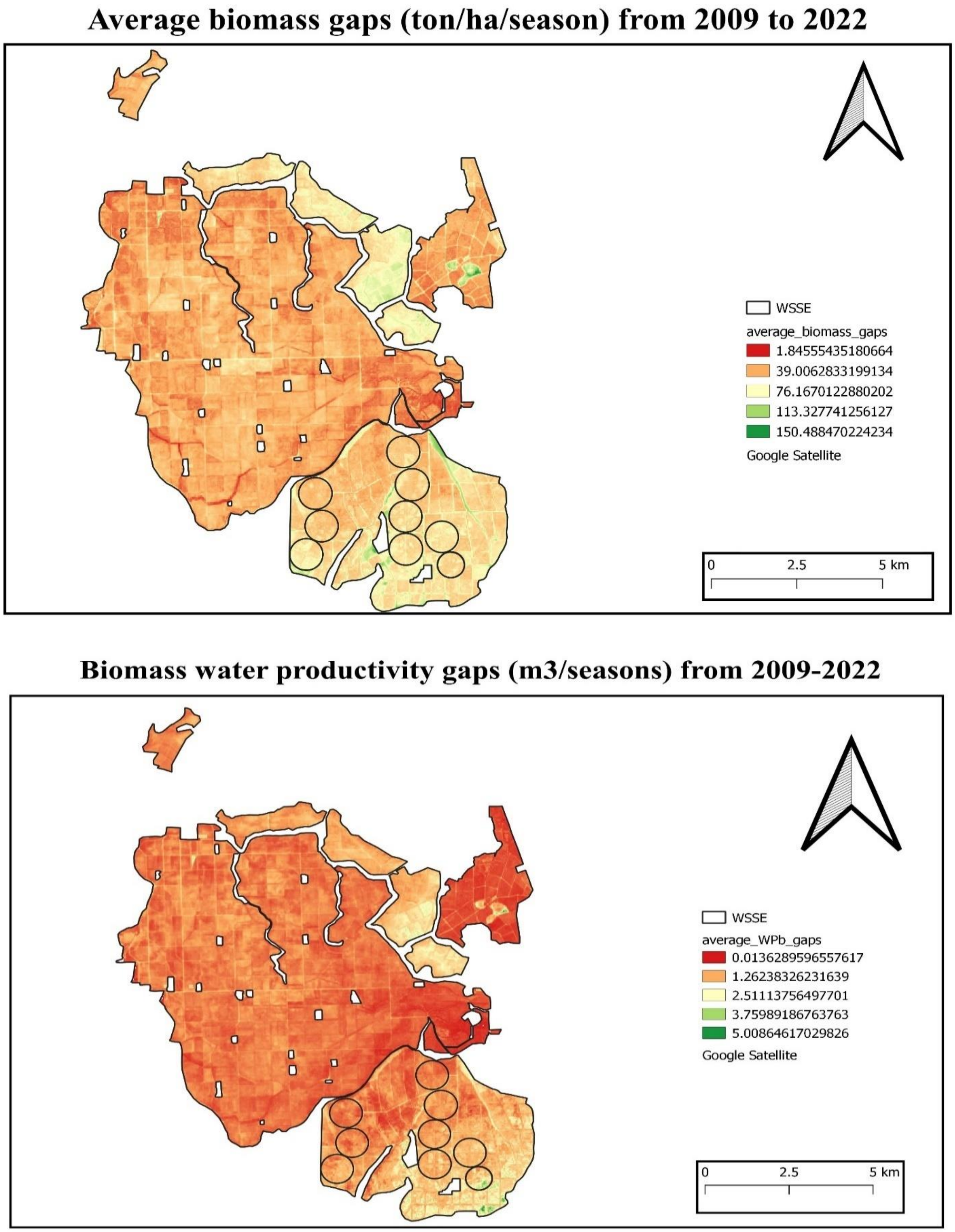

Figure 4.19 Spatial variation of biomass gaps (ton/ha/season) (a) and biomass water productivity gaps (b) at Wonji irrigation scheme.

4.8 Zonal statistics

The zonal statistics findings help to emphasize the regional differences in agricultural productivity and resource usage to better develop and implement tailored crop management and improvement strategies in different zones. Figure 4.18 presents the 19 zones on ID 1 to 19 of Wonji Shoa to show significant variations in yield, water productivity, and yield gaps across different zones from 7/1/2009 to 6/30/2022.

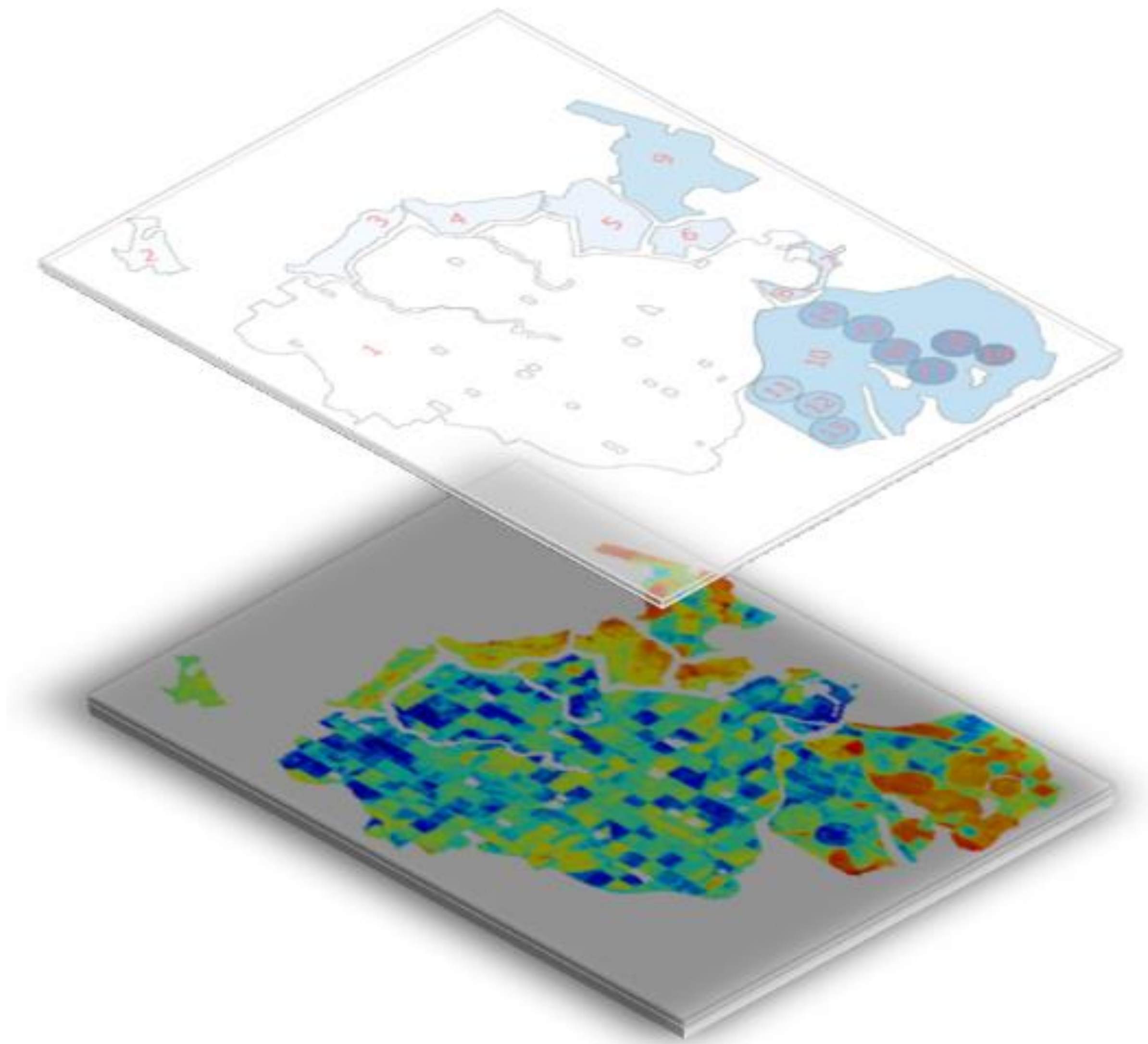

Figure 4.20 The 19 zones on the IDs 1 to 19 of WSSE show significant variations in yield, water productivity, and yield gaps across different zones from 7/1/2009 to 6/30/2022.

From 7/1/2009 to 6/30/2010, zone 4 had the highest yield mean (171.4 ton/ha/season) and the highest water productivity (9.75 kg/m^3), while zone 18 had the lowest yield mean (16.93 ton/ha/season) and the lowest water productivity (4.44 kg/m^3). This indicates that higher average yields tend to have more efficient water usage. The yield gap means, which represents the difference between potential and actual yields, shows significant room for improvement in many zones. Zone 4 has the smallest yield gap (22.3 ton/ha/season), while zone 18 has the largest (162.07 ton/ha/season), implying that zone 18 has the most potential for increased yield. Figure 4.19 shows the average yield, crop yield water productivity (WPb), and yield gap variation for different zones for the period 2009-2010. The remaining annual figures are shown in Appendix A.12.

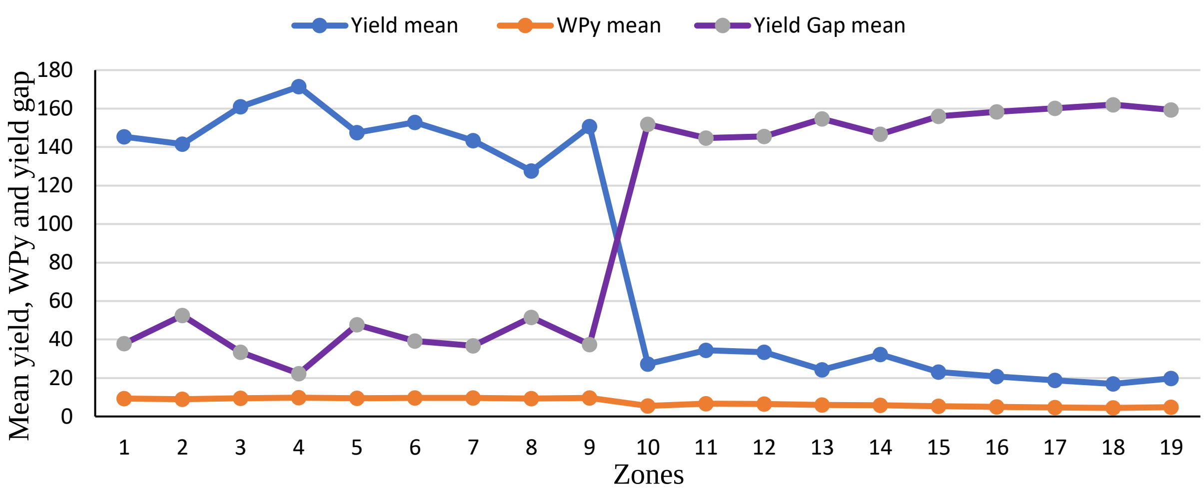

Figure 4.21 Average yield, Crop Yield water productivity (WPb), and Yield gap for different zones from 2009 to 2010.

Between 7/1/2010 and 6/30/2011, Zone 7 had the highest average crop yield at 156.5 ton/ha/season and the highest water productivity for crop production at 9.71 kg/m^3. In contrast, Zone 13 had the lowest crop yield (21.03 ton/ha/season) and the highest yield gap (131.47 ton/ha/season), while Zone 10 had the lowest water productivity (6.13 kg/m^3). Zone 8 performed more efficiently, with the lowest yield gap at 6.73 ton/ha/season. From 7/1/2011 to 6/30/2012, the highest average yield was in zone 4 (139.9 ton/ha/season) and the lowest in zone 13 (27.38 ton/ha/year). Zone 8 had the highest water productivity (8.45 kg/m^3), while zone 13 had the lowest (5.86 kg/m^3). The largest yield gap was in zone 13 (130.02 ton/ha/season) and the smallest in zone 4 (27.03 ton/ha/season), indicating better performance in zone 4. From 7/1/2012 to 6/30/2013, the highest average yield was in zone 12 (166.9 ton/ha/season) and the lowest in zone 13 (60.74 ton/ha/season). The highest water productivity was in zone 7 (9.58 kg/m^3), and the lowest in zone 13 (7.53 kg/m^3). The largest yield gap was in zone 13 (99.86) and the smallest in zone 8 (10.03), indicating better performance in zone 8.

Between 7/1/2013 and 6/30/2014, zone 11 had the highest average crop yield (166.9 ton/ha/season), while zone 8 had the lowest (109.3 ton/ha/season). Water productivity was highest in zone 19 (10.23 kg/m^3) and lowest in zone 1 (9.07 kg/m^3). The yield gap was largest in zone 6 (58.64 ton/ha/season) and smallest in zone 14 (12.41 ton/ha/season), indicating greater potential for crop yield improvement in zone 6. From 7/1/2014 to 6/30/2015, zone 7 has the highest average yield (158.1 ton/ha/season), while zone 13 has the lowest average yield (111.6 ton/ha/season). The highest water productivity (WPb mean) is seen in zone 7 (9.29 kg/m^3), and the lowest is in zone 1 (8.42 kg/m^3). The highest Yield Gap mean is observed in Zone 13 (49.21 ton/ha/season), whereas the lowest is in Zone 12 (12.78 ton/ha/season).

Between 7/1/2015 and 6/30/2016, zone 7 had the highest average yield (186.6 ton/ha/season) and water productivity (9.32 kg/m^3), while zone 18 had the lowest average yield (65.98 ton/ha/season) and water productivity (7.29 kg/m^3). The highest yield gap was observed in zone 18 (110.62 ton/ha/season), indicating greater potential for improvement, while the lowest was in zone 14 (12.84 ton/ha/season), implying less potential for improvement. From 7/1/2016 to 6/30/2017, the average crop yield varied across zones, with Zone 3 having the lowest yield (62.4 ton/ha/season) and Zone 8 having the highest (148.6 ton/ha/season). Water productivity was overall high, ranging from 7.11 kg/m^3 in Zone 3 to 8.67 kg/m^3 in Zone 19. There were significant yield gaps, with the mean value ranging from 10.2 in Zone 18 to 84.1 ton/ha/year in Zone 3.

Between 7/1/2017 and 6/30/2018, the crop yield mean varied from a low of 40.39 ton/ha/season in Zone 5 to a high of 169.7 ton/ha/season in Zone 7. The WPb mean (Crop Yield water productivity) ranged from a low of 5.55 kg/m^3 in Zone 5 to a high of 9.83 kg/m^3 in Zone 7. The yield gap means varied from a low of 15.61 ton/ha/season in Zone 8 to a high of 124.61 ton/ha/season in Zone 5, indicating the greater potential for improvement in these areas. Between July 2018 and June 2019, average crop yields ranged from 47.13 to 159.4

tons/ha/season across different zones, and water productivity varied from 5.66 to 8.77 $\mathrm{kg/m^3}$. This indicates significant differences in water productivity among zones. The yield gap was between 17.31 and 115.97 tons/ha/season, suggesting potential for improvement in some zones through better management practices and resource use.

Between 7/1/2019 and 6/30/2020, the highest average yield was in Zone 7 (186.6 tons/ha/season) and the lowest was in Zone 6 (43.89 tons/ha/season). The highest WPb mean was in Zone 12 (10.04 $\mathrm{kg/m^3}$) and the lowest in Zone 6 (5.33 $\mathrm{kg/m^3}$). The widest yield gap mean was in Zone 6 (128.41 tons/ha/season) and the narrowest was in Zone 14 (10.36 tons/ha/season). Between 7/1/2020 and 6/30/2021, zone 7 showed the best water resource usage for crop production with the highest average yield (183.8 ton/ha/season) and water productivity (9.23 $\mathrm{kg/m^3}$). On the other hand, zone 6 had the lowest efficiency with an average yield of 30.228 ton/ha/season and water productivity of 4.29 $\mathrm{kg/m^3}$. The largest yield gap was in zone 6, with 119.18 ton/ha/season, while the smallest was in zone 8 with 12.29 ton/ha/season. From 7/1/2021 to 6/30/2022, the highest average crop yield was in Zone 7 at 168.6 ton/ha/season, and the lowest was in Zone 6 at 57.48 ton/ha/season, indicating favorable conditions for crop growth in Zone 7. The crop yield water productivity varied between zones, with the highest efficiency (8.89 $\mathrm{kg/m^3}$) in Zone 11 and the lowest (5.73 $\mathrm{kg/m^3}$) in Zone 6. Zone 7 had the smallest yield gap and was closer to achieving its potential yield, while Zone 6 had the largest yield gap, indicating significant room for improvement.

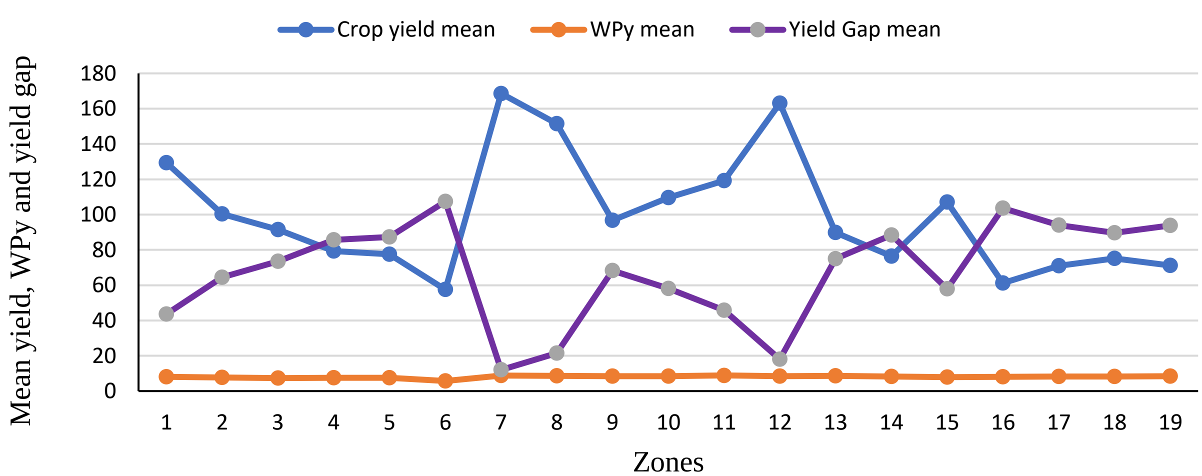

Figure 4.22 Average yield, Crop Yield water productivity (WPb), and Yield gap for different zones from 2021-2022.

5 CONCLUSIONS AND RECOMMENDATIONS

5.1 Conclusions

This study examines the spatiotemporal variability of land and water productivity and other irrigation performance indicators for average of thirteen growing seasons (2009-2022) at Wonji Shoa, sugarcane plantation. The seasonal monitoring of sugarcane production at Wonji sugar estate using WaPOR from 2009 to 2022 has demonstrated good results in assessing B and WPb. A strong statistical correlation was observed in the linear WPb trend analysis for seasonal Biomass (B) over seasonal ETa. This supports the established agronomic principles governing photosynthesis and crop water consumption are accurately represented in the WaPOR data. These positive findings indicate the strong potential for the WaPOR method to be effectively applied to large-scale and consistent agricultural production system.

The temporal variation of water consumption in the period 2009-2022 shows generally increasing trend, indicating that the goals of the ABWAP for reducing water use have not been met. The spatial distribution analysis exhibited that the fields in the Wonji Main, Wake Tio expansion, Hargitti, Bishola, and northwestern parts of the Dodota site had the highest $ETact$ and the highest land productivity (B). The overall uniformity of irrigation in the Wonji estate is fairly balanced, with water being adequately distributed throughout the area. However, furrow and sprinkler-irrigated areas are less efficient in even distribution. In contrast, the center pivot irrigated areas demonstrate the best performance in terms of achieving uniformity.

The spatial distribution of the average beneficial fraction from 2009-2022, revealed that furrow irrigation methods had the highest beneficial fraction (0.8289), closely followed by sprinkler-irrigated areas (0.8203), and center pivot irrigated areas lower (0.8033). This means that a larger portion of the water applied to crops was used for transpiration, promoting crop growth in the fields of Wonji main, Kuriftu, Boku, and Adulala. On the other hand, a lower beneficial fraction in the WakeMia, WakeTio, and some parts of Dodota fields suggested that more water was lost to non-beneficial processes, such as soil surface evaporation and deep drainage below the root zone. Considering the room for improvement, farmers and irrigation managers in areas with lower beneficial fractions should consider adopting more efficient methods to decrease water wastage and enhance water-use efficiency. The areas irrigated through furrow irrigation exhibit the highest adequacy levels at 0.70 which shows that the crop water requirements were also quite well met. In comparison, sprinkler-irrigated areas have an adequacy of 0.65, while those using center pivot irrigation have an adequacy of 0.64. This is primarily attributed to the relatively lower water consumption in these methods.

The temporal distribution of land productivity reveals similar trends and ranges, indicating no significant differences in the patterns and no noticeable changes over time. The yield estimates based on WaPOR were found to be comparable with observed yields with an average difference of 24.68%. The spatial distribution of biomass in the Wonji Shoa irrigation scheme, categorized by irrigation methods, shows that furrow irrigation achieved the highest B (120.4 tons/ha/year), followed by sprinkler-irrigated areas (115.8 tons/ha/year), and center pivot-irrigated areas (110.5 tons/ha/year). The higher B in furrow irrigation can be attributed to increased seasonal ETa values. Some lower-performing areas with B were observed in Boku, Adulala, Wake Mia, Wake Tio, and the southeasternmost Dodota fields, with biomass production ranging from 54 to 96 tons/ha/year. On the other hand, higher performing areas with B were found in Bishola and Hargitti, Wonji main, Kuriftu, and Wake Tio expansion, with biomass production ranging from 139-181 tons/ha/year. There is room for improvement for least productive schemes to enhance their efficiency and increase overall productivity.

The temporal findings revealed that the average WPb decreased over time, meaning that over time more water was needed to produce the same amount of biomass. The average water productivity (WPb) was 8.3 kg/m^3, with sprinkler-irrigated areas ranking highest with an 8.5 kg/m^3 WPb, followed by center pivot and furrow-irrigated areas with an 8.3 kg/m^3 WPb. The spatial distribution of WPb showed that certain areas, including Hargitti, Bishola, Wonji main, Kuriftu, Wake Tio expansion, and parts of Boku and Adulala schemes, exhibit higher WPb values ranging from 8.6-10 kg/m^3. Conversely, some sites, such as parts of Wake Mia, Wake Tio, and northeastern Dodota fields, display lower WPb values ranging from 5.7-8 kg/m^3. There is certainly potential for improvement in the lower biomass water productivity schemes.

The spatial distribution of production gaps showed that from 2009-2022, a 39.0 ton/ha/year average production gap was observed in the areas of Wonji main, Kuriftu, Hargitti, and Bishola, where the furrow irrigation method was used, as well as in the WakeTio expansion, where sprinkler irrigation methods were employed. On the other hand, the areas of Boku, Adulala, WakeMia, and WakeTio, which also utilized furrow irrigation, along with the center of WakeTio expansion and Dodota (both implementing sprinkler and center pivot irrigations), experienced a 13-year average production gap ranging from 76.2 to 113.2 ton/ha/year. In the Wonji main, Hargitti, Bishola, and Kuriftu regions where furrow irrigation methods are used, the 13-year average water productivity gap (WPb) is 0.014 $\mathrm{kg/m^3}$ /year. On the other hand, in Boku, Adulala, WakeMia, WakeTio, and Dodota regions that employ both sprinkler and center pivot systems, the water productivity gap varies from 1.26 to 3.8 $\mathrm{kg/m^3}$ /year.

The analysis of zonal statistics from 2009 to 2022 highlights significant spatial variations in crop yield, water productivity, and yield gap across different zones. Zones such as 4, 7, and 8 have consistently displayed high crop yields and water productivity, indicating efficient water use and good agricultural performance. In contrast, zones 13 and 18 have struggled with low crop yields and water productivity, suggesting a need for improvement in these areas.

By closing the biomass gaps at Wonji Shoa, the 13-season average biomass production could be increased from 119.9 tons/ha/year across 10,987 ha to the target biomass of 162.4 tons/ha/year. This would result in an additional biomass production of 466,947.5 tons/year. Furthermore, closing the biomass water productivity gap at Wonji Shoa would raise the 13-year average biomass water productivity from 8.3 $\mathrm{kg/m^3}$ to the target of 8.5 $\mathrm{kg/m^3}$.

5.2 Recommendations

The study demonstrates the potential of using RS-derived data to pinpoint areas with the highest land and water productivity, as well as detecting spatial variability in performance linked to plant stress. However, the underlying causes for this variability cannot be determined solely from RS-derived data. The study's findings regarding plant stress are supported by field observations and previous research, which suggest that factors such as farm management, inputs, waterlogging, and salinity contribute to variations in land productivity. As a result, accurate interpretation of the data, diagnosing productivity gaps, and development of practical solutions can only be achieved when WaPOR analyses and results are combined with observed field data. This additional information helps to better understand the production context of the fields and investigate the constraints faced. Subsequent studies could additionally consider socio-economic performance indicators, such as social water productivity (e.g., employment per water use or land use) and economic water productivity (economic return per water or land use), which could help to conduct comprehensive performance assessment of irrigation schemes.

REFERENCES

Allen, R. G., Pereira, L. S., Raes, D., & Smith, M. (1998). Crop evapotranspiration-Guidelines for computing crop water requirements-FAO Irrigation and drainage paper 56. Fao, Rome, 300(9), D05109.

Alemayehu, T., Bastiaanssen, S., Bremer, K., Cherinet, Y., Chevalking, S., Girma, M. 2020. Water Productivity Analyses Using WaPOR Database. A Case Study of Wonji, Ethiopia. WaterPIP technical report series. IHE Delft Institute for Water Education, Delft, the Netherlands

Araya, A., Stroosnijder, L., Girmay, G., & Keesstra, S. D. (2011). Crop coefficient, yield response to water stress and water productivity of teff (Eragrostis tef (Zucc.). Agricultural Water Management, 98(5), 775–783.

Bakkes, J. A. (2009). Getting into the Right Lane for 2050. A primer for EU debate.

Baldocchi, D. D. (2003). Assessing the eddy covariance technique for evaluating carbon dioxide exchange rates of ecosystems: Past, present and future. Global Change Biology, 9(4), 479–492.

Barideh, R., & Nasimi, F. (2022). Investigating the changes in agricultural land use and actual evapotranspiration of the Urmia Lake basin based on FAO's WaPOR database. Agricultural Water Management, 264, 107509.

Bastiaanssen, W. G., & Ali, S. (2003). A new crop yield forecasting model based on satellite measurements applied across the Indus Basin, Pakistan. Agriculture, Ecosystems & Environment, 94(3), 321–340.

Bastiaanssen, W. G., & Bos, M. G. (1999). Irrigation performance indicators based on remotely sensed data: A review of literature. Irrigation and Drainage Systems, 13, 291–311.

Bastiaanssen, W. G. M., Cheema, M. J. M., Immerzeel, W. W., Miltenburg, I. J., & Pelgrum, H. (2012). Surface energy balance and actual evapotranspiration of the transboundary Indus Basin estimated from satellite measurements and the ETLook model. Water Resources Research, 48(11).

Bastiaanssen, W. G. M., Menenti, M., Feddes, R. A., & Holtslag, A. A. M. (1998). A remote sensing surface energy balance algorithm for land (SEBAL). 1. Formulation. Journal of Hydrology, 212–213, 198–212. https://doi.org/10.1016/S0022-1694(98)00253-4

Bastiaanssen, W. G., Molden, D. J., & Makin, I. W. (2000). Remote sensing for irrigated agriculture: Examples from research and possible applications. Agricultural Water Management, 46(2), 137–155.

Bastiaanssen, W. G., & Steduto, P. (2017). The water productivity score (WPS) at global and regional level: Methodology and first results from remote sensing measurements of wheat, rice and maize. Science of the Total Environment, 575, 595–611.

Bastiaanssen, W. G., Van der Wal, T., & Visser, T. N. M. (1996). Diagnosis of regional evaporation by remote sensing to support irrigation performance assessment. Irrigation and Drainage Systems, 10, 1–23.

Blatchford, M. L., Karimi, P., Bastiaanssen, W. G. M., & Nouri, H. (2018). From global goals to local gains—A framework for crop water productivity. ISPRS International Journal of Geo-Information, 7(11), 414.

Blatchford, M. L., Mannaerts, C. M., Njuki, S. M., Nouri, H., Zeng, Y., Pelgrum, H., Wonink, S., & Karimi, P. (2020). Evaluation of WaPOR V2 evapotranspiration products across Africa. Hydrological Processes, 34(15), 3200–3221.

Blatchford, M. L., Mannaerts, C. M., Zeng, Y., Nouri, H., & Karimi, P. (2019). Status of accuracy in remotely sensed and in-situ agricultural water productivity estimates: A review. Remote Sensing of Environment, 234, 111413.

Bos, M. G. (1997). Performance indicators for irrigation and drainage. Irrigation and Drainage Systems, 11(2), 119–137.

Bos, M. G., Burton, M. A., & Molden, D. J. (2005). Diagnosing irrigation performance. Irrigation and Drainage Performance Assessment: Practical Guidelines, 87–116. https://doi.org/10.1079/9780851999678.0087

Casley, D. J., & Kumar, K. (1988). The collection, analysis and use of monitoring and evaluation data. The World Bank.

Chukalla, A. D., Mul, M. L., Van Der Zaag, P., Van Halsema, G., Mubaya, E., Muchanga, E., Den Besten, N., & Karimi, P. (2022). A framework for irrigation performance assessment using WaPOR data: The case of a sugarcane estate in Mozambique. Hydrology and Earth System Sciences, 26(10), 2759–2778.

Chukalla, A. D., Mul, M., Tran, B., & Karimi, P. (2021). Standardized protocol for land and water productivity analyses using WaPOR (1.1) [Jupyter Notebook]. https://doi.org/10.5281/zenodo.4641360

Chukalla, A. D., Mul, M., van Halsema, G., van der Zaag, P., Uyttendaele, T., & Karimi, P. (2020). Water Productivity Analyses using the WaPOR Database. A Case Study in Xinavane, Mozambique, IHE Delft Institute for Water Education, Delft, the Netherlands.

Chukalla, A., Mul, M., Halsema, G. V., Zaag, P., & Uyttendaele, T. (2021). Water Productivity Analyses using the WaPOR Database. https://www.semanticscholar.org/paper/Water-Productivity-Analyses-using-the-WaPOR-Chukalla-Mul/f43f778f162a68364ffd56ad16b92c4aa239a05b

Clemmens, A. J., & Molden, D. J. (2007). Water uses and productivity of irrigation systems. Irrigation Science, 25, 247–261.

Colaço, A. F., & Bramley, R. G. V. (2018). Do crop sensors promote improved nitrogen management in grain crops? Field Crops Research, 218, 126–140. https://doi.org/10.1016/j.fcr.2018.01.007

Conrad, C., Usman, M., Morper-Busch, L., & Schönbrodt-Stitt, S. (2020). Remote sensing-based assessments of land use, soil and vegetation status, crop production and water use in irrigation systems of the Aral Sea Basin. A review. Water Security, 11, 100078.

de Wit, C. T. (1958). Transpiration and crop yields.

Dejen, Z. A. (2014). Hydraulic and Operational Performance of Irrigation System in View of Interventions for Water Saving and Sustainability [PhD Thesis]. UNESCO-IHE Institute for Water Education Delft, The Netherlands.

Dejen, Z. A. (2015). Hydraulic and operational performance of irrigation schemes in view of water saving and sustainability: Sugar estates and community managed schemes In Ethiopia. Wageningen University and Research.

Di Gregorio, A. (2005). Land cover classification system: Classification concepts and user manual: LCCS (Vol. 2). Food & Agriculture Org.

Du, M., & Noguchi, N. (2017). Monitoring of Wheat Growth Status and Mapping of Wheat Yield's within-Field Spatial Variations Using Color Images Acquired from UAV-camera System. Remote Sensing, 9(3), Article 3. https://doi.org/10.3390/rs9030289

Edreira, J. I. R., Guilpart, N., Sadras, V., Cassman, K. G., van Ittersum, M. K., Schils, R. L., & Grassini, P. (2018). Water productivity of rainfed maize and wheat: A local to global perspective. Agricultural and Forest Meteorology, 259, 364–373.

FAO. (1998). Chapter 6. ETc - single crop coefficient (Kc). In FAO (Red.), Crop Evapotranspiration. Guidelines for computing crop water requirements. (Reprinted in 2000 ed., pp. 103–114). FAO.

FAO. (2001). Lecture notes on the major soils of the world. In World Soil Resources Reports, 94 (p. 334). Food and Agriculture Organization of the United Nations Rome, Italy.

FAO. (2019). WaPOR Database methodology: Level 3 data: Using remote sensing in support of solutions to reduce agricultural water productivity gaps. FAO. https://www.fao.org/documents/card/en?details=CA3750EN%2f

FAO. (2020). WaPOR Database Methodology: Version 2 Release, April 2020. FAO Rome, Itay.

FAO and IHE Delft. (2019). WaPOR quality assessment: Technical report on the data quality of the WaPOR FAO database version 1.0. FAO and IHE Delft. https://www.fao.org/documents/card/en?details=CA4895EN%2f

FAO Water Productivity. (n.d.). Retrieved May 21, 2023, from https://wapor.apps.fao.org/home/WAPOR_2/1

Fao: WFP and WHO. 2019. The state of food security... - Google Scholar. (n.d.). Retrieved May 29, 2023, from https://scholar.google.com/scholar_lookup?title=The State of Food Security and Nutrition in the World Safeguarding Against Economic Slowdowns and Down turns & author=FAO& publication year=2019

Fernandez-Ordoñez, Yolanda. M., & Soria-Ruiz, J. (2017). Maize crop yield estimation with remote sensing and empirical models. 2017 IEEE International Geoscience and Remote Sensing Symposium (IGARSS). https://doi.org/10.1109/IGARSS.2017.8127638

Ferreira, E., Mannaerts, C. M., Dantas, A. A., & Maathuis, B. H. (2016). Surface energy balance system (SEBS) and satellite data for monitoring water consumption of irrigated sugarcane. Engenharia Agrícola, 36, 1176–1185.

Foken, T. (2008). The energy balance closure problem: An overview. Ecological Applications, 18(6), 1351–1367.

Foley, J. A., Ramankutty, N., Brauman, K. A., Cassidy, E. S., Gerber, J. S., Johnston, M., Mueller, N. D., O'Connell, C., Ray, D. K., & West, P. C. (2011). Solutions for a cultivated planet. Nature, 478(7369), 337–342.

Geerts, S., & Raes, D. (2009). Deficit irrigation as an on-farm strategy to maximize crop water productivity in dry areas. Agricultural Water Management, 96(9), 1275–1284.

Gemechu, M. G., Hulluka, T. A., & Wakjira, Y. C. (2020). Analysis of spatiotemporal variability of water productivity in Ethiopian sugar estates: Using open access remote sensing source. Annals of GIS, 26(4), 395–405. https://doi.org/10.1080/19475683.2020.1812716

Girma, M. M. A., & Seleshi, B. (2007). Irrigation practices in Ethiopia: Characteristics of selected irrigation schemes (Vol. 124). IWMI.

Girma, A. (2020). Interview: Water Productivity and Sugarcane Production in Wonji-Shoa Sugar Estate, Ethiopia

Gonzalez-Rodriguez, S., & Fernandez-Marcos, M. L. (2018). Phosphate sorption and desorption by two contrasting volcanic soils of equatorial Africa. PeerJ, 6, e5820.

Goswami, D., Kalita, P. K., Cooke, R. A. C., & McIsaac, G. F. (2009). Nitrate-N loadings through subsurface environment to agricultural drainage ditches in two flat Midwestern (USA) watersheds. Agricultural Water Management, 96(6), 1021–1030.

Group, W. W. (1998). World reference base for soil resources. FAO World Soil Resources Report, 84.

Hellegers, P., Soppe, R., Perry, C. J., & Bastiaanssen, W. G. M. (2009). Combining remote sensing and economic analysis to support decisions that affect water productivity. Irrigation Science, 27, 243–251.

Hess, T. M., Sumberg, J., Biggs, T., Georgescu, M., Haro-Monteagudo, D., Jewitt, G., Ozdogan, M., Marshall, M., Thenkabail, P., & Daccache, A. (2016). A sweet deal? Sugarcane, water and agricultural transformation in Sub-Saharan Africa. Global Environmental Change, 39, 181–194.

Higgins, S., Schellberg, J., & Bailey, J. S. (2019). Improving productivity and increasing the efficiency of soil nutrient management on grassland farms in the UK and Ireland using precision agriculture technology. European Journal of Agronomy, 106, 67–74.

Hirwa, H., Zhang, Q., Li, F., Qiao, Y., Measho, S., Muhirwa, F., Xu, N., Tian, C., Cheng, H., Chen, G., Ngwijabagabo, H., Turyasingura, B., & Itangishaka, A. C. (2022). Water Accounting and Productivity Analysis to Improve Water Savings of Nile River Basin, East Africa: From Accountability to Sustainability. Agronomy, 12(4), Article 4. https://doi.org/10.3390/agronomy12040818

Hong, M., Bremer, D. J., & van der Merwe, D. (2019). Thermal imaging detects early drought stress in turfgrass utilizing small unmanned aircraft systems. Agrosystems, Geosciences & Environment, 2(1), 1–9.

Janssens, A. (2022). Spatial and temporal analysis in land and water productivity using WaPOR data. A case study of the sugarcane plantations of Metahara, Ethiopia [Master's Thesis].

Jensen, T., Apan, A., Young, F., & Zeller, L. (2007). Detecting the attributes of a wheat crop using digital imagery acquired from a low-altitude platform. Computers and Electronics in Agriculture, 59(1), 66–77. https://doi.org/10.1016/j.compag.2007.05.004

Jin, X., Liu, S., Baret, F., Hemerlé, M., & Comar, A. (2017). Estimates of plant density of wheat crops at emergence from very low altitude UAV imagery. Remote Sensing of Environment, 198, 105–114.

Karimi, P., Bongani, B., Blatchford, M., & de Fraiture, C. (2019). Global Satellite-Based ET Products for the Local Level Irrigation Management: An Application of Irrigation Performance Assessment in the Sugarbelt of Swaziland. Remote Sensing, 11(6), Article 6. https://doi.org/10.3390/rs11060705

Karimi, P., David, S., & Bastiaanssen, W. G. (2011). Mapping crop water productivity in the Nile basin through combined use of remote sensing and census data.

Khanal, S., Fulton, J., Klopfenstein, A., Douridas, N., & Shearer, S. (2018). Integration of high resolution remotely sensed data and machine learning techniques for spatial prediction of soil properties and corn yield. Computers and Electronics in Agriculture, 153, 213–225. https://doi.org/10.1016/j.compag.2018.07.016

Khanal, S., Kc, K., Fulton, J. P., Shearer, S., & Ozkan, E. (2020). Remote sensing in agriculture—Accomplishments, limitations, and opportunities. Remote Sensing, 12(22), 3783.

Kulkarni, S. S., Bajwa, S. G., & Huitink, G. (2010). Investigation of the effects of soil compaction in cotton. Transactions of the ASABE, 53(3), 667–674.

Li, H., Zheng, L., Lei, Y., Li, C., Liu, Z., & Zhang, S. (2008). Estimation of water consumption and crop water productivity of winter wheat in North China Plain using remote sensing technology. Agricultural Water Management, 95(11), 1271–1278.

Licker, R., Johnston, M., Foley, J. A., Barford, C., Kucharik, C. J., Monfreda, C., & Ramankutty, N. (2010). Mind the gap: How do climate and agricultural management explain the 'yield gap'of croplands around the world? Global Ecology and Biogeography, 19(6), 769–782.

Lobell, D. B., Ortiz-Monasterio, J. I., Addams, C. L., & Asner, G. P. (2002). Soil, climate, and management impacts on regional wheat productivity in Mexico from remote sensing. Agricultural and Forest Meteorology, 114(1–2), 31–43.

Lobell, D. B., Thau, D., Seifert, C., Engle, E., & Little, B. (2015). A scalable satellite-based crop yield mapper. Remote Sensing of Environment, 164, 324–333. https://doi.org/10.1016/j.rse.2015.04.021

López-Granados, F., Torres-Sánchez, J., De Castro, A.-I., Serrano-Pérez, A., Mesas-Carrascosa, F.-J., & Peña, J.-M. (2016). Object-based early monitoring of a grass weed in a grass crop using high resolution UAV imagery. Agronomy for Sustainable Development, 36(4), 67. https://doi.org/10.1007/s13593-016-0405-7

Mali, S. (2016). Basic concepts of water productivity. Indian Council for Research.

Metameta_waterpip_wp1_wonji_reduced-main_report.pdf. (n.d.). Retrieved May 19, 2023, fromhttps://waterpip.un-ihe.org/sites/waterpip.un-ihe.org/files/metameta_waterpip_wp1_wonji_reduced-main_report.pdf

Molden, D. J., & Gates, T. K. (1990a). Performance measures for evaluation of irrigation-water-delivery systems. Journal of Irrigation and Drainage Engineering, 116(6), 804–823.

Molden, D. J., Sakthivadivel, R., Perry, C. J., & De Fraiture, C. (1998). Indicators for comparing performance of irrigated agricultural systems (Vol. 20). Iwmi.

Möller, M., Alchanatis, V., Cohen, Y., Meron, M., Tsipris, J., Naor, A., Ostrovsky, V., Sprintsin, M., & Cohen, S. (2007). Use of thermal and visible imagery for estimating crop water status of irrigated grapevine*. Journal of Experimental Botany, 58(4), 827–838. https://doi.org/10.1093/jxb/erl115

Morel, J., Todoroff, P., Bégué, A., Bury, A., Martiné, J.-F., & Petit, M. (2014). Toward a satellite-based system of sugarcane yield estimation and forecasting in smallholder farming conditions: A case study on Reunion Island. Remote Sensing, 6(7), 6620–6635.

Mul, M., & Bastiaanssen, W. (2019). WaPOR quality assessment: Technical report on the data quality of the WaPOR FAO database version 1.0, Rome, 134pp.

Mulianga, B., Bégué, A., Simoes, M., & Todoroff, P. (2013). Forecasting regional sugarcane yield based on time integral and spatial aggregation of MODIS NDVI. Remote Sensing, 5(5), 2184–2199.

Murphy, J., Casley, D. J., & Curry, J. J. (1991). Farmers' estimations as a source of production data: Methodological guidelines for cereals in Africa. The World Bank.

Mutiro, J., Makurira, H., Senzanje, A., & Mul, M. L. (2006). Water productivity analysis for smallholder rainfed systems: A case study of Makanya catchment, Tanzania. Physics and Chemistry of the Earth, Parts A/B/C, 31(15–16), 901–909.

Naz, B. S., Ale, S., & Bowling, L. C. (2009). Detecting subsurface drainage systems and estimating drain spacing in intensively managed agricultural landscapes. Agricultural Water Management, 96(4), 627–637.

Nock, C. A., Vogt, R. J., & Beisner, B. E. (2016). Functional Traits. In Encyclopedia of Life Sciences (pp. 1–8). John Wiley & Sons, Ltd. https://doi.org/10.1002/9780470015902.a0026282

Norman, D. W. (1995). The farming systems approach to development and appropriate technology generation. Food & Agriculture Org.

Palanisamy, S., Selvaraj, R., Ramesh, T., & Ponnusamy, J. (2019). Applications of Remote Sensing in Agriculture—A Review. International Journal of Current Microbiology and Applied Sciences, 8, 2270–2283. https://doi.org/10.20546/ijcmas.2019.801.238

Peña, J. M., Torres-Sánchez, J., de Castro, A. I., Kelly, M., & López-Granados, F. (2013). Weed mapping in early-season maize fields using object-based analysis of unmanned aerial vehicle (UAV) images. PloS One, 8(10), e77151.

Profile–Ethiopia, F. A. C. (2016). Food and Agriculture Organization of the United Nations (FAO). Rome, Italy.

Ramirez, O. A., Misra, S., & Field, J. (2003). Crop-yield distributions revisited. American Journal of Agricultural Economics, 85(1), 108–120.

Rana, G., & Katerji, N. (2000). Measurement and estimation of actual evapotranspiration in the field under Mediterranean climate: A review. European Journal of Agronomy, 13(2), 125–153. https://doi.org/10.1016/S1161-0301(00)00070-8

Renschler, C. S., & Flanagan, D. C. (2008). Site-specific decision-making based on RTK GPS survey and six alternative elevation data sources: Soil erosion predictions. Transactions of the ASABE, 51(2), 413–424.

Renschler, C. S., Flanagan, D. C., Engel, B. A., Kramer, L. A., & Sudduth, K. A. (2002). Site–specific decision–making based on RTK GPS survey and six alternative elevation data sources: Watershed topography and delineation. Transactions of the ASAE, 45(6), 1883.

Rijsberman, F. R. (2006). Water scarcity: Fact or fiction? Agricultural Water Management, 80(1–3), 5–22.

Ruffeis, D., Loiskandl, W., Spendlingwimmer, R., Schonerklee, M., Awulachew, S. B., Boelee, E., & Wallner, K. (2008). Environmental impact analysis of two large scale irrigation schemes in Ethiopia.

Safi, A. R., Karimi, P., Mul, M., Chukalla, A., & de Fraiture, C. (2022). Translating open-source remote sensing data to crop water productivity improvement actions. Agricultural Water Management, 261, 107373. https://doi.org/10.1016/j.agwat.2021.107373

Sawasawa, H. (2003). Crop yield estimation: Integrating RS, GIS, and management factors. International Institute for Geo-Information Science and Earth Observation, Enschede The Netherlands.

Simaika, J. B. (1982). Estimation of crop areas and yields in agricultural statistics. Estimation of Crop Areas and Yields in Agricultural Statistics. https://www.cabdirect.org/cabdirect/abstract/19826744064

Smith, D. M., Inman-Bamber, N. G., & Thorburn, P. J. (2005). Growth and function of the sugarcane root system. Field Crops Research, 92(2–3), 169–183.

Soliman, M. S. M., Abdel-Rahman, E. M., El-Saadany, E. F., & Mansour, R. R. (2008). A wideband vibration-based energy harvester. Journal of Micromechanics and Microengineering, 18(11), 115021.

Steduto, P., & Albrizio, R. (2005a). Resource use efficiency of field-grown sunflower, sorghum, wheat and chickpea: II. Water use efficiency and comparison with radiation use efficiency. Agricultural and Forest Meteorology, 130(3–4), 269–281.

Steduto, P., & Albrizio, R. (2005b). Resource use efficiency of field-grown sunflower, sorghum, wheat and chickpea: II. Water use efficiency and comparison with radiation use efficiency. Agricultural and Forest Meteorology, 130(3–4), 269–281.

Steduto, P., Hsiao, T. C., & Fereres, E. (2007). On the conservative behavior of biomass water productivity. Irrigation Science, 25, 189–207.

Sud: Synthesis of Literature and Framework under... - Google Scholar. (n.d.). Retrieved May 27, 2023, from https://scholar.google.com/scholar_lookup?title=Synthesis of Literature and Framework A Research on Improving Methods -for Estimating Crop Area Yield and Production Under Mixed Repeated and Continuous Cropping (Working Paper No.205)&author=U.C.Sud & publication_year=2016

Turral, H., Burke, J., & Faurès, J.-M. (2011). Climate change, water and food security. Food and agriculture organization of the United Nations (FAO).

UN. 2019. World Population Prospect. United Nation: Global.

UNESCO World Water Assessment Programme (WWAP), 2019. The United Nations World Water Development Report 2019: Leaving No One Behind. UNESCO World Water Assessment Programme (WWAP). Paris.

Verma, V., Marchant, T., & Scott, C. (1988). Evaluation of crop-cut methods and farmer reports for estimating crop production: Results of a methodological study in five African countries.

Villalobos, F. J., & Fereres, E. (2016). Principles of agronomy for sustainable agriculture. Springer.

Wang, L., Tian, Y., Yao, X., Zhu, Y., & Cao, W. (2014). Predicting grain yield and protein content in wheat by fusing multi-sensor and multi-temporal remote-sensing images. Field Crops Research, 164, 178–188. https://doi.org/10.1016/j.fcr.2014.05.001

Wang, Z. J., Wang, J. H., Liu, L. Y., Huang, W. J., Zhao, C. J., & Wang, C. Z. (2004). Prediction of grain protein content in winter wheat (Triticum aestivum L.) using plant pigment ratio (PPR). Field Crops Research, 90(2), 311–321. https://doi.org/10.1016/j.fcr.2004.04.004

WATPRO: A remote sensing-based model for mapping water productivity of wheat—ScienceDirect. (n.d.). Retrieved April 6, 2023, from https://www.sciencedirect.com/science/article/abs/pii/S037837741000185X

Yadeta, D., Kebede, A., & Tessema, N. (2020). Climate change posed agricultural drought and potential of rainy season for effective agricultural water management, Kesem sub-basin, Awash Basin, Ethiopia. Theoretical and Applied Climatology, 140, 653–666.

Yilma, W. A. (2017). Computation and spatial observation of water productivity in Awash River Basin [PhD Thesis]. UNESCO-IHE.

Zwart, S. J., & Bastiaanssen, W. G. (2004). Review of measured crop water productivity values for irrigated wheat, rice, cotton and maize. Agricultural Water Management, 69(2), 115–133.

Zwart, S. J., Bastiaanssen, W. G., de Fraiture, C., & Molden, D. J. (2010). A global benchmark map of water productivity for rainfed and irrigated wheat. Agricultural Water Management, 97(10), 1617–1627.

Zwart, S. J., & Bastiaanssen, W. G. M. (2007). SEBAL for detecting spatial variation of water productivity and scope for improvement in eight irrigated wheat systems. Agricultural Water Management, 89(3), 287–296. https://doi.org/10.1016/j.agwat.2007.02.002

Zwart, S. J., & Leclert, L. M. C. (2010). A remote sensing-based irrigation performance assessment: A case study of the Office du Niger in Mali. Irrigation Science, 28(5), 371–385. https://doi.org/10.1007/s00271-009-0199-3

APPENDICES

Appendix A

Appendix A. 1 Relationship between biomass vs transpiration (T) at Wonji from 2009/2022.

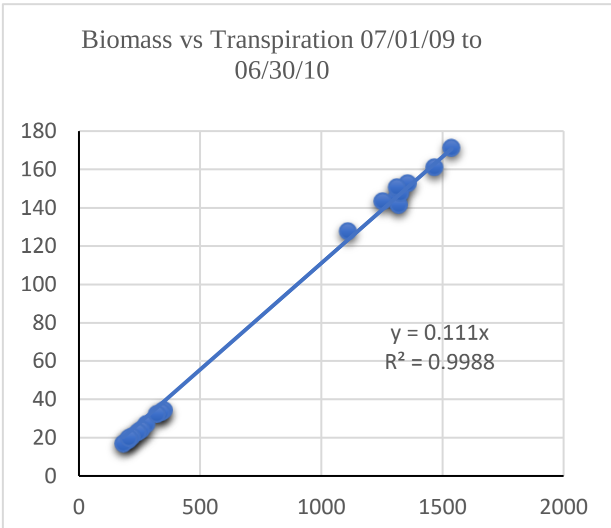

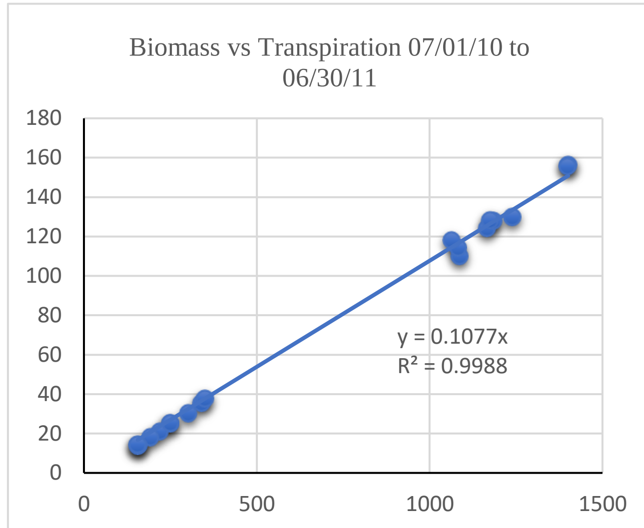

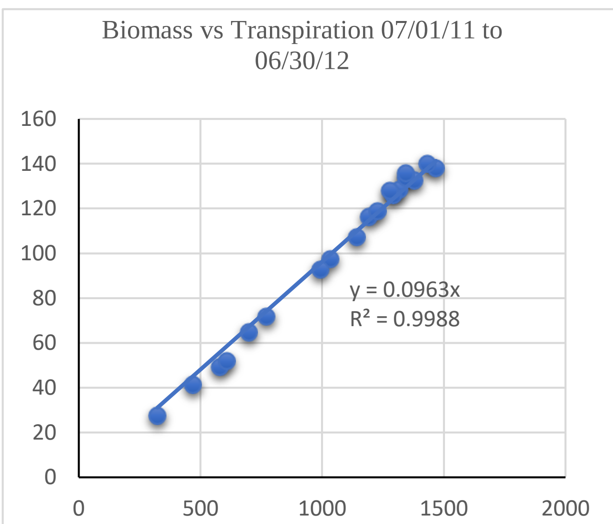

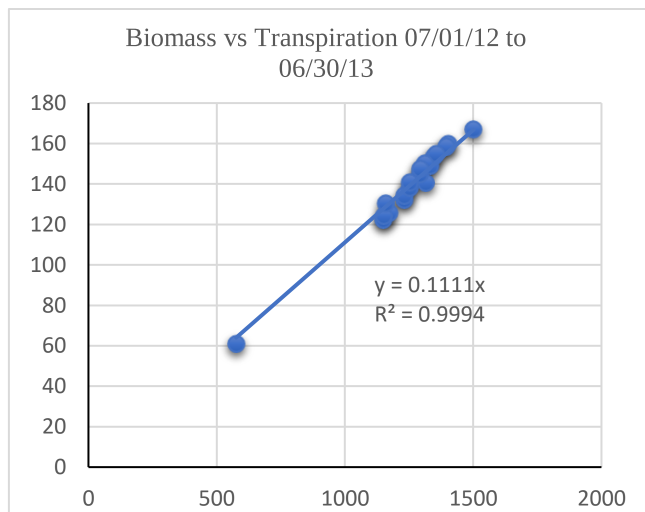

.

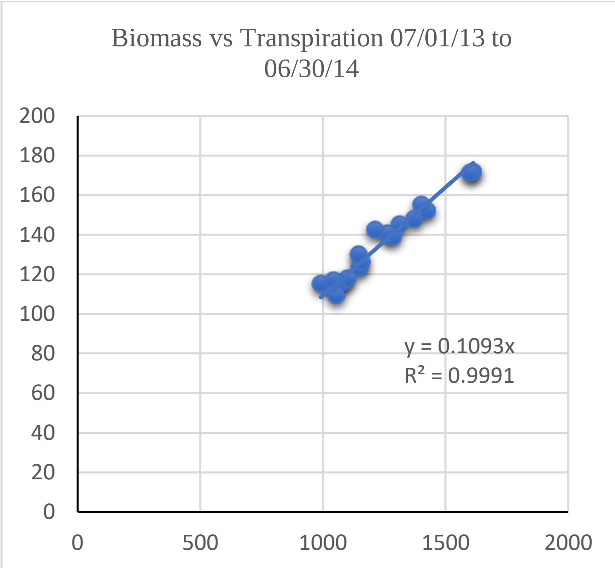
Biomass vs Transpiration 07/01/13 to 06/30/14
y = 0.1093x
R² = 0.9991
0 20 40 60 80 100 120 140 160 180 200
0 500 1000 1500 2000

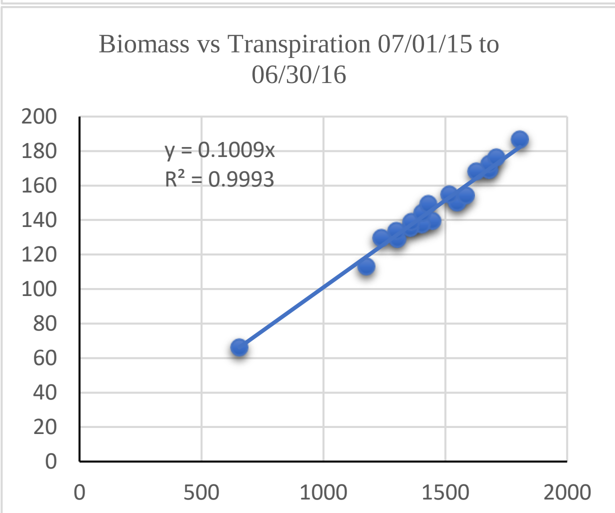
Biomass vs Transpiration 07/01/15 to 06/30/16
y = 0.1009x
R² = 0.9993
0 20 40 60 80 100 120 140 160 180 200
0 500 1000 1500 2000

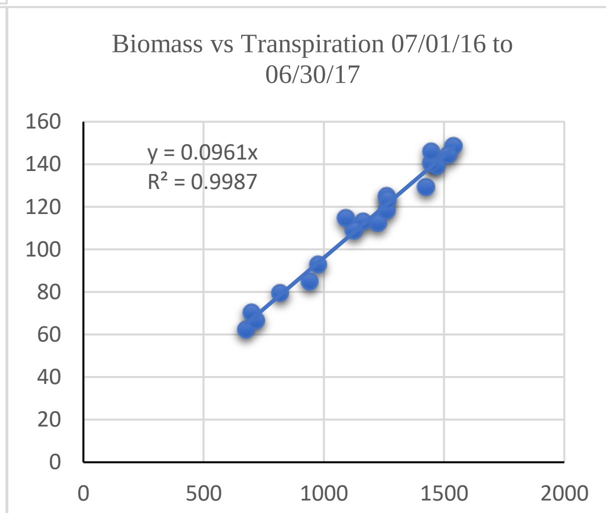
Biomass vs Transpiration 07/01/16 to 06/30/17
y = 0.0961x
R² = 0.9987
0 20 40 60 80 100 120 140 160
0 500 1000 1500 2000

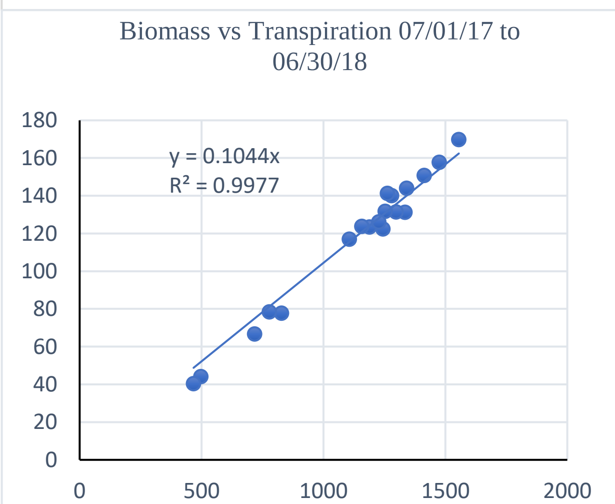
Biomass vs Transpiration 07/01/17 to 06/30/18
y = 0.1044x
R² = 0.9977
0 20 40 60 80 100 120 140 160 180
0 500 1000 1500 2000

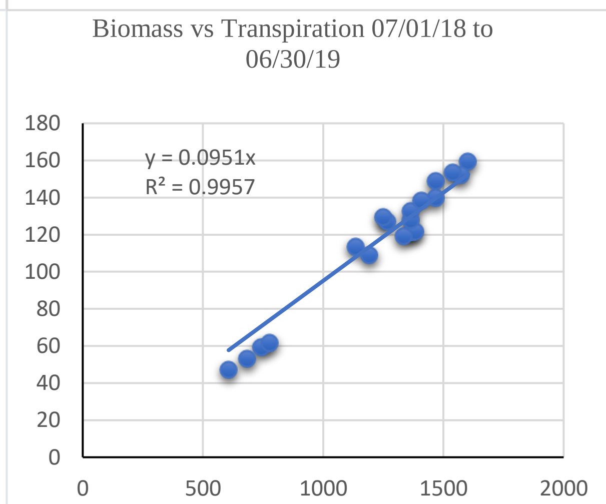
Biomass vs Transpiration 07/01/18 to 06/30/19
y = 0.0951x
R² = 0.9957
0 20 40 60 80 100 120 140 160 180
0 500 1000 1500 2000

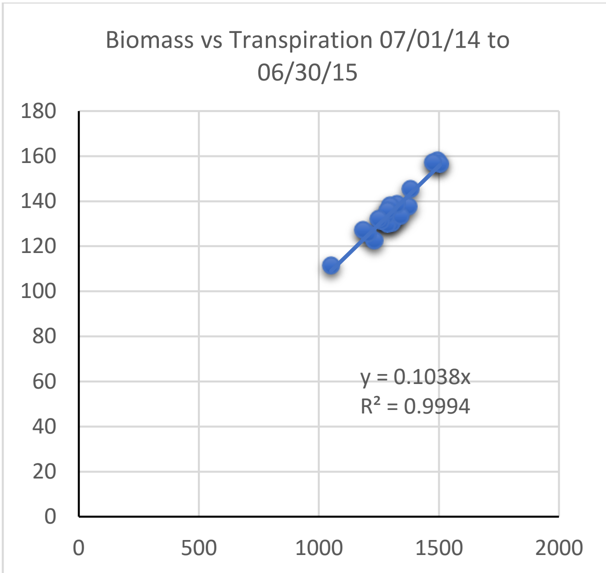
Biomass vs Transpiration 07/01/14 to 06/30/15
180
160
140
120
100
80
60
40
20
0
0
500
1000
1500
2000
y = 0.1038x
R² = 0.9994

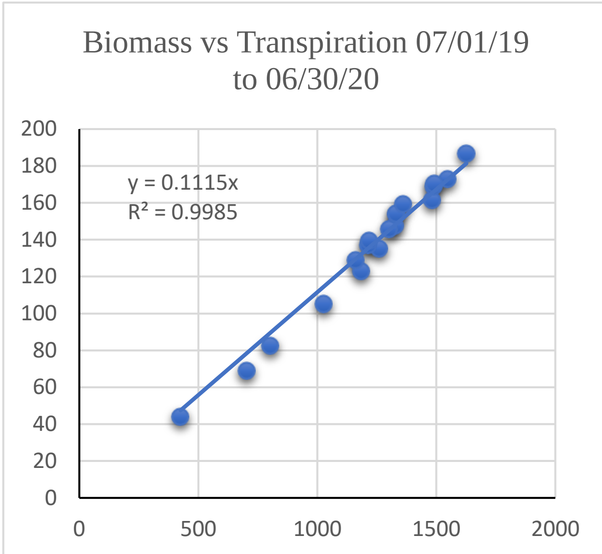

Biomass vs Transpiration 07/01/19 to 06/30/20
y = 0.1115x
R² = 0.9985
200
180
160
140
120
100
80
60
40
20
0
0
500
1000
1500
2000

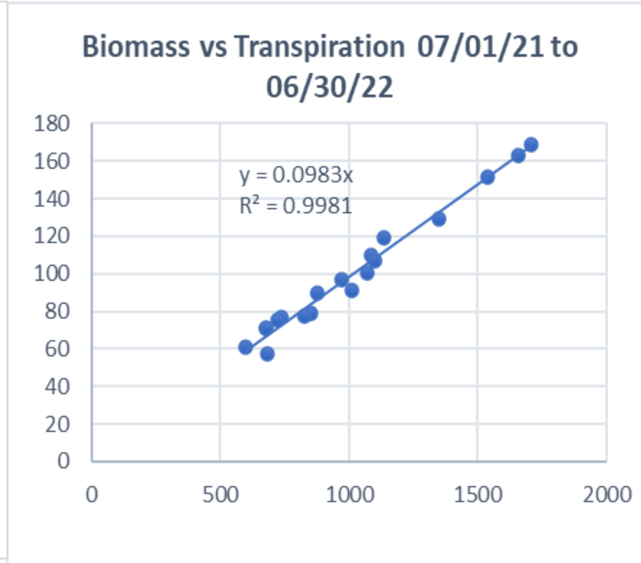

Biomass vs Transpiration 07/01/21 to 06/30/22
y = 0.0983x
R² = 0.9981
180
160
140
120
100
80
60
40
20
0
0
500
1000
1500
2000

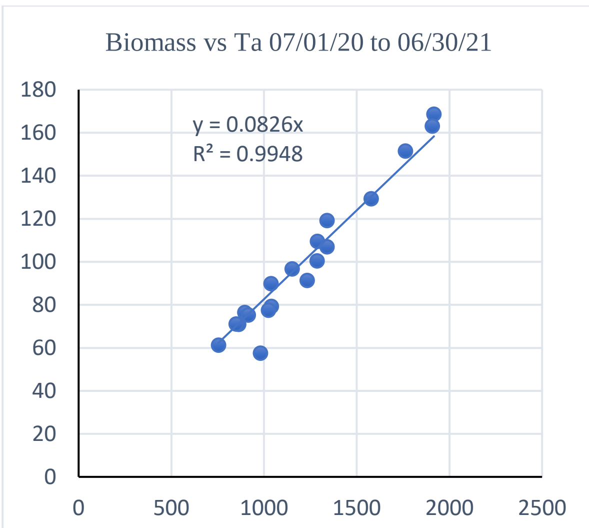

Biomass vs Ta 07/01/20 to 06/30/21
y = 0.0826x
R² = 0.9948
180
160
140
120
100
80
60
40
20
0
0
500
1000
1500
2000
2500

Appendix A. 2 Relationship between biomass vs ETa at Wonji from 2009/2022.

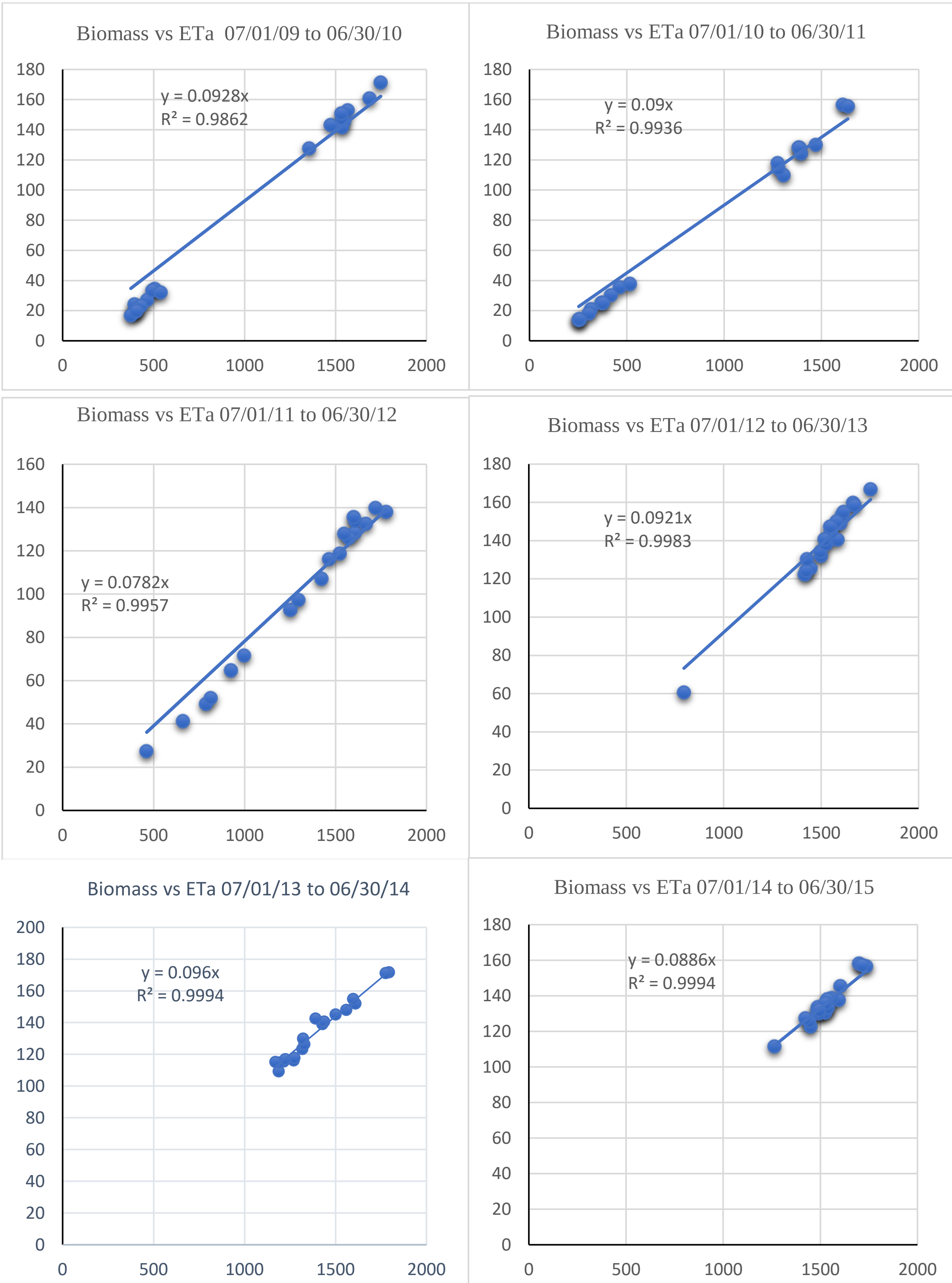

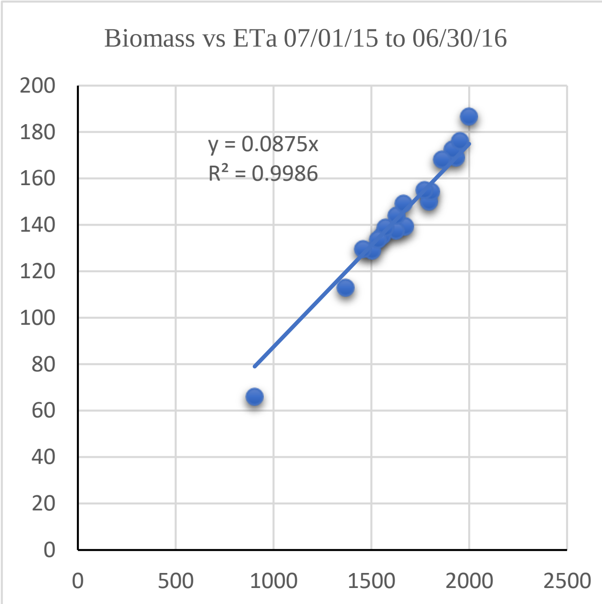
Biomass vs ETa 07/01/15 to 06/30/16
y = 0.0875x
R² = 0.9986
200
180
160
140
120
100
80
60
40
20
0
0
500
1000
1500
2000
2500

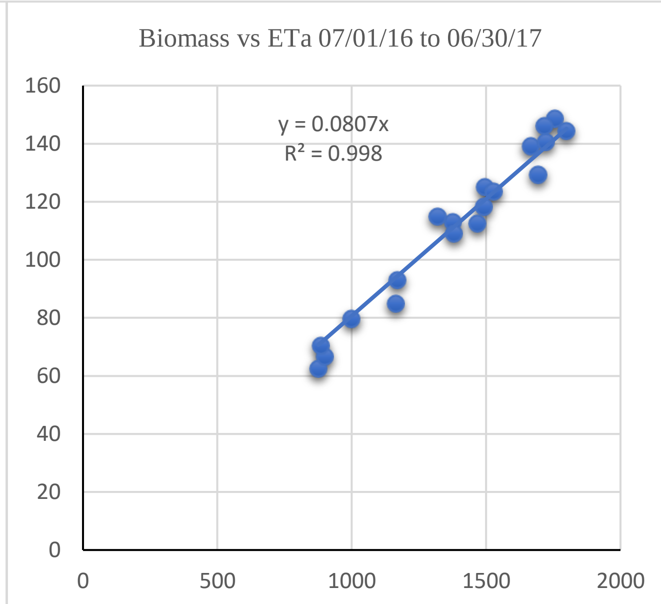
Biomass vs ETa 07/01/16 to 06/30/17
y = 0.0807x
R² = 0.998
160
140
120
100
80
60
40
20
0
0
500
1000
1500
2000

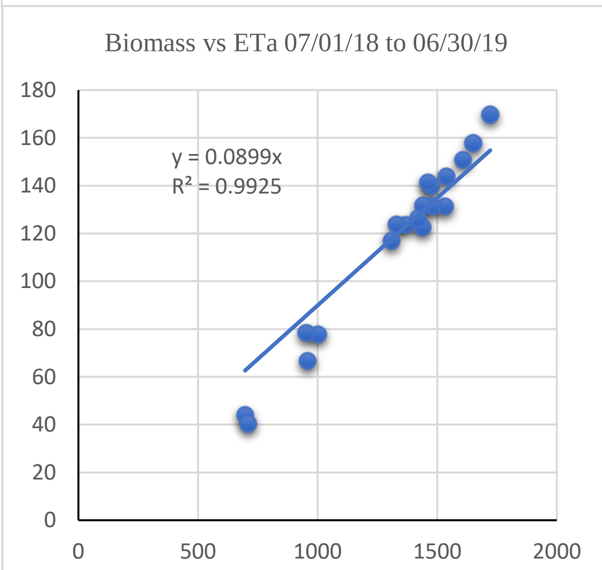
Biomass vs ETa 07/01/18 to 06/30/19
y = 0.0899x
R² = 0.9925
180
160
140
120
100
80
60
40
20
0
0
500
1000
1500
2000

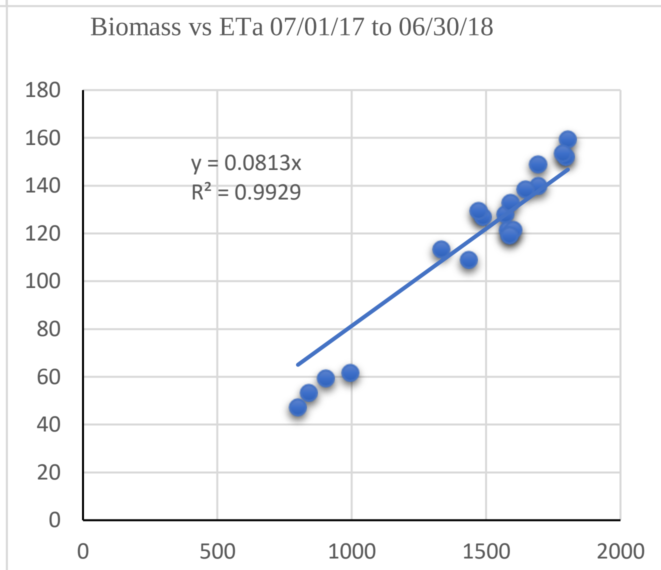
Biomass vs ETa 07/01/17 to 06/30/18
y = 0.0813x
R² = 0.9929
180
160
140
120
100
80
60
40
20
0
0
500
1000
1500
2000

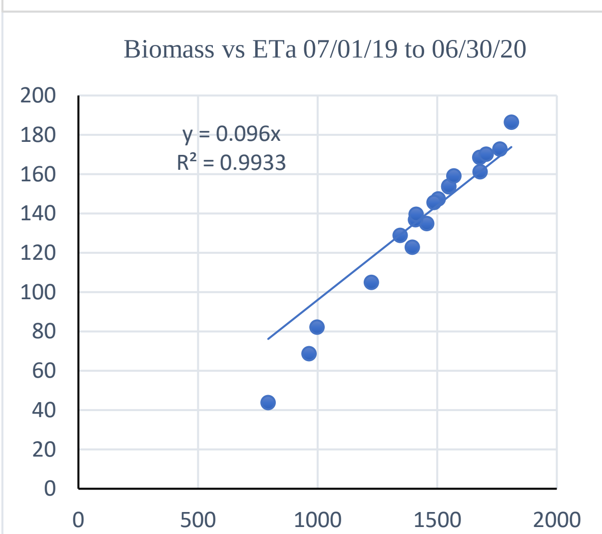
Biomass vs ETa 07/01/19 to 06/30/20
y = 0.096x
R² = 0.9933
200
180
160
140
120
100
80
60
40
20
0
0
500
1000
1500
2000

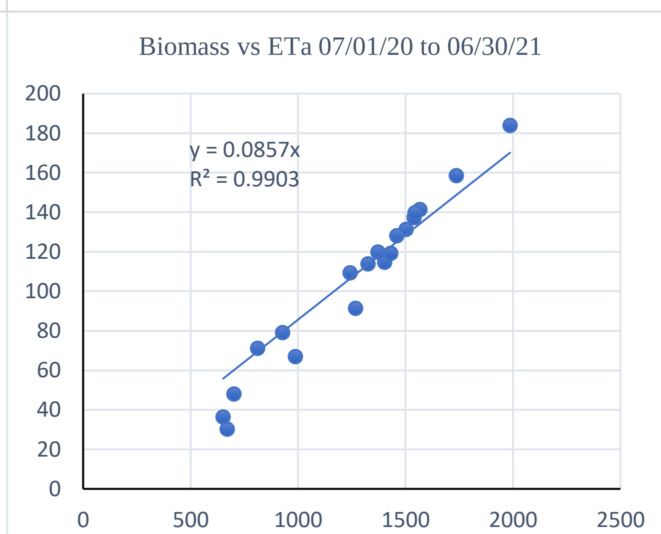
Biomass vs ETa 07/01/20 to 06/30/21
y = 0.0857x
R² = 0.9903
200
180
160
140
120
100
80
60
40
20
0
0
500
1000
1500
2000
2500

Appendix A. 3 Spatial distribution of actual ET of sugarcane at Wonji Shoa from 2009-2022.

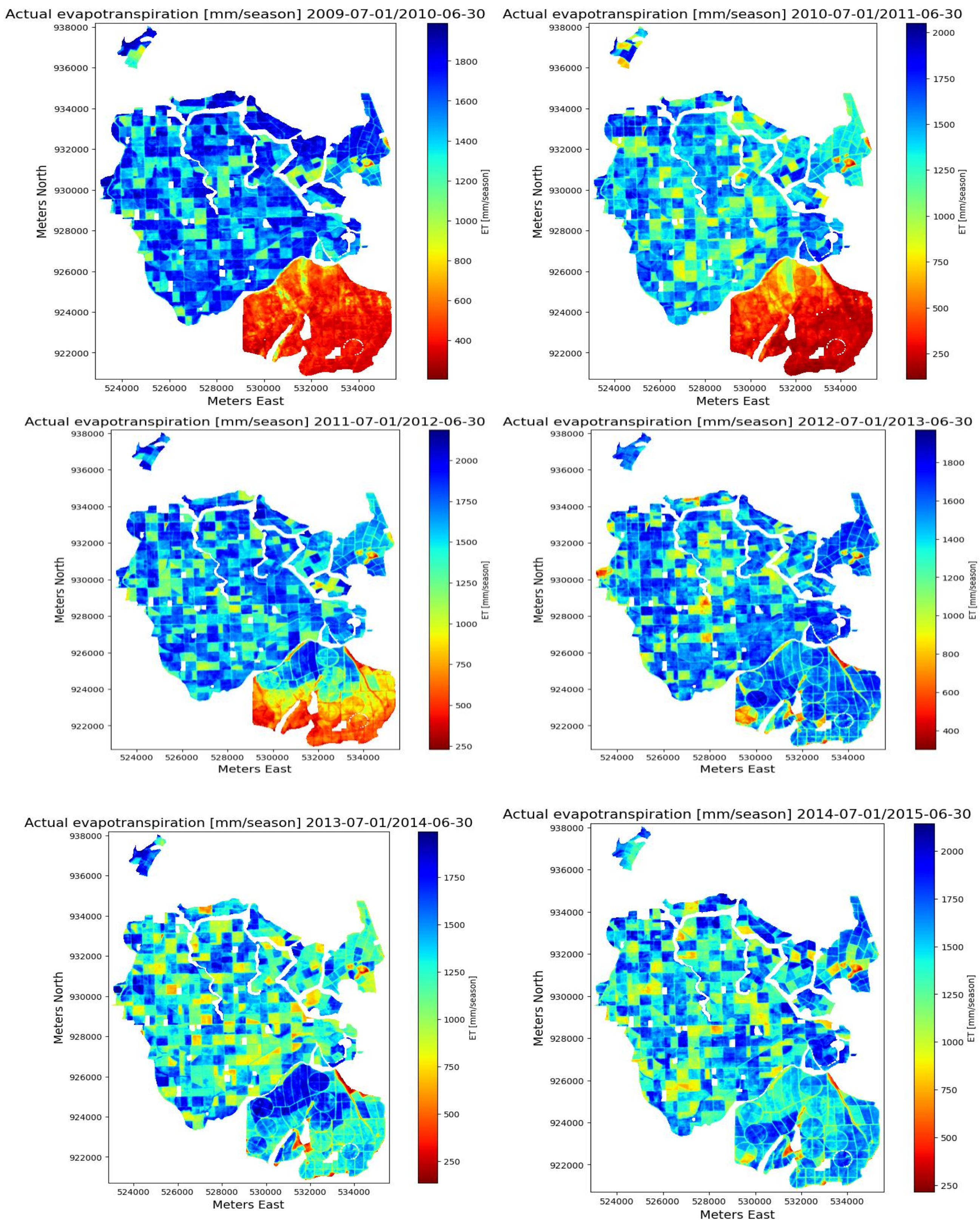

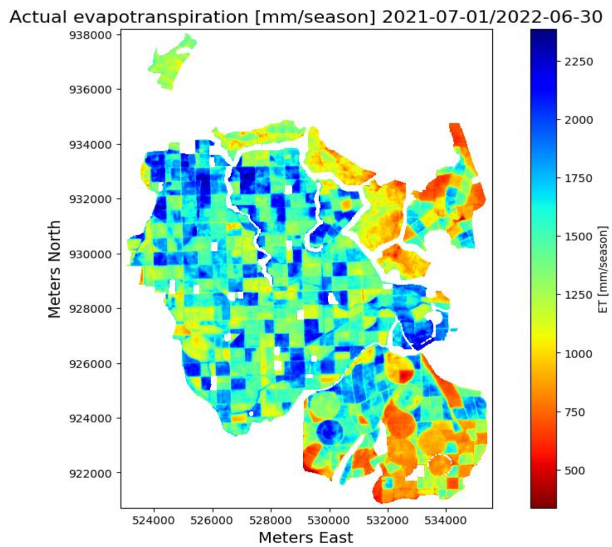
Actual evapotranspiration [mm/season] 2021-07-01/2022-06-30
Meters North
Meters East
ET [mm/season]

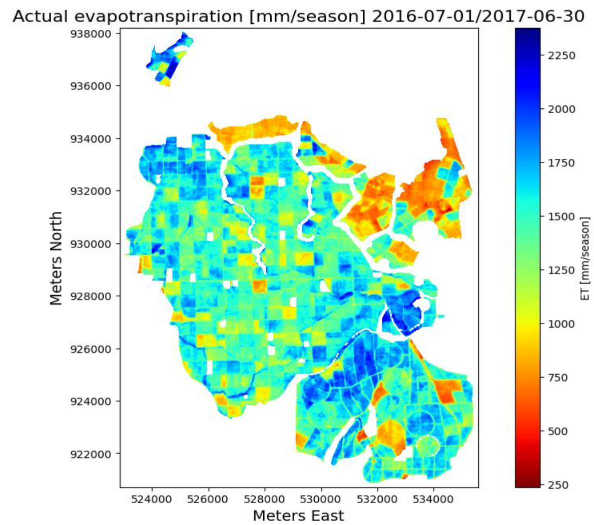
Actual evapotranspiration [mm/season] 2016-07-01/2017-06-30
Meters North
Meters East
ET [mm/season]

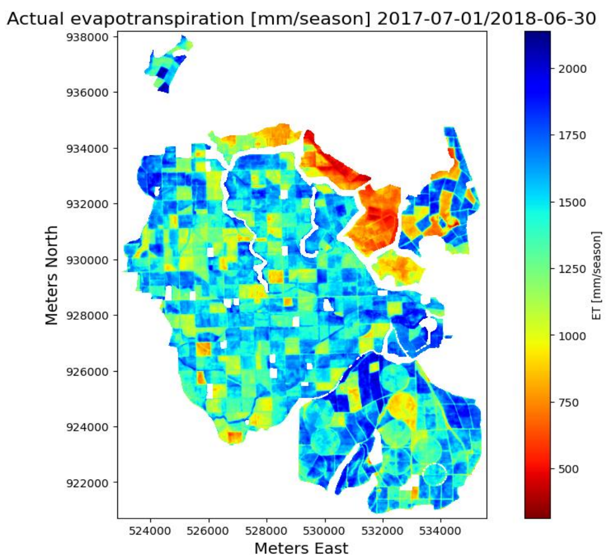
Actual evapotranspiration [mm/season] 2017-07-01/2018-06-30
Meters North
Meters East
ET [mm/season]

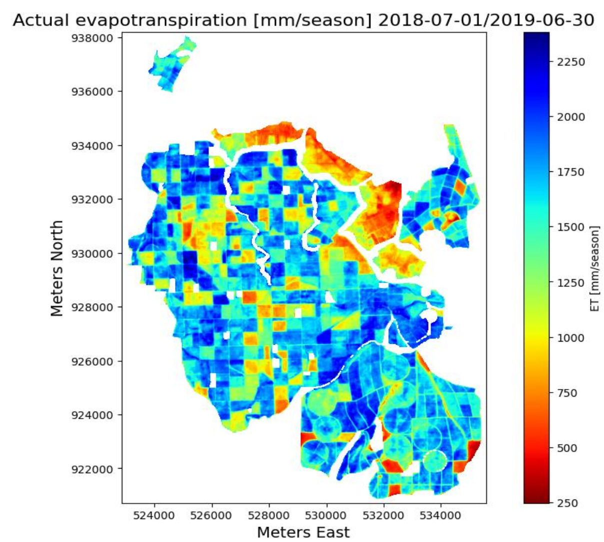
Actual evapotranspiration [mm/season] 2018-07-01/2019-06-30
Meters North
Meters East
ET [mm/season]

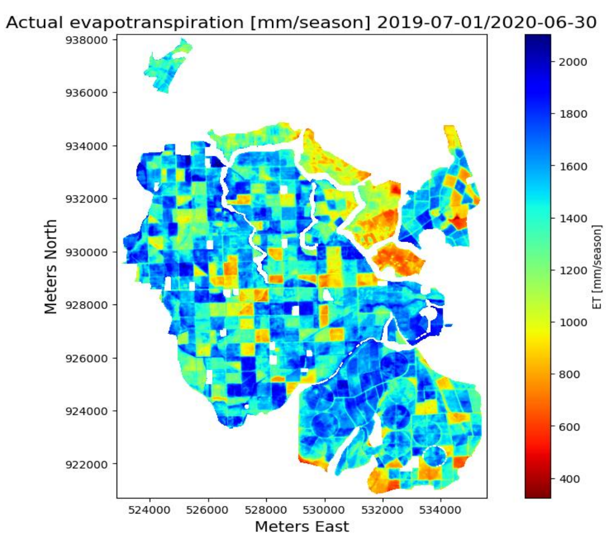
Actual evapotranspiration [mm/season] 2019-07-01/2020-06-30
Meters North
Meters East
ET [mm/season]

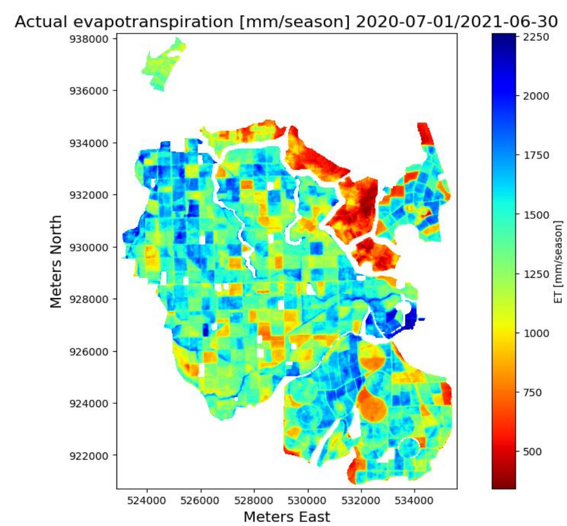
Actual evapotranspiration [mm/season] 2020-07-01/2021-06-30
Meters North
Meters East
ET [mm/season]

Appendix A. 4 Spatial distribution of the efficiency of sugarcane at Wonji Shoa from 2009 to 2022.

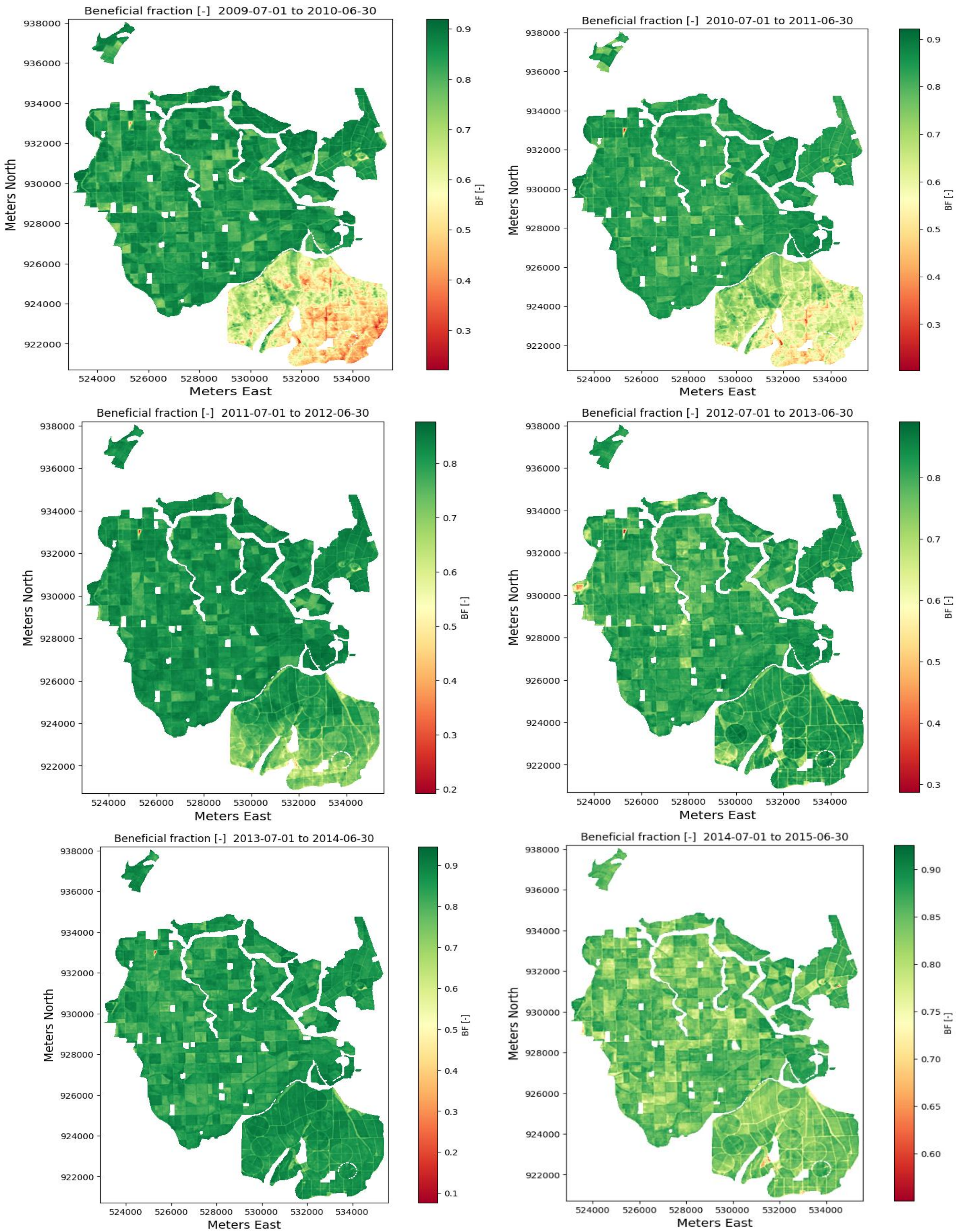

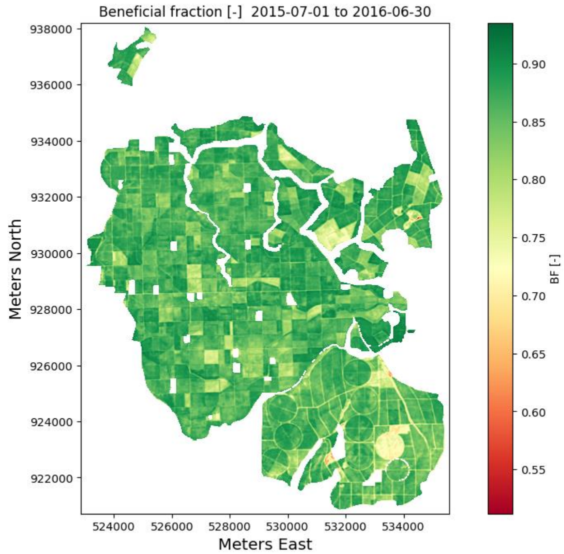
Beneficial fraction [-] 2015-07-01 to 2016-06-30
Meters North
Meters East
BF [-]

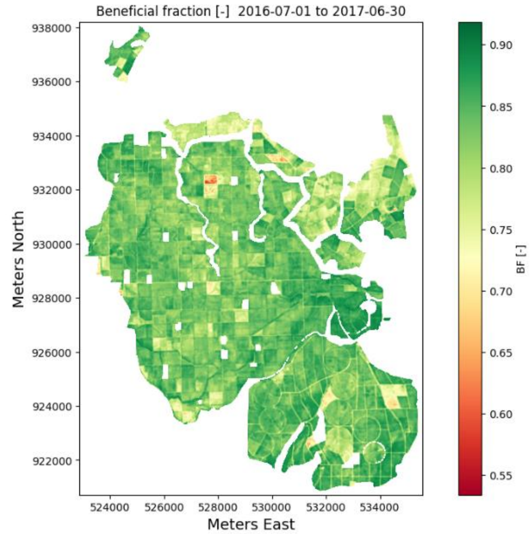
Beneficial fraction [-] 2016-07-01 to 2017-06-30
Meters North
Meters East
BF [-]

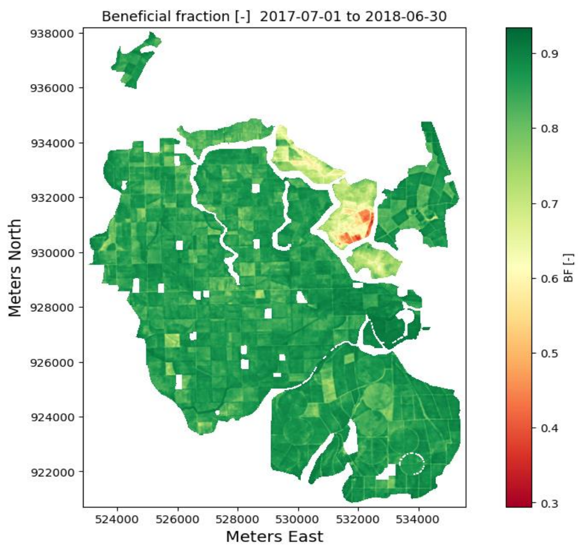
Beneficial fraction [-] 2017-07-01 to 2018-06-30
Meters North
Meters East
BF [-]

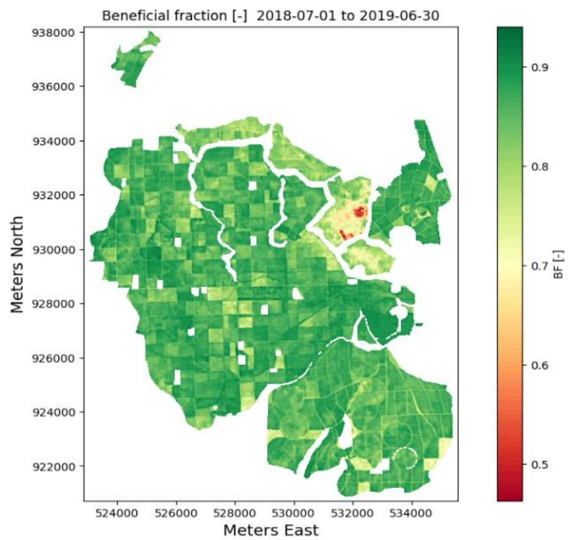
Beneficial fraction [-] 2018-07-01 to 2019-06-30
Meters North
Meters East
BF [-]

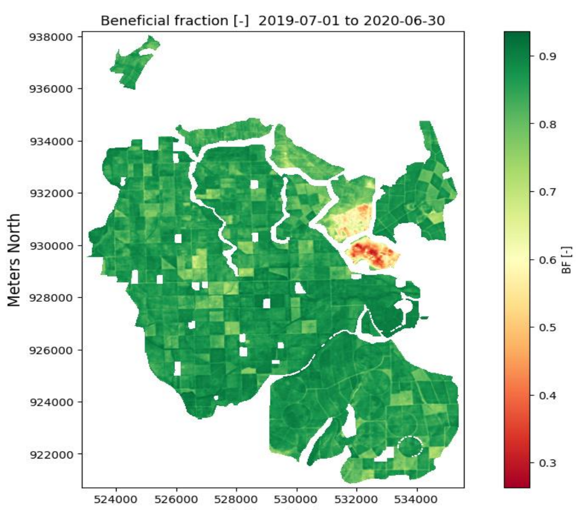
Beneficial fraction [-] 2019-07-01 to 2020-06-30
Meters North
Meters East
BF [-]

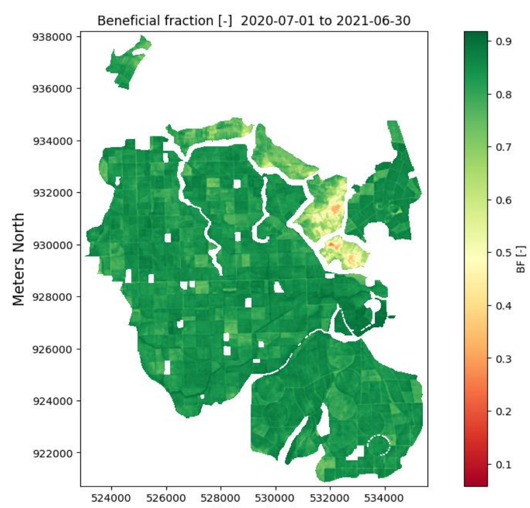
Beneficial fraction [-] 2020-07-01 to 2021-06-30
Meters North
Meters East
BF [-]

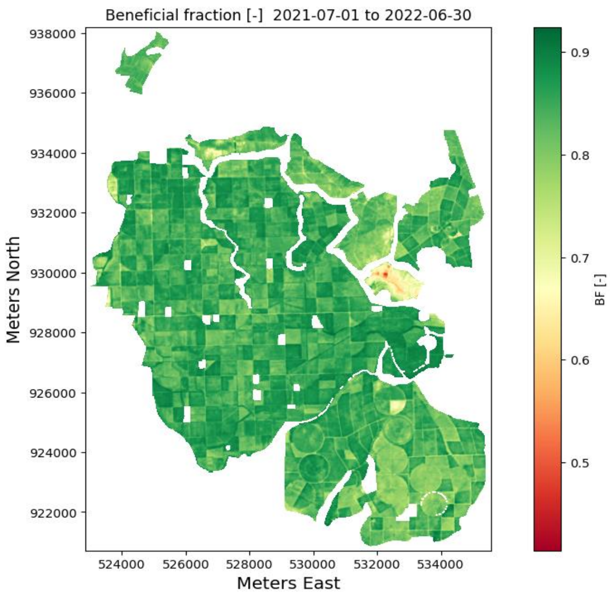

Appendix A. 5 Spatial distribution of relative evapotranspiration (Adequacy)of sugarcane at Wonji Shoa from 2009/2010 to 2021/2022.

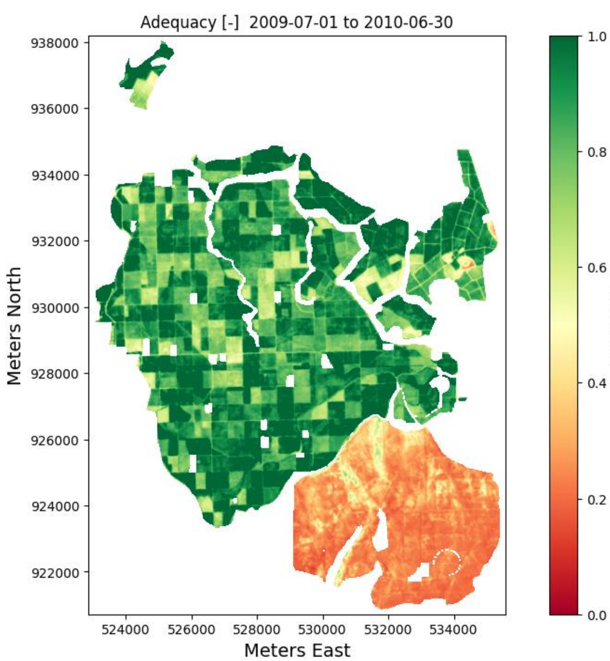

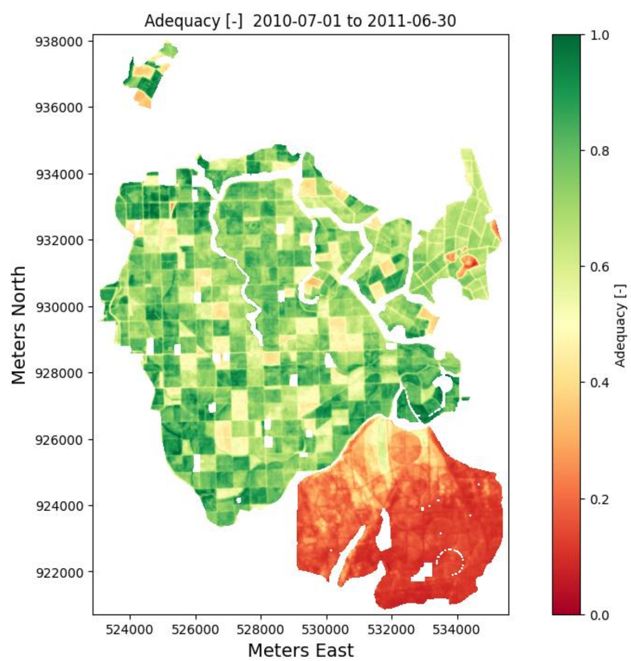

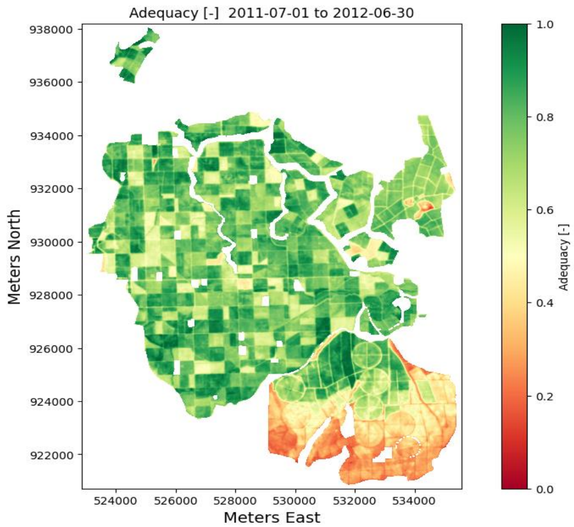
Adequacy [-] 2011-07-01 to 2012-06-30
Meters North
Meters East
Adequacy [-]

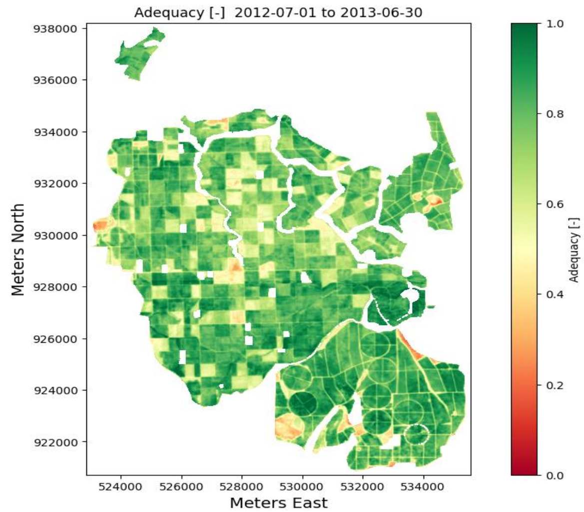
Adequacy [-] 2012-07-01 to 2013-06-30
Meters North
Meters East
Adequacy [-]

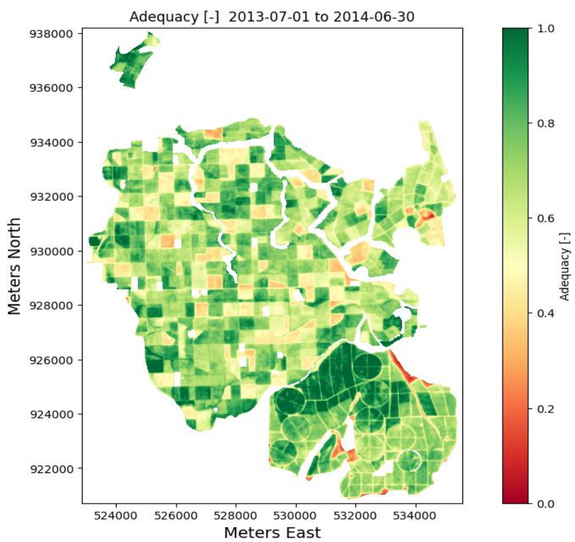
Adequacy [-] 2013-07-01 to 2014-06-30
Meters North
Meters East
Adequacy [-]

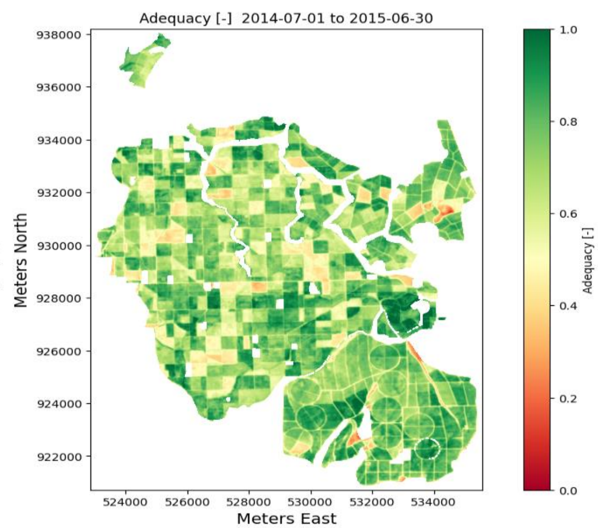
Adequacy [-] 2014-07-01 to 2015-06-30
Meters North
Meters East
Adequacy [-]

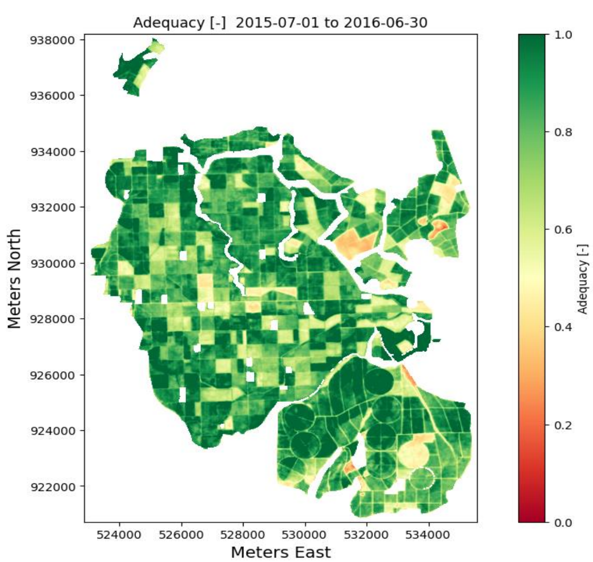
Adequacy [-] 2015-07-01 to 2016-06-30
Meters North
Meters East
Adequacy [-]

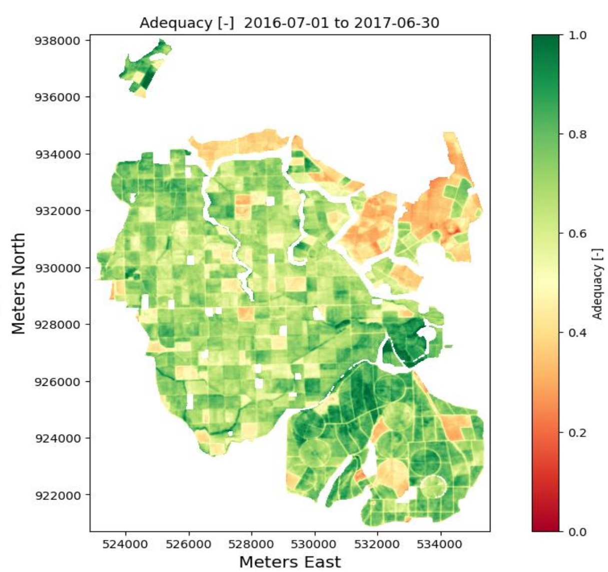
Adequacy [-] 2016-07-01 to 2017-06-30
Meters North
Meters East
Adequacy [-]

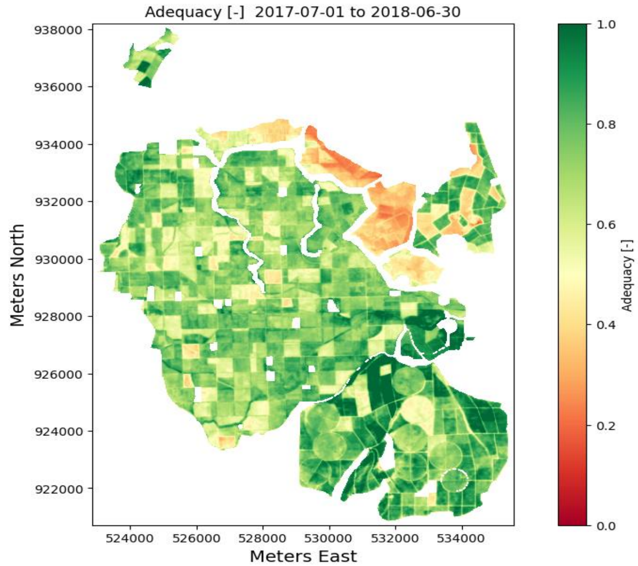
Adequacy [-] 2017-07-01 to 2018-06-30
Meters North
938000
936000
934000
932000
930000
928000
926000
924000
922000
524000
526000
528000
530000
532000
534000
Meters East
Adequacy [-]
0.0
0.2
0.4
0.6
0.8
1.0

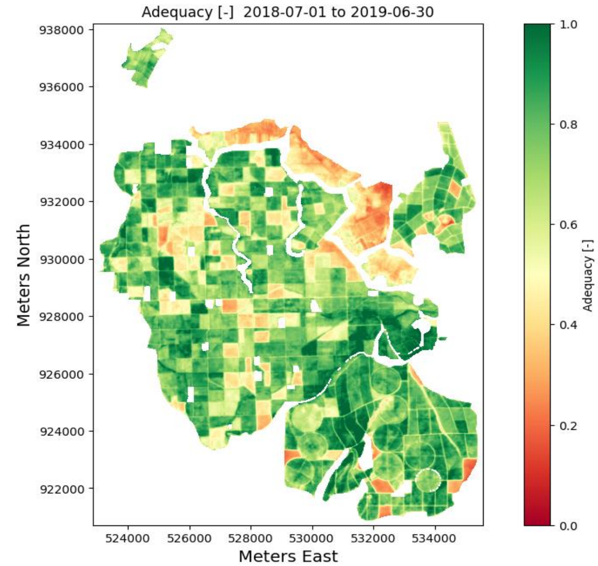
Adequacy [-] 2018-07-01 to 2019-06-30
Meters North
938000
936000
934000
932000
930000
928000
926000
924000
922000
524000
526000
528000
530000
532000
534000
Meters East
Adequacy [-]
0.0
0.2
0.4
0.6
0.8
1.0

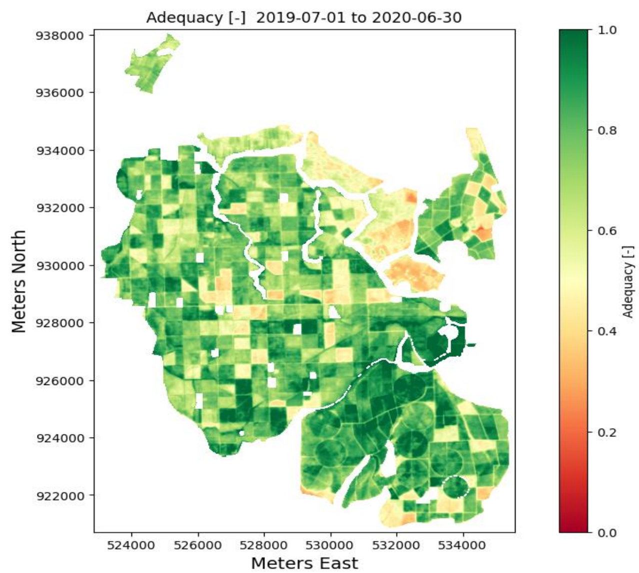
Adequacy [-] 2019-07-01 to 2020-06-30
Meters North
938000
936000
934000
932000
930000
928000
926000
924000
922000
524000
526000
528000
530000
532000
534000
Meters East
Adequacy [-]
0.0
0.2
0.4
0.6
0.8
1.0

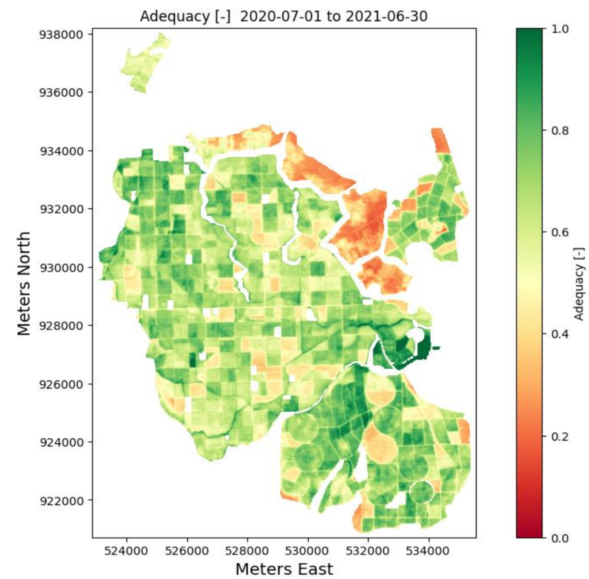
Adequacy [-] 2020-07-01 to 2021-06-30
Meters North
938000
936000
934000
932000
930000
928000
926000
924000
922000
524000
526000
528000
530000
532000
534000
Meters East
Adequacy [-]
0.0
0.2
0.4
0.6
0.8
1.0

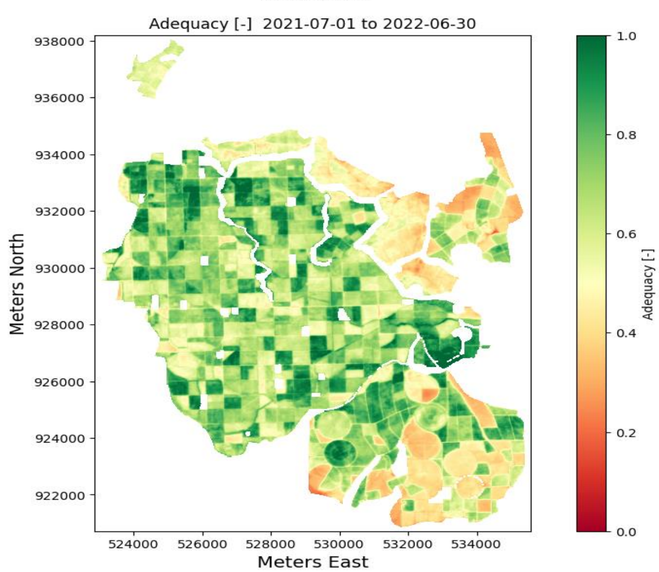
Adequacy [-] 2021-07-01 to 2022-06-30
Meters North
938000
936000
934000
932000
930000
928000
926000
924000
922000
524000
526000
528000
530000
532000
534000
Meters East
Adequacy [-]
0.0
0.2
0.4
0.6
0.8
1.0

Appendix A. 6 Spatial distribution of biomass of sugarcane at Wonji Shoa from 2009 to 2022.

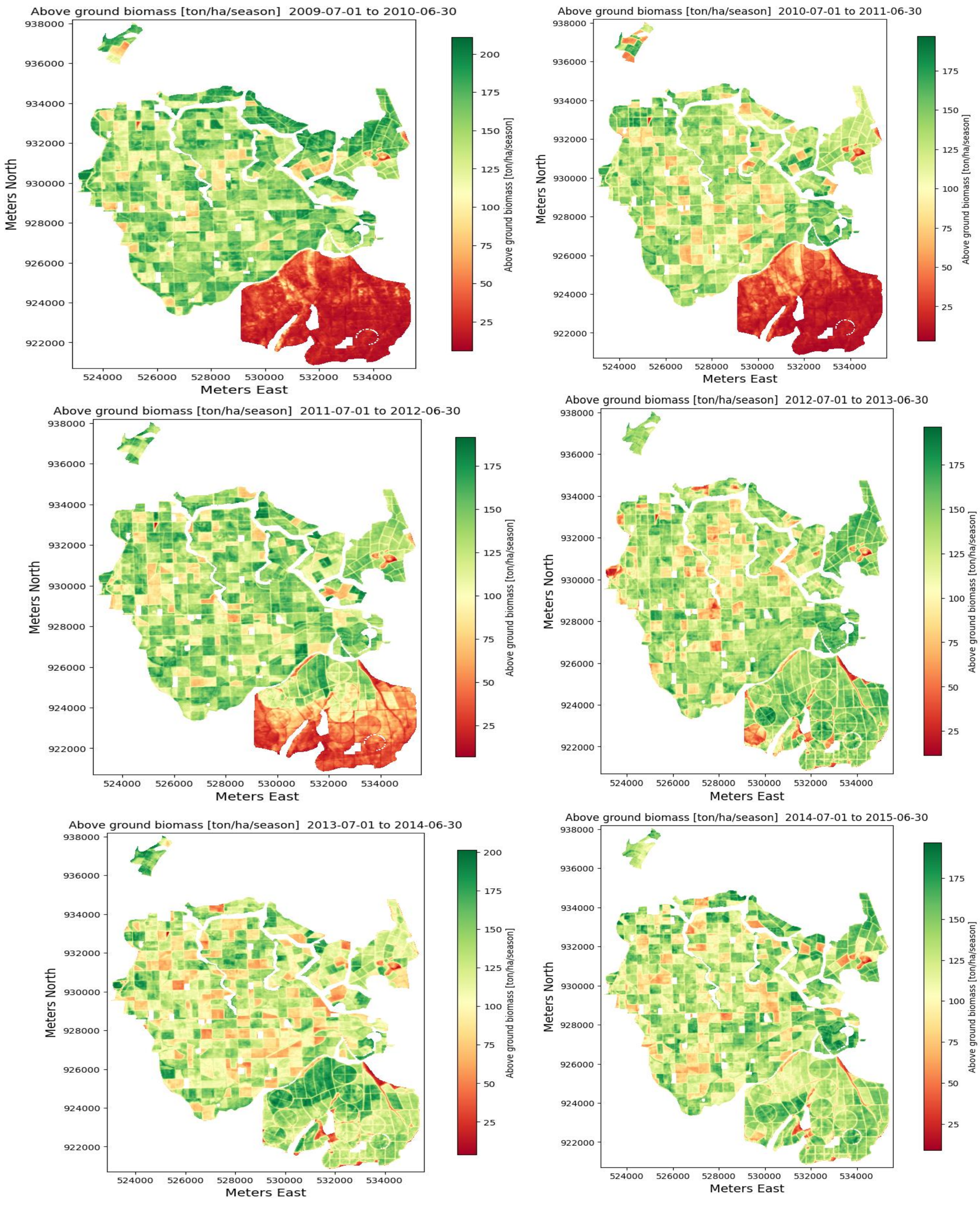

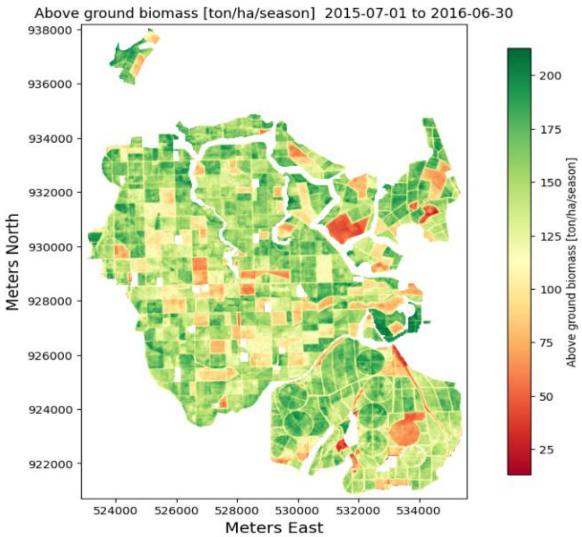
Above ground biomass [ton/ha/season] 2015-07-01 to 2016-06-30
Meters North
Meters East
Above ground biomass [ton/ha/season]

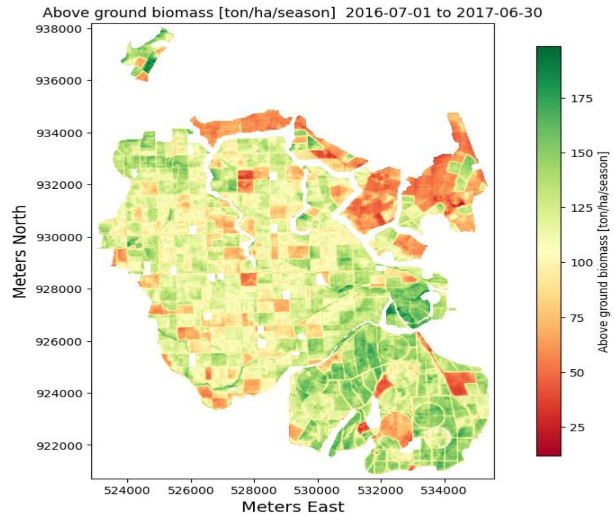
Above ground biomass [ton/ha/season] 2016-07-01 to 2017-06-30
Meters North
Meters East
Above ground biomass [ton/ha/season]

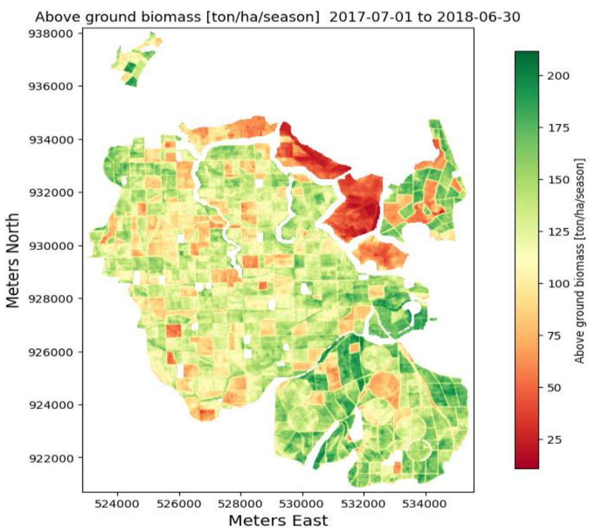
Above ground biomass [ton/ha/season] 2017-07-01 to 2018-06-30
Meters North
Meters East
Above ground biomass [ton/ha/season]

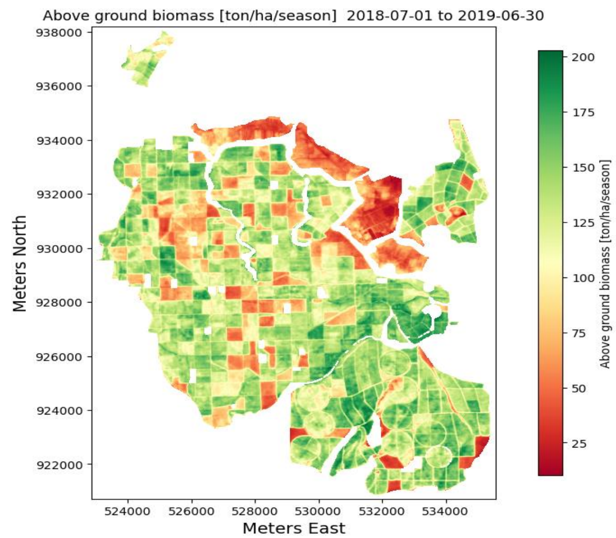
Above ground biomass [ton/ha/season] 2018-07-01 to 2019-06-30
Meters North
Meters East
Above ground biomass [ton/ha/season]

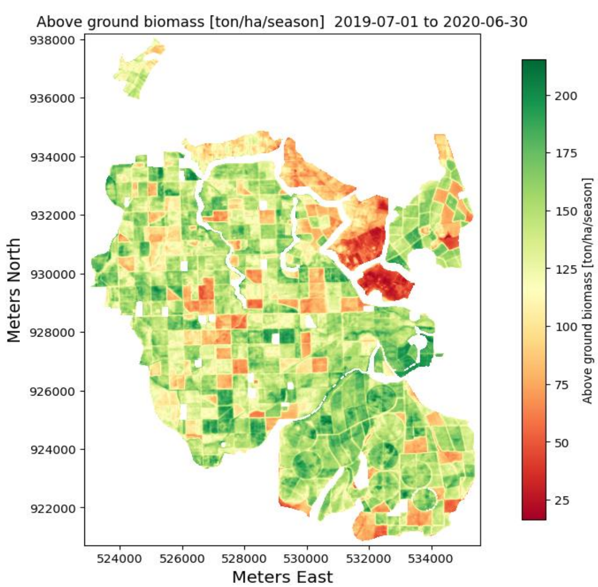
Above ground biomass [ton/ha/season] 2019-07-01 to 2020-06-30
Meters North
Meters East
Above ground biomass [ton/ha/season]

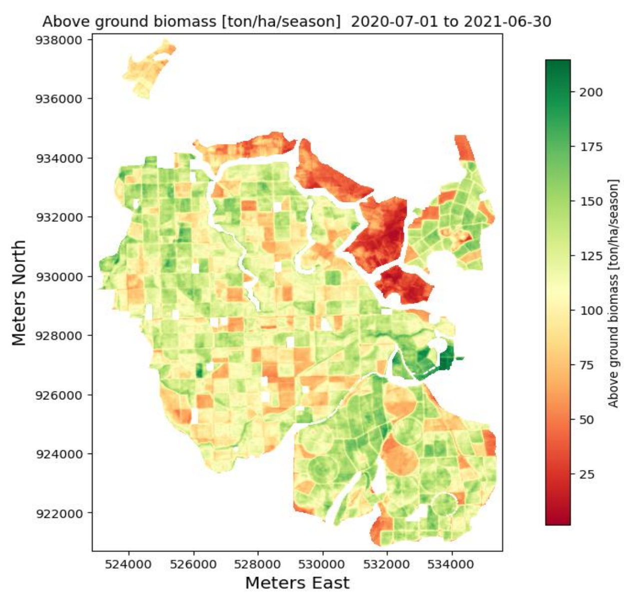
Above ground biomass [ton/ha/season] 2020-07-01 to 2021-06-30
Meters North
Meters East
Above ground biomass [ton/ha/season]

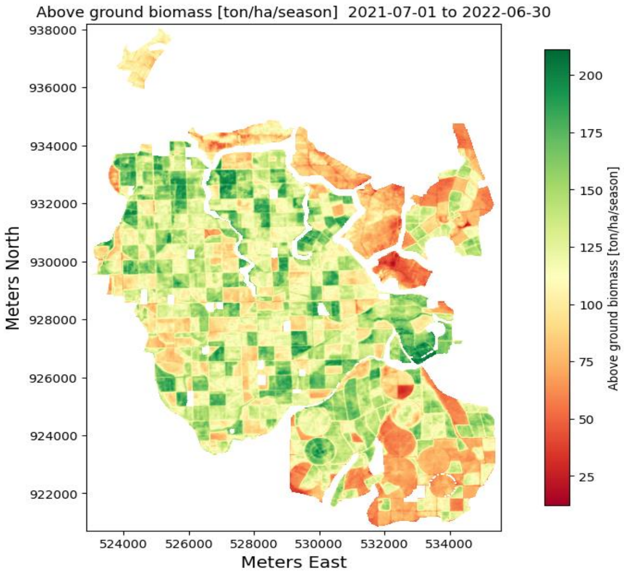

Appendix A. 7 Spatial distribution of biomass WP of sugarcane at Wonji Shoa from

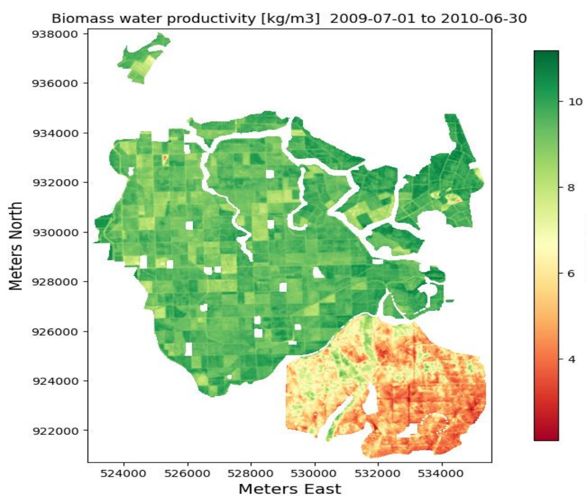

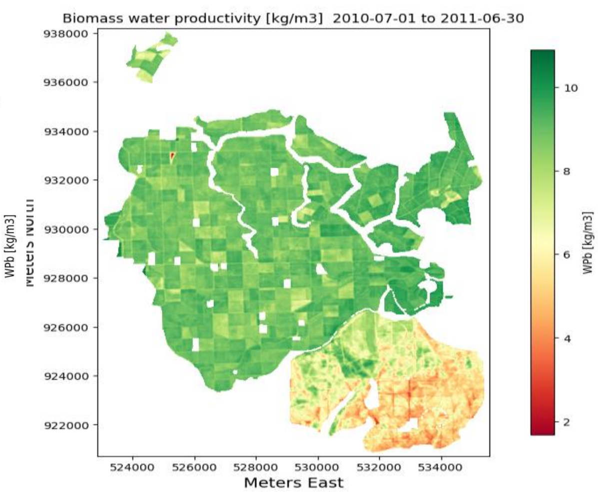

2009/2022.

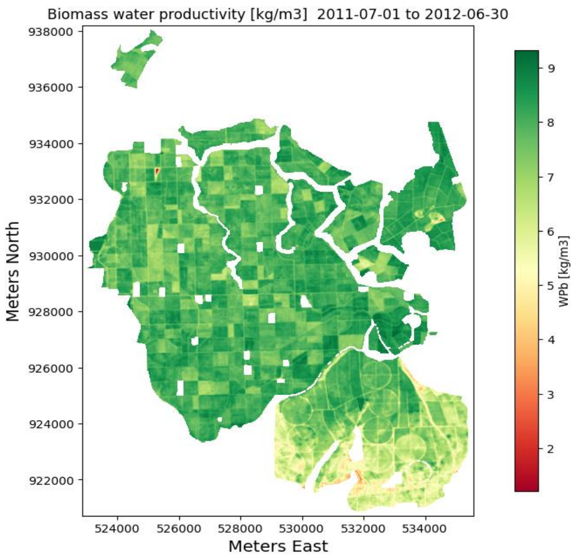
Biomass water productivity [kg/m3] 2011-07-01 to 2012-06-30
Meters North
Meters East
WPb [kg/m3]
938000
936000
934000
932000
930000
928000
926000
924000
922000
524000
526000
528000
530000
532000
534000
9
8
7
6
5
4
3
2

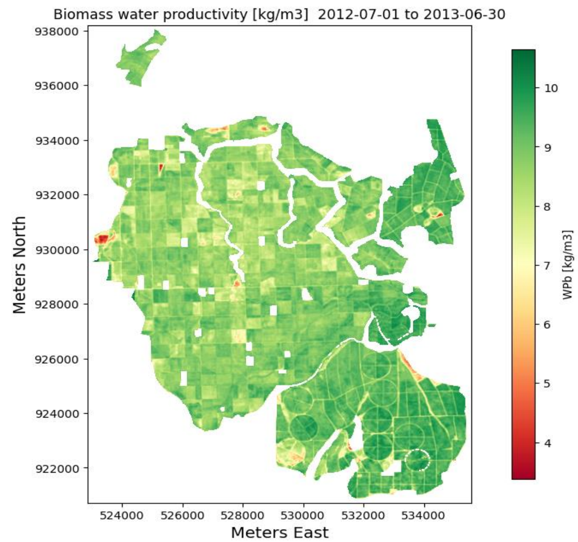
Biomass water productivity [kg/m3] 2012-07-01 to 2013-06-30
Meters North
Meters East
WPb [kg/m3]
938000
936000
934000
932000
930000
928000
926000
924000
922000
524000
526000
528000
530000
532000
534000
10
9
8
7
6
5
4

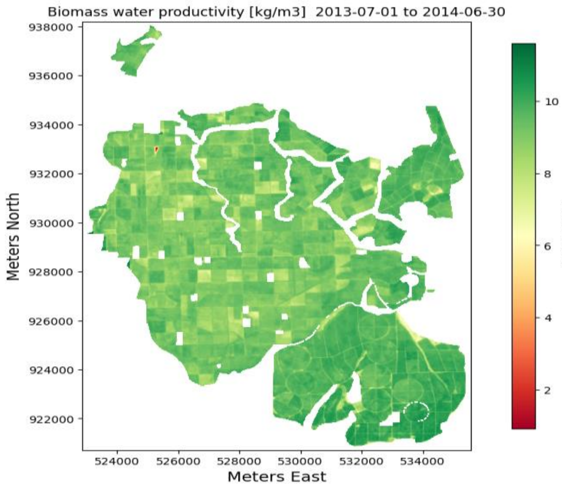
Biomass water productivity [kg/m3] 2013-07-01 to 2014-06-30
Meters North
Meters East
WPb [kg/m3]

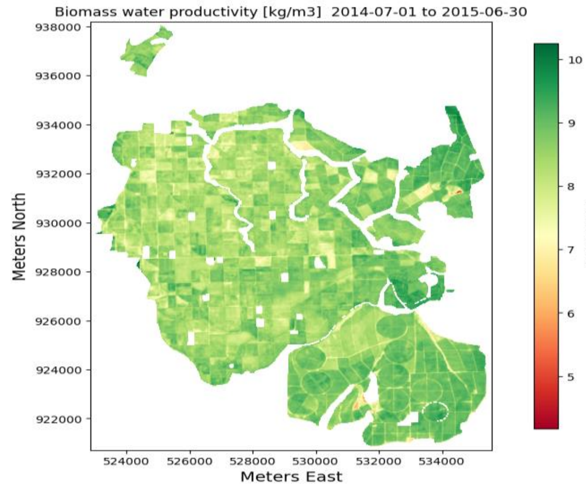
Biomass water productivity [kg/m3] 2014-07-01 to 2015-06-30
Meters North
Meters East
WPb [kg/m3]

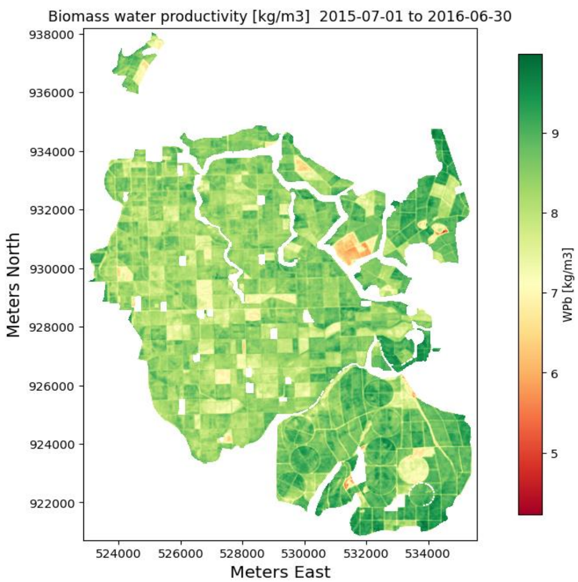
Biomass water productivity [kg/m3] 2015-07-01 to 2016-06-30
Meters North
Meters East
WPb [kg/m3]

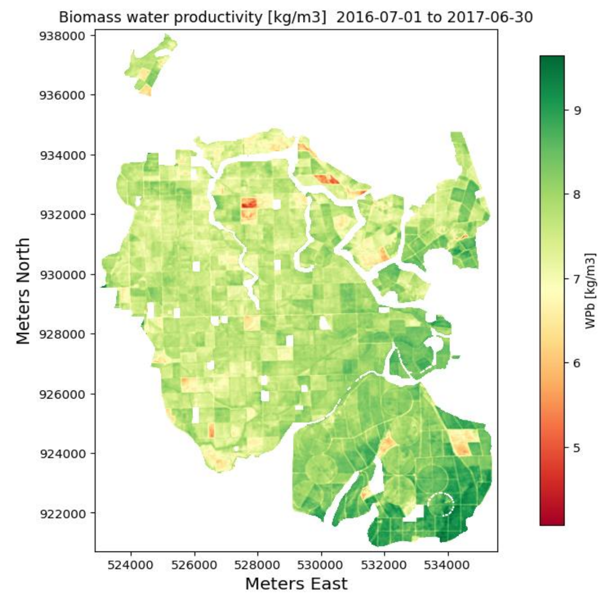
Biomass water productivity [kg/m3] 2016-07-01 to 2017-06-30
Meters North
Meters East
WPb [kg/m3]

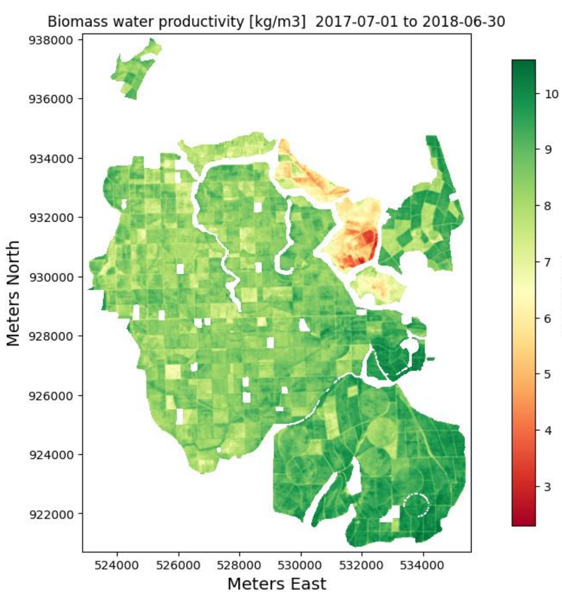
Biomass water productivity [kg/m3] 2017-07-01 to 2018-06-30
Meters North
Meters East
WPb [kg/m3]

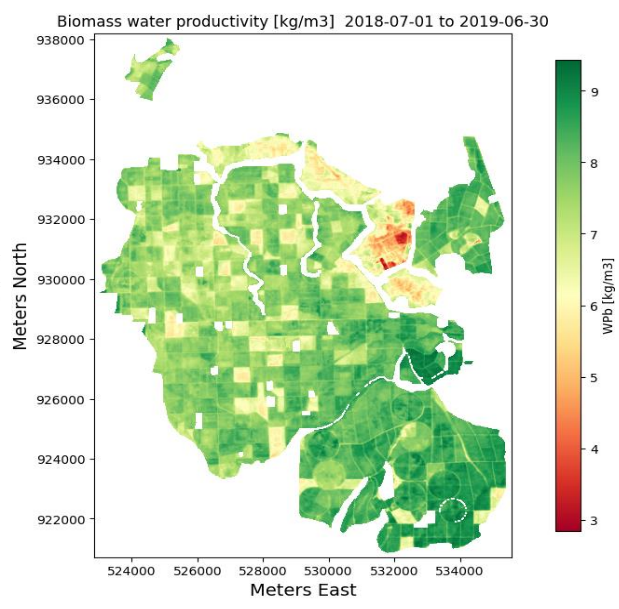
Biomass water productivity [kg/m3] 2018-07-01 to 2019-06-30
Meters North
Meters East
WPb [kg/m3]

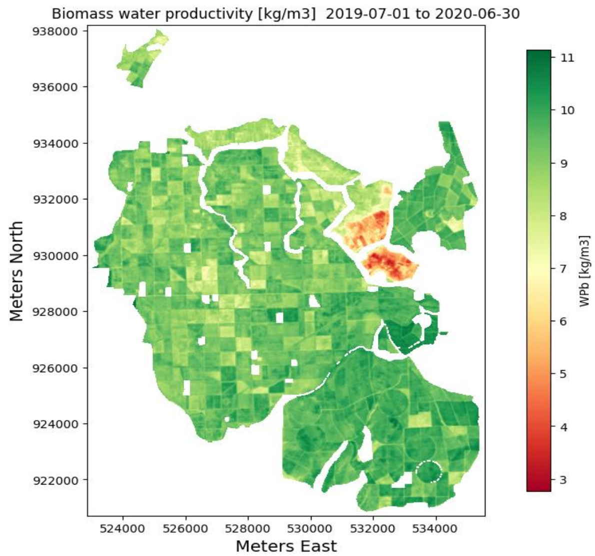
Biomass water productivity [kg/m3] 2019-07-01 to 2020-06-30
Meters North
Meters East
WPb [kg/m3]

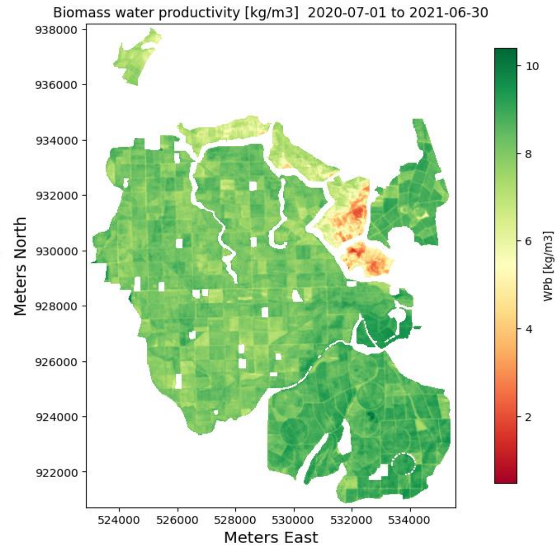
Biomass water productivity [kg/m3] 2020-07-01 to 2021-06-30
Meters North
Meters East
WPb [kg/m3]

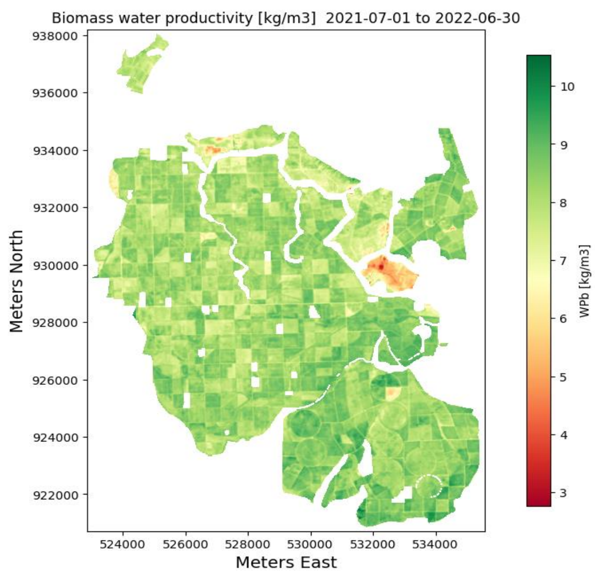
Biomass water productivity [kg/m3] 2021-07-01 to 2022-06-30
Meters North
Meters East
WPb [kg/m3]

Appendix A. 8 Biomass and biomass WP targets at Wonji Shoa from 2009/2010 to 2021/2022.

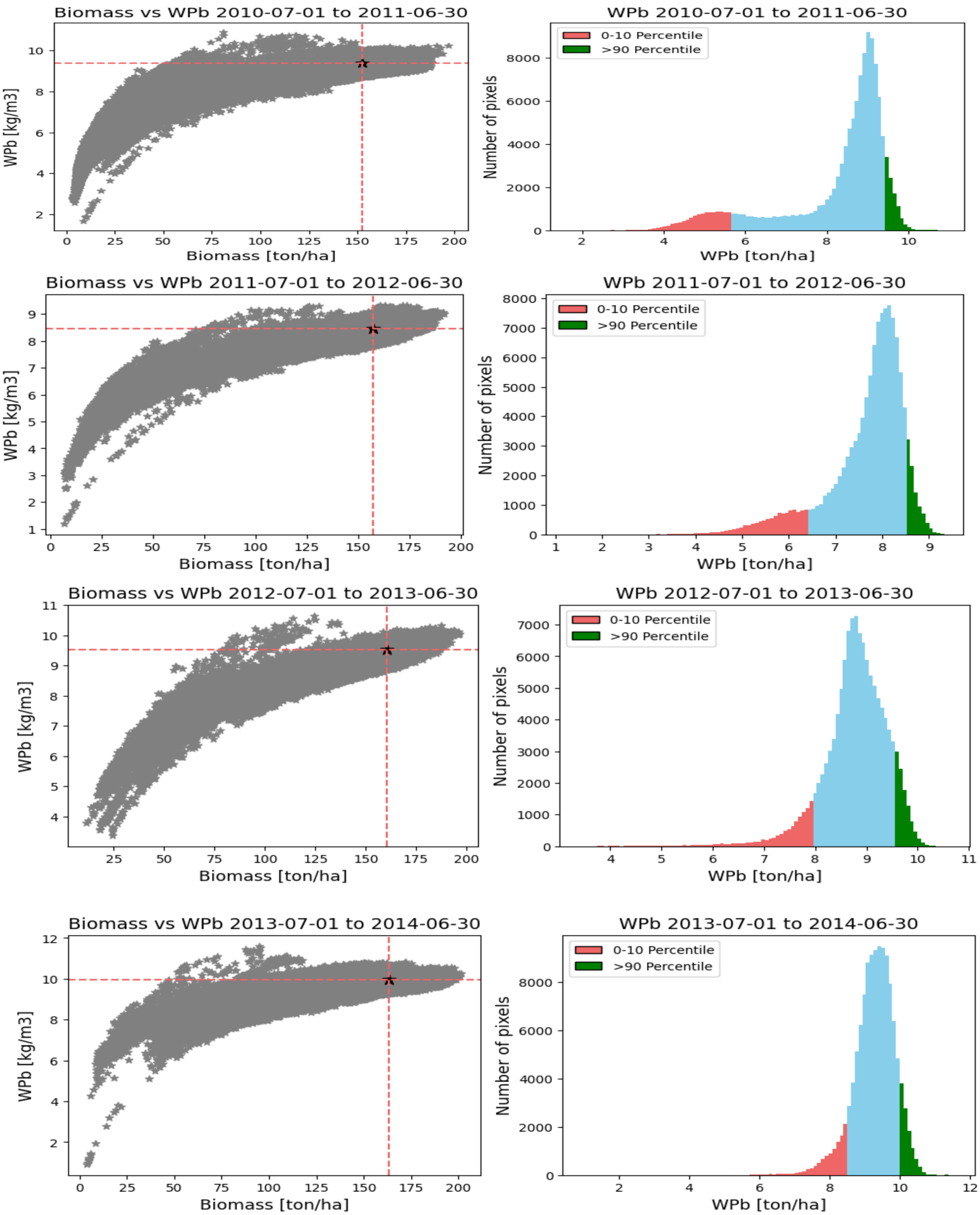

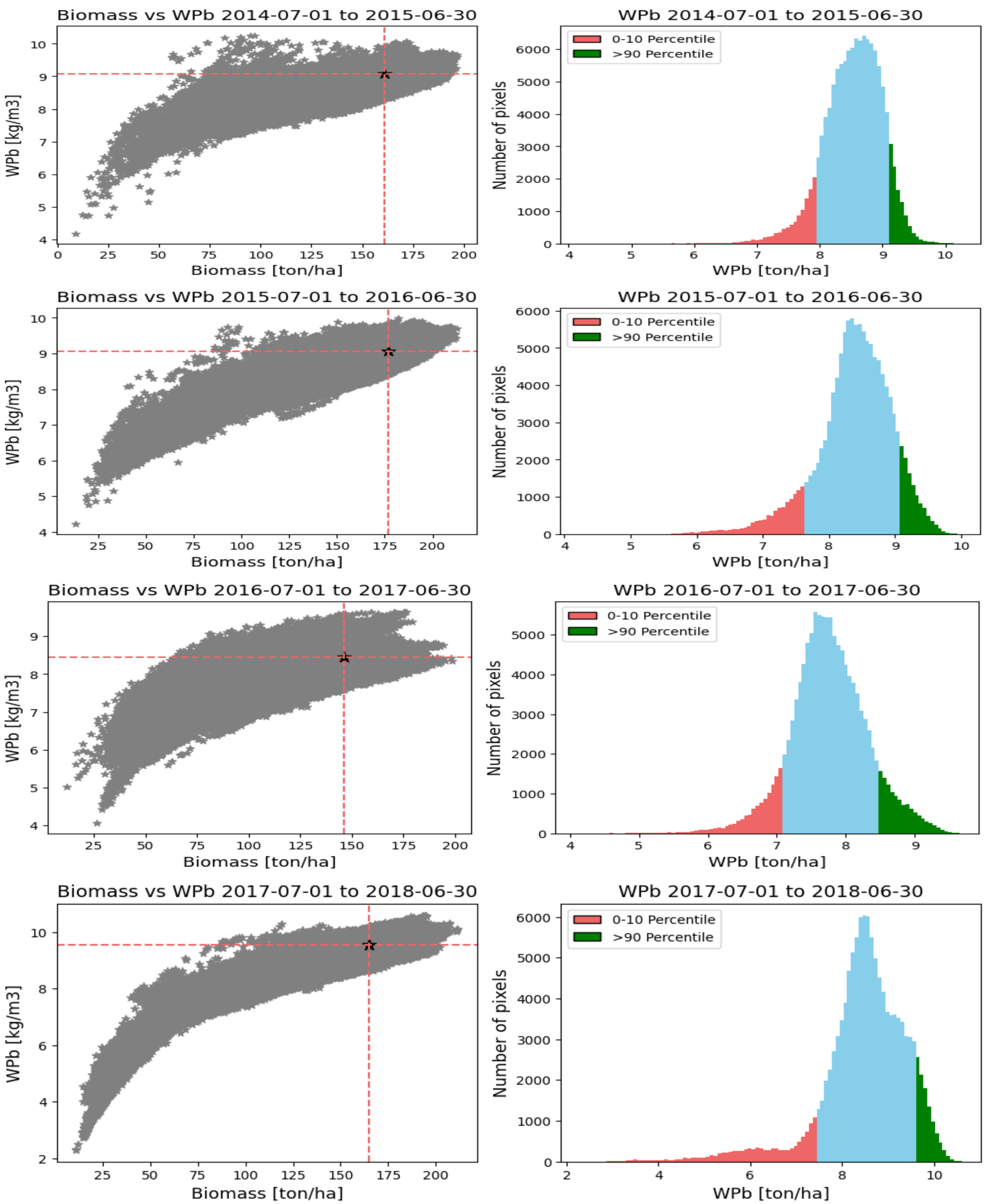
Biomass vs WPb 2014-07-01 to 2015-06-30
WPb [kg/m3]
Biomass [ton/ha]
WPb 2014-07-01 to 2015-06-30
0-10 Percentile
>90 Percentile
Number of pixels
WPb [ton/ha]
Biomass vs WPb 2015-07-01 to 2016-06-30
WPb [kg/m3]
Biomass [ton/ha]
WPb 2015-07-01 to 2016-06-30
0-10 Percentile
>90 Percentile
Number of pixels
WPb [ton/ha]
Biomass vs WPb 2016-07-01 to 2017-06-30
WPb [kg/m3]
Biomass [ton/ha]
WPb 2016-07-01 to 2017-06-30
0-10 Percentile
>90 Percentile
Number of pixels
WPb [ton/ha]
Biomass vs WPb 2017-07-01 to 2018-06-30
WPb [kg/m3]
Biomass [ton/ha]
WPb 2017-07-01 to 2018-06-30
0-10 Percentile
>90 Percentile
Number of pixels
WPb [ton/ha]

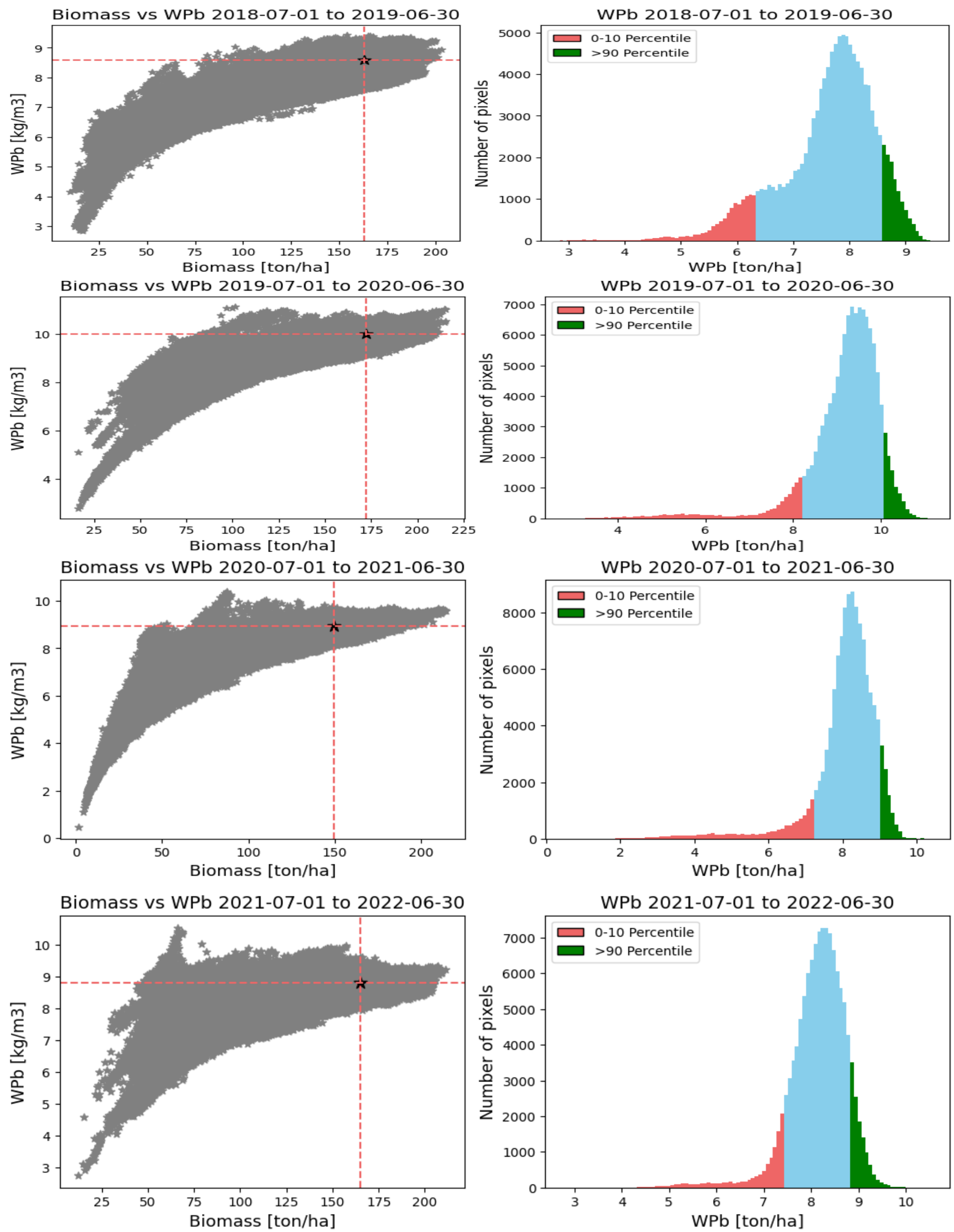
Biomass vs WPb 2018-07-01 to 2019-06-30
WPb [kg/m3]
Biomass [ton/ha]
WPb 2018-07-01 to 2019-06-30
0-10 Percentile
>90 Percentile
Number of pixels
WPb [ton/ha]
Biomass vs WPb 2019-07-01 to 2020-06-30
WPb [kg/m3]
Biomass [ton/ha]
WPb 2019-07-01 to 2020-06-30
0-10 Percentile
>90 Percentile
Number of pixels
WPb [ton/ha]
Biomass vs WPb 2020-07-01 to 2021-06-30
WPb [kg/m3]
Biomass [ton/ha]
WPb 2020-07-01 to 2021-06-30
0-10 Percentile
>90 Percentile
Number of pixels
WPb [ton/ha]
Biomass vs WPb 2021-07-01 to 2022-06-30
WPb [kg/m3]
Biomass [ton/ha]
WPb 2021-07-01 to 2022-06-30
0-10 Percentile
>90 Percentile
Number of pixels
WPb [ton/ha]

Appendix A. 9 Targets spots (areas where yield and WP greater than or equal to the 90 percentile) at Wonji Shoa from 2009/2022.

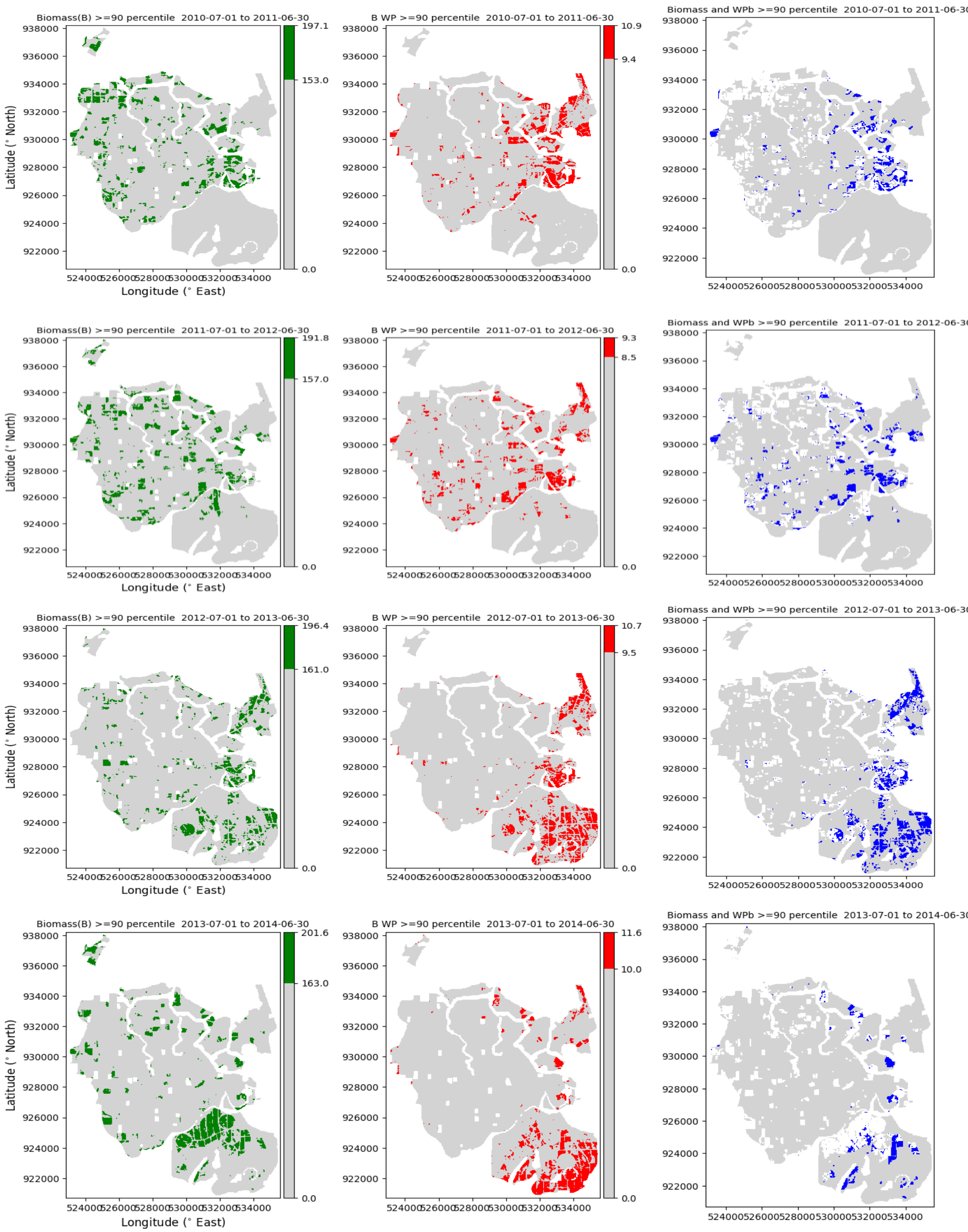

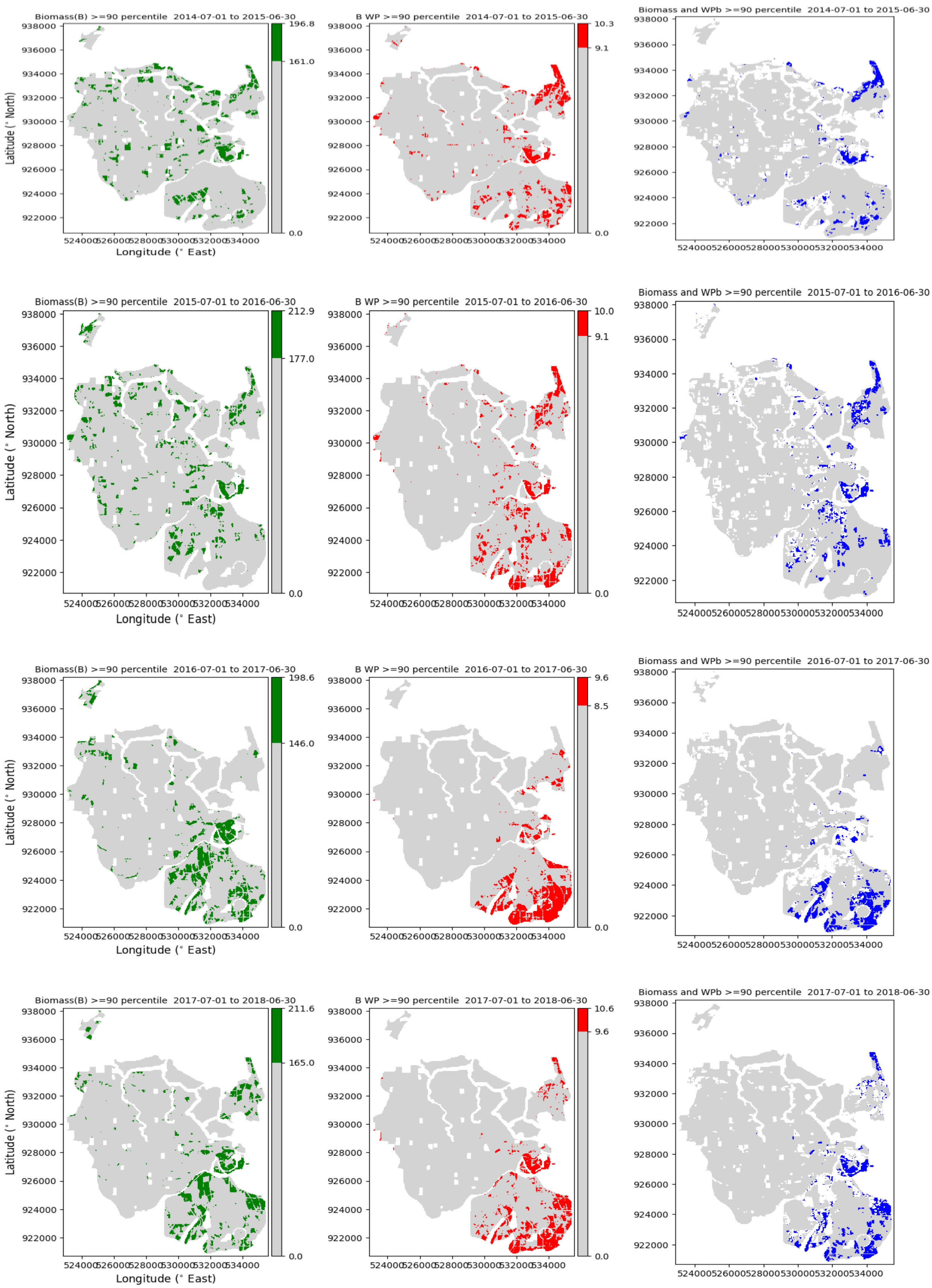
Biomass(B) >=90 percentile 2014-07-01 to 2015-06-30
196.8
161.0
0.0
B WP >=90 percentile 2014-07-01 to 2015-06-30
10.3
9.1
0.0
Biomass and WPb >=90 percentile 2014-07-01 to 2015-06-30
Biomass(B) >=90 percentile 2015-07-01 to 2016-06-30
212.9
177.0
0.0
B WP >=90 percentile 2015-07-01 to 2016-06-30
10.0
9.1
0.0
Biomass and WPb >=90 percentile 2015-07-01 to 2016-06-30
Biomass(B) >=90 percentile 2016-07-01 to 2017-06-30
198.6
146.0
0.0
B WP >=90 percentile 2016-07-01 to 2017-06-30
9.6
8.5
0.0
Biomass and WPb >=90 percentile 2016-07-01 to 2017-06-30
Biomass(B) >=90 percentile 2017-07-01 to 2018-06-30
211.6
165.0
0.0
B WP >=90 percentile 2017-07-01 to 2018-06-30
10.6
9.6
0.0
Biomass and WPb >=90 percentile 2017-07-01 to 2018-06-30
Latitude (° North)
Longitude (° East)
938000
936000
934000
932000
930000
928000
926000
924000
922000
524000
526000
528000
530000
532000
534000

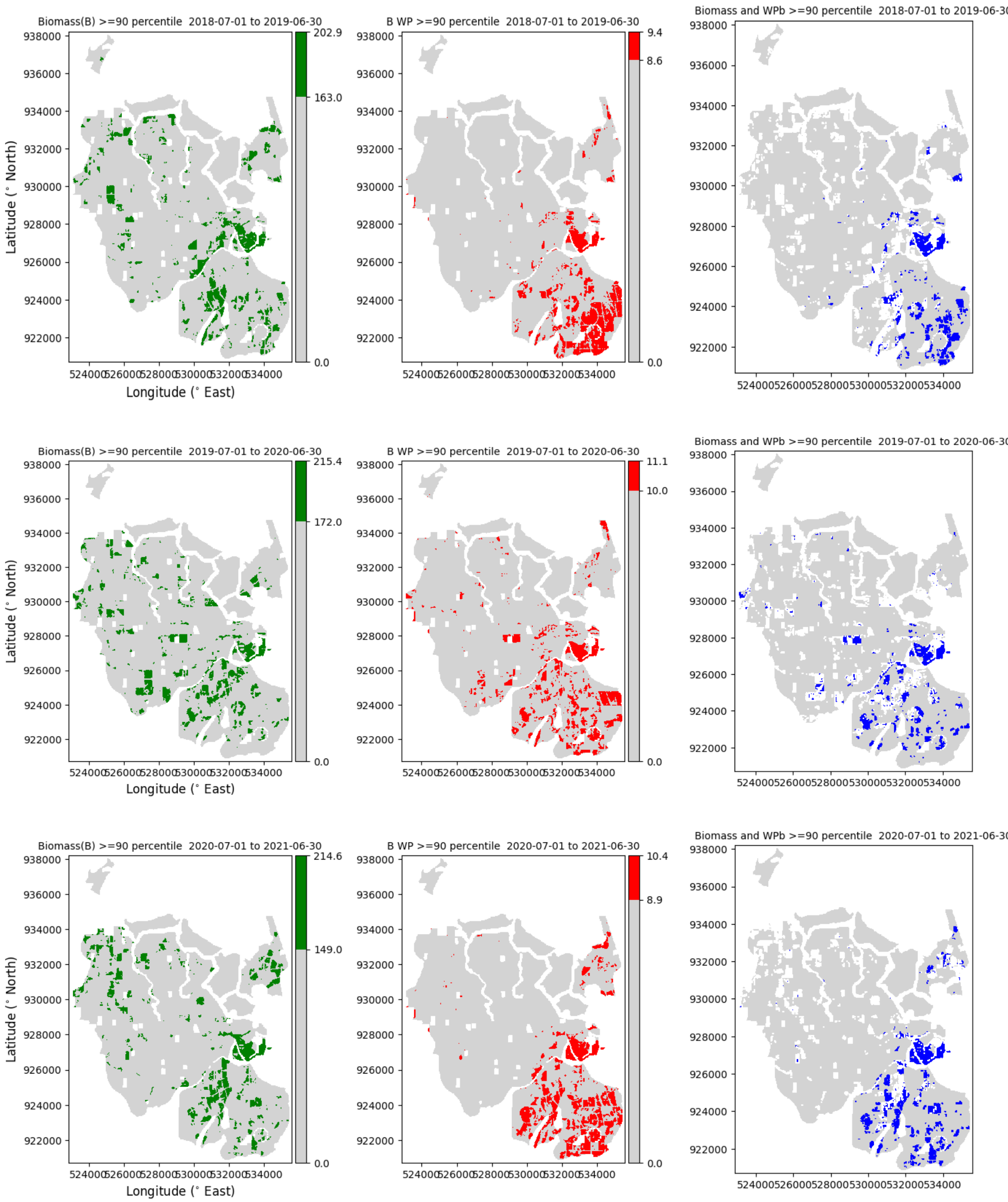
Biomass(B) >=90 percentile 2018-07-01 to 2019-06-30
202.9
163.0
0.0
B WP >=90 percentile 2018-07-01 to 2019-06-30
9.4
8.6
0.0
Biomass and WPb >=90 percentile 2018-07-01 to 2019-06-30
Biomass(B) >=90 percentile 2019-07-01 to 2020-06-30
215.4
172.0
0.0
B WP >=90 percentile 2019-07-01 to 2020-06-30
11.1
10.0
0.0
Biomass and WPb >=90 percentile 2019-07-01 to 2020-06-30
Biomass(B) >=90 percentile 2020-07-01 to 2021-06-30
214.6
149.0
0.0
B WP >=90 percentile 2020-07-01 to 2021-06-30
10.4
8.9
0.0
Biomass and WPb >=90 percentile 2020-07-01 to 2021-06-30
Latitude (° North)
Longitude (° East)
938000
936000
934000
932000
930000
928000
926000
924000
922000
524000
526000
528000
530000
532000
534000

Appendix A. 10 Spatial distribution of biomass gaps of sugarcane at Wonji Shoa from 2009 /2022

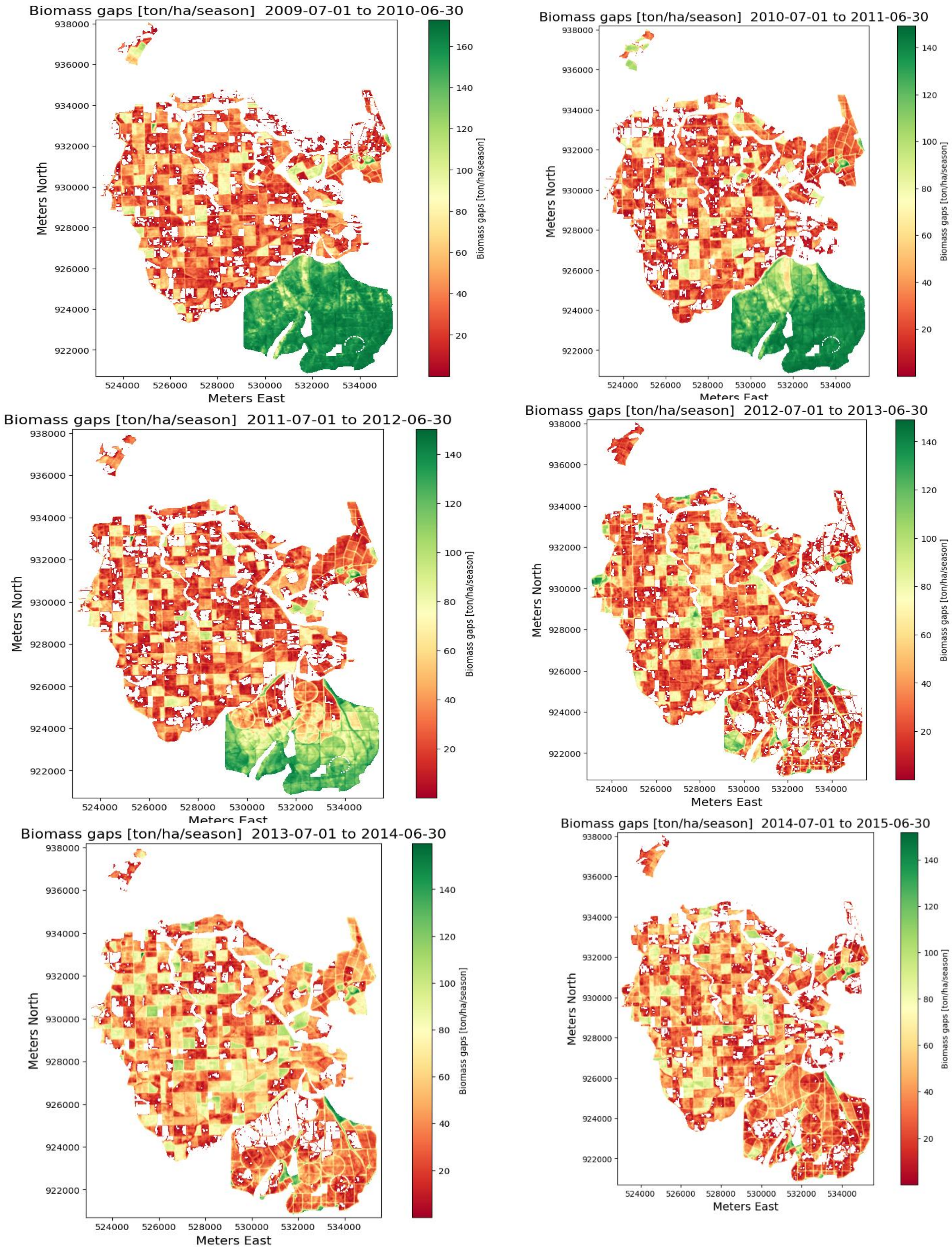

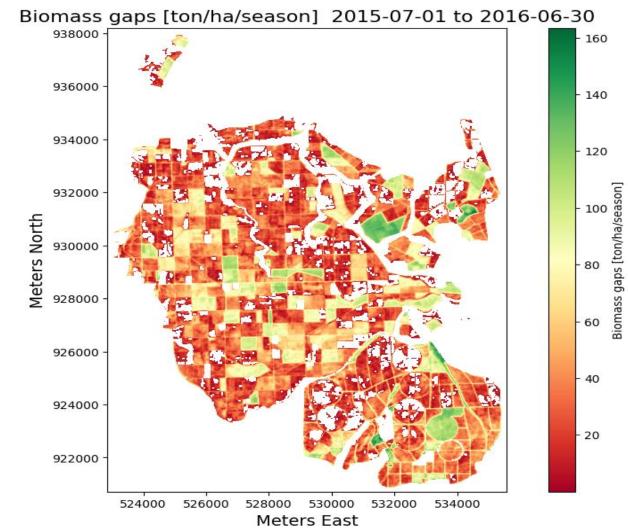
Biomass gaps [ton/ha/season] 2015-07-01 to 2016-06-30
Meters North
Meters East
Biomass gaps [ton/ha/season]

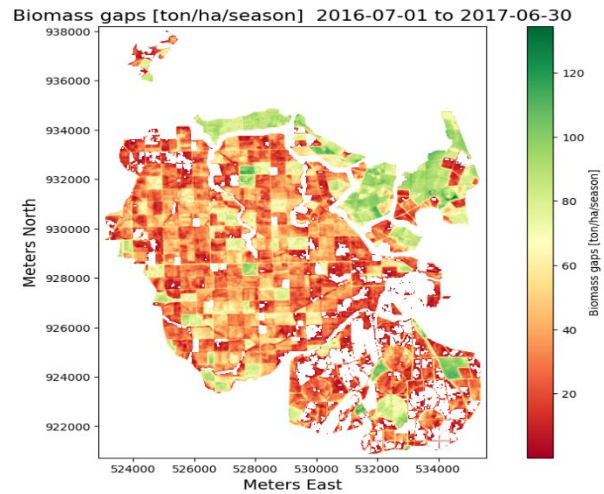
Biomass gaps [ton/ha/season] 2016-07-01 to 2017-06-30
Meters North
Meters East
Biomass gaps [ton/ha/season]

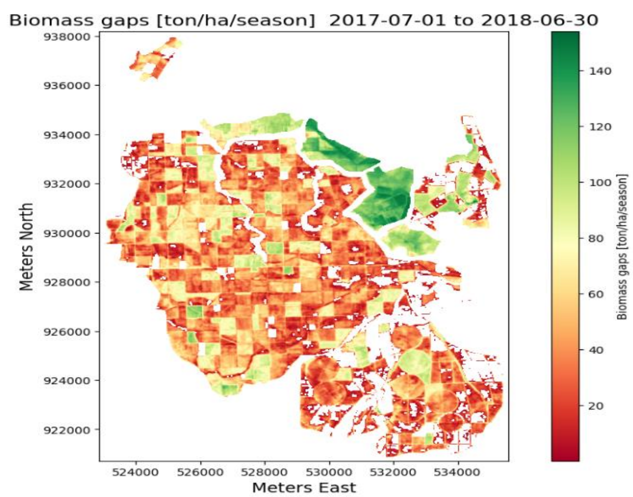
Biomass gaps [ton/ha/season] 2017-07-01 to 2018-06-30
Meters North
Meters East
Biomass gaps [ton/ha/season]

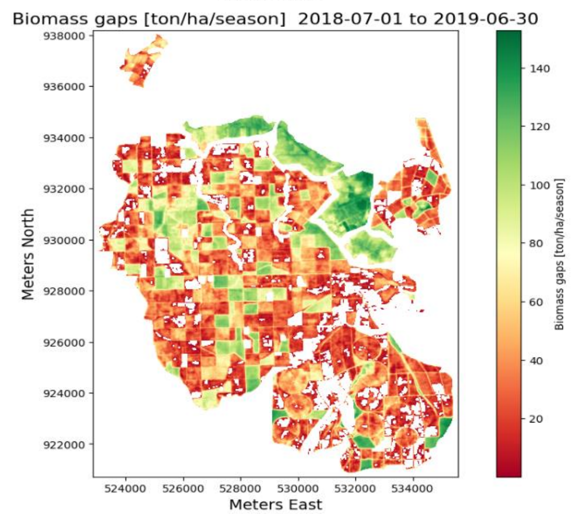
Biomass gaps [ton/ha/season] 2018-07-01 to 2019-06-30
Meters North
Meters East
Biomass gaps [ton/ha/season]

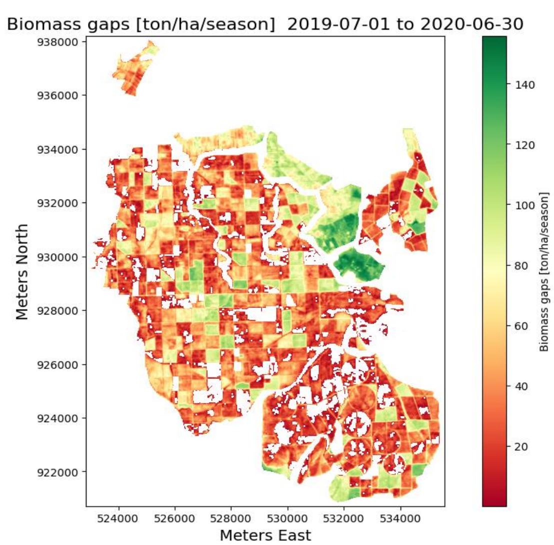
Biomass gaps [ton/ha/season] 2019-07-01 to 2020-06-30
Meters North
Meters East
Biomass gaps [ton/ha/season]

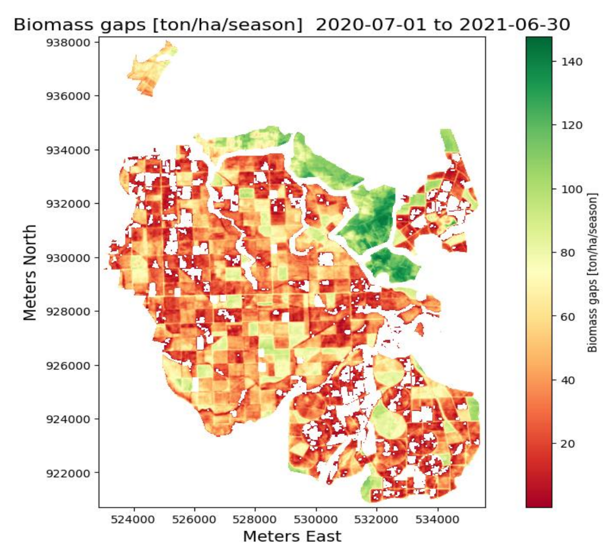
Biomass gaps [ton/ha/season] 2020-07-01 to 2021-06-30
Meters North
Meters East
Biomass gaps [ton/ha/season]

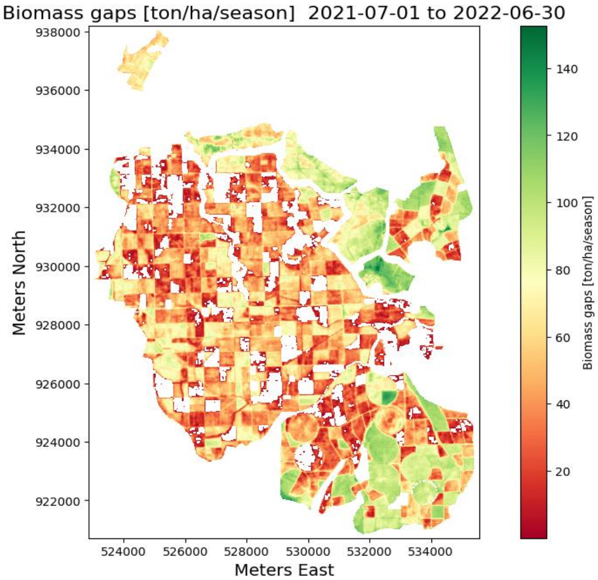

Appendix A. 11 Spatial distribution of biomass water productivity gaps of sugarcane at Wonji Shoa from 2009 to 2022.

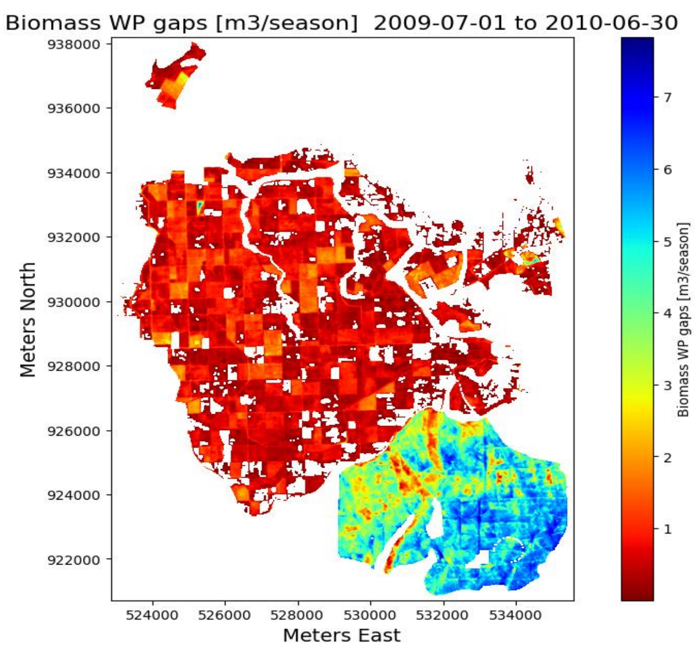

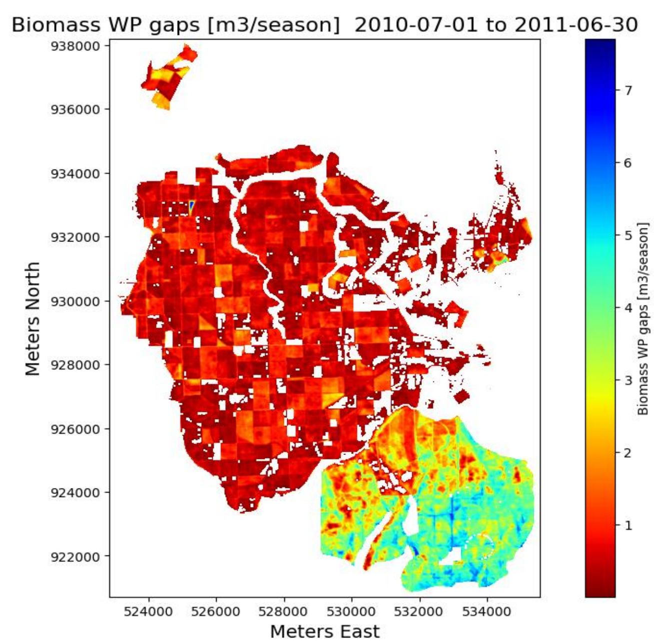

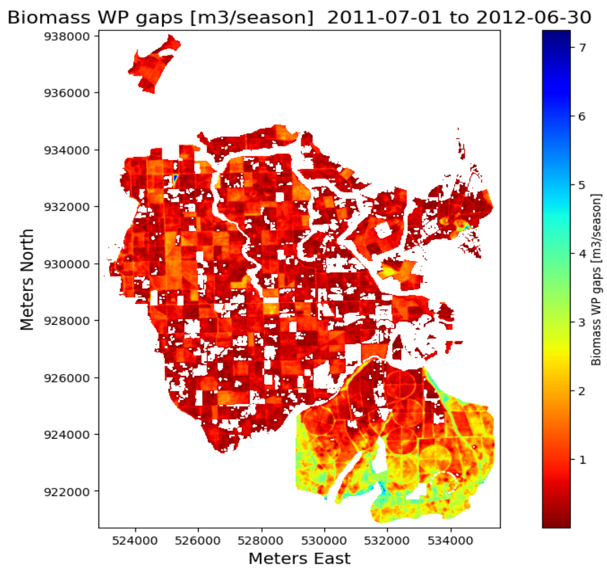
Biomass WP gaps [m3/season] 2011-07-01 to 2012-06-30
Meters North
Meters East
Biomass WP gaps [m3/season]
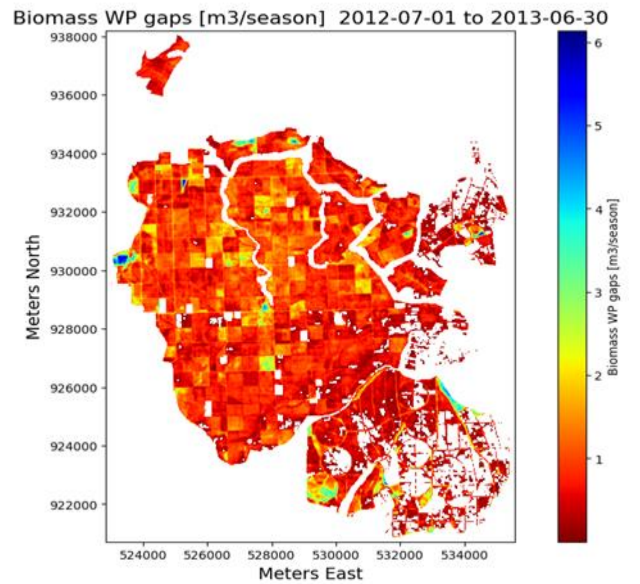
Biomass WP gaps [m3/season] 2012-07-01 to 2013-06-30
Meters North
Meters East
Biomass WP gaps [m3/season]
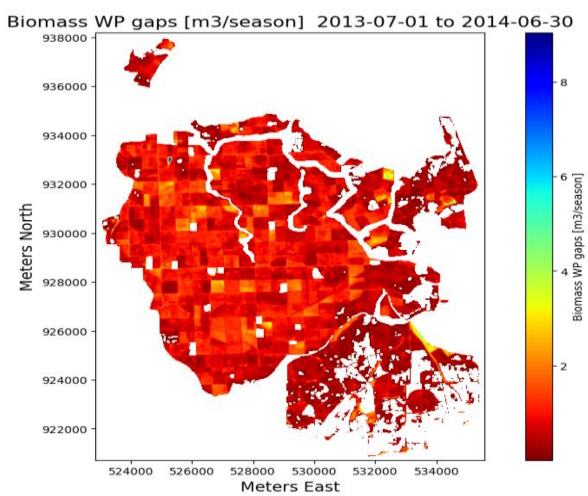
Biomass WP gaps [m3/season] 2013-07-01 to 2014-06-30
Meters North
Meters East
Biomass WP gaps [m3/season]
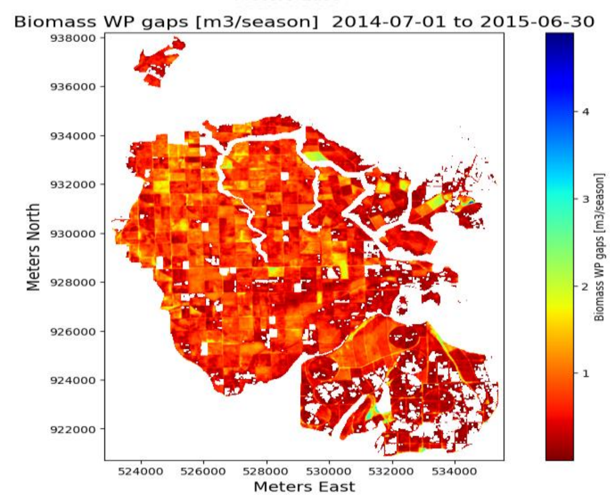
Biomass WP gaps [m3/season] 2014-07-01 to 2015-06-30
Meters North
Meters East
Biomass WP gaps [m3/season]
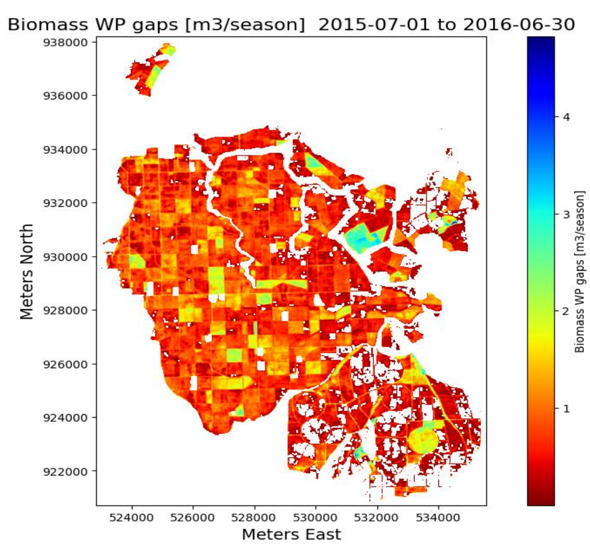
Biomass WP gaps [m3/season] 2015-07-01 to 2016-06-30
Meters North
Meters East
Biomass WP gaps [m3/season]
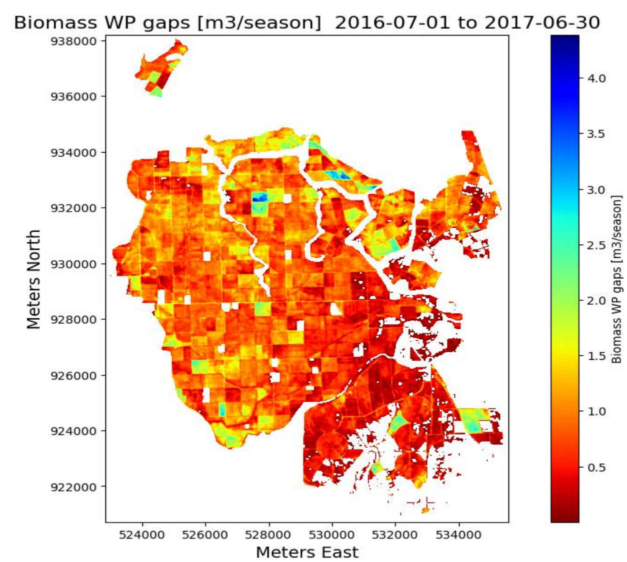
Biomass WP gaps [m3/season] 2016-07-01 to 2017-06-30
Meters North
Meters East
Biomass WP gaps [m3/season]

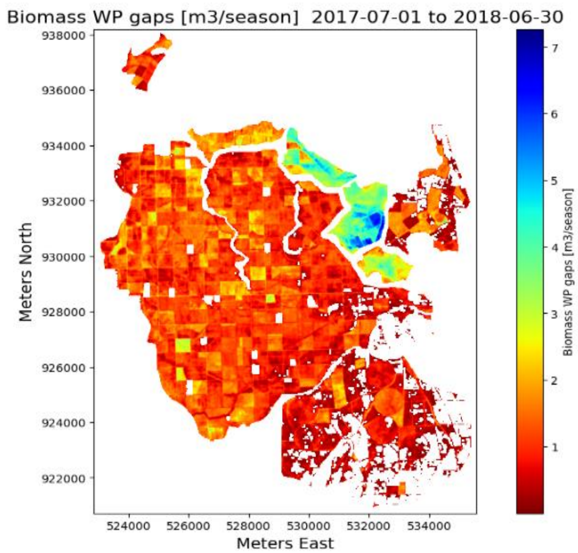
Biomass WP gaps [m3/season] 2017-07-01 to 2018-06-30
Meters North
Meters East
Biomass WP gaps [m3/season]

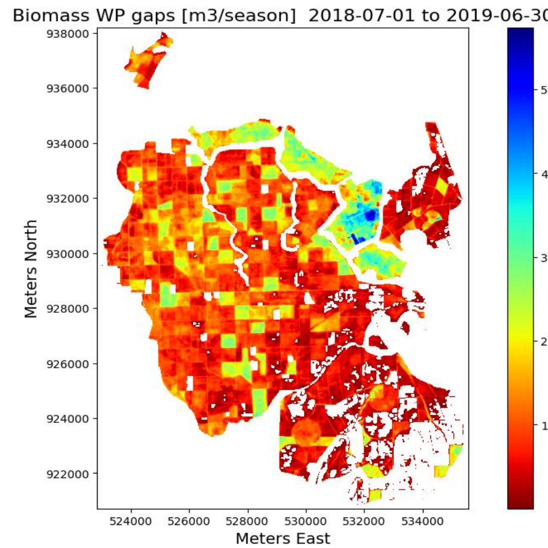
Biomass WP gaps [m3/season] 2018-07-01 to 2019-06-30
Meters North
Meters East
Biomass WP gaps [m3/season]

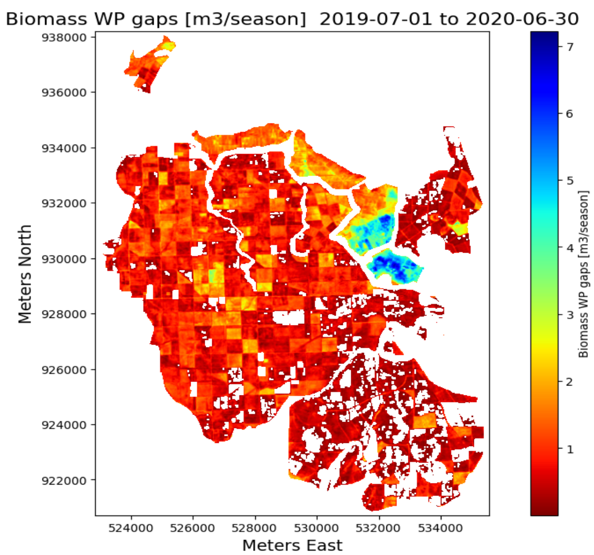
Biomass WP gaps [m3/season] 2019-07-01 to 2020-06-30
Meters North
Meters East
Biomass WP gaps [m3/season]

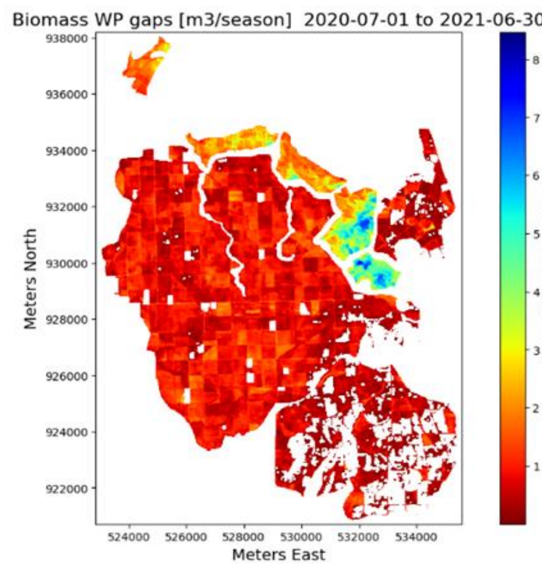
Biomass WP gaps [m3/season] 2020-07-01 to 2021-06-30
Meters North
Meters East
Biomass WP gaps [m3/season]

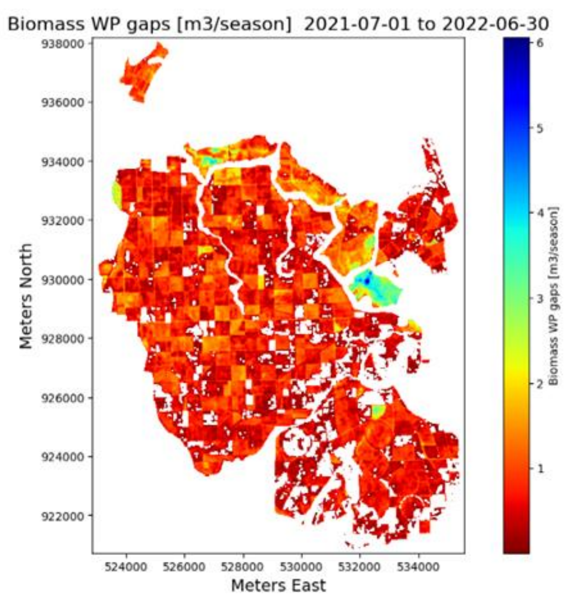
Biomass WP gaps [m3/season] 2021-07-01 to 2022-06-30
Meters North
Meters East
Biomass WP gaps [m3/season]

Appendix A. 12 Average yield, Crop Yield water productivity (WPb), and Yield gap for different zones during the period of 7/1/2009 to 6/30/2022.

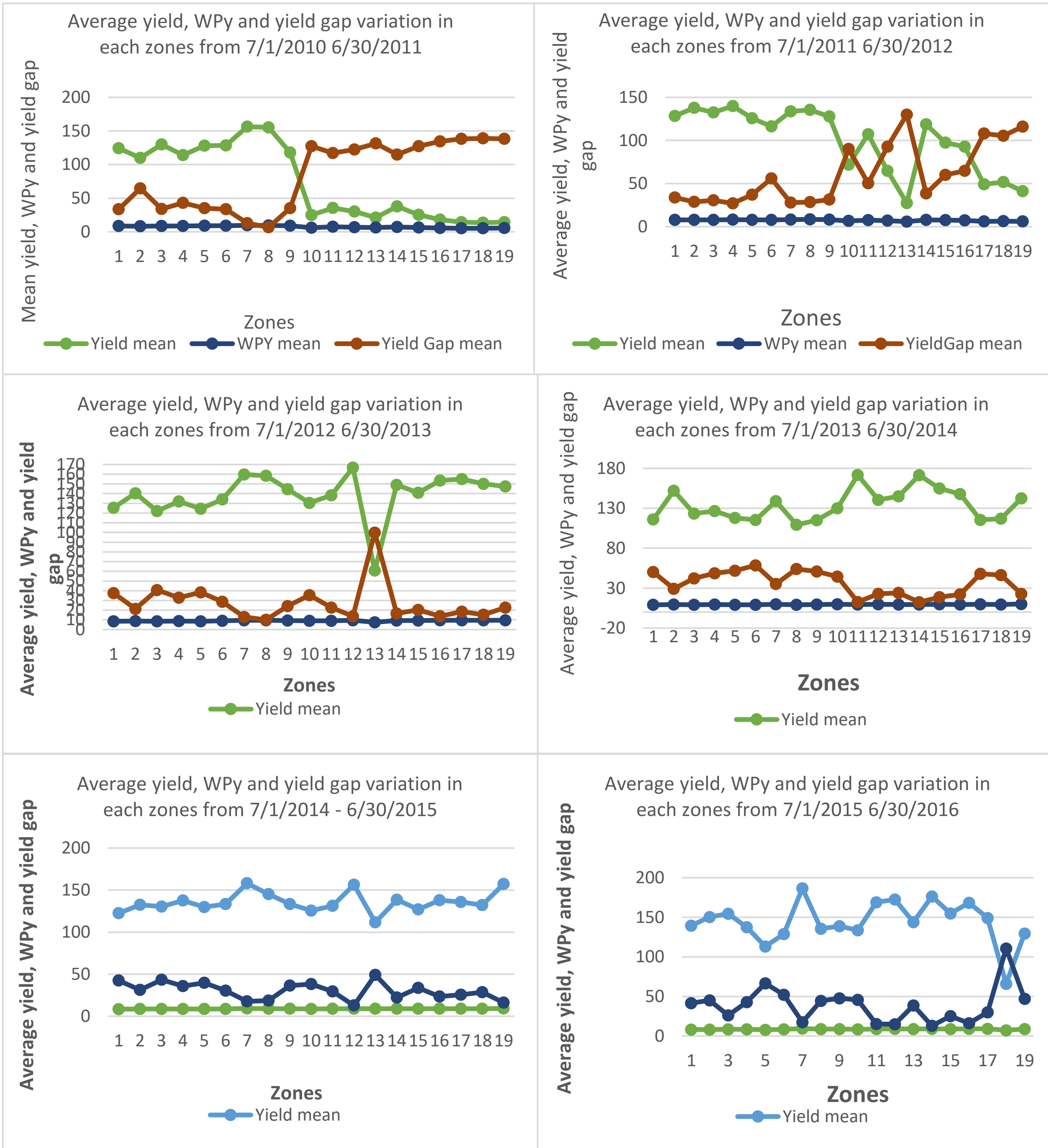

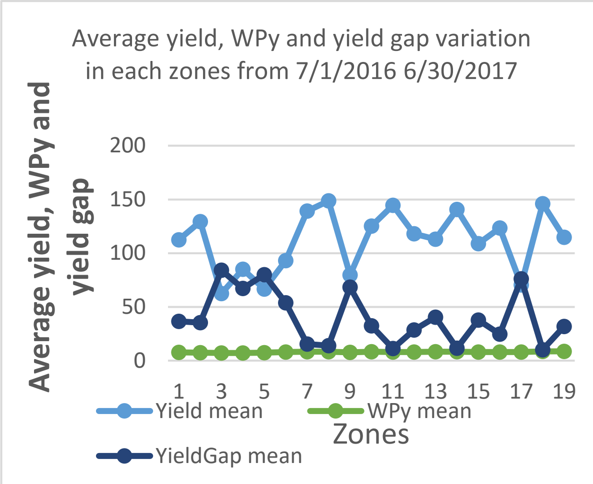
Average yield, WPy and yield gap variation in each zones from 7/1/2016 6/30/2017
Average yield, WPy and yield gap
200
150
100
50
0
1 3 5 7 9 11 13 15 17 19
Zones
Yield mean
WPy mean
YieldGap mean

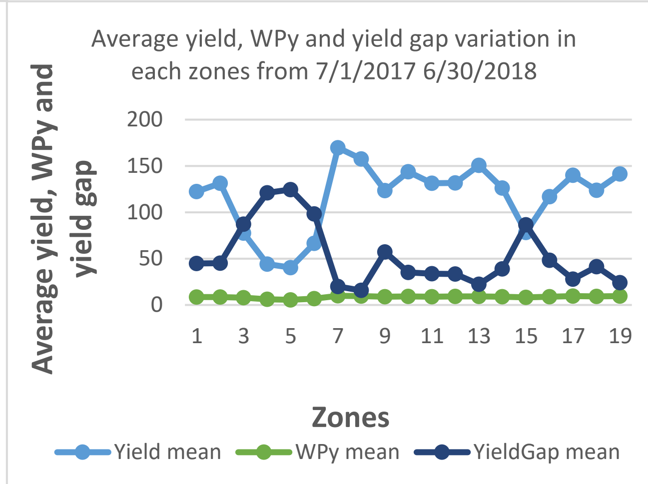
Average yield, WPy and yield gap variation in each zones from 7/1/2017 6/30/2018
Average yield, WPy and yield gap
200
150
100
50
0
1 3 5 7 9 11 13 15 17 19
Zones
Yield mean
WPy mean
YieldGap mean

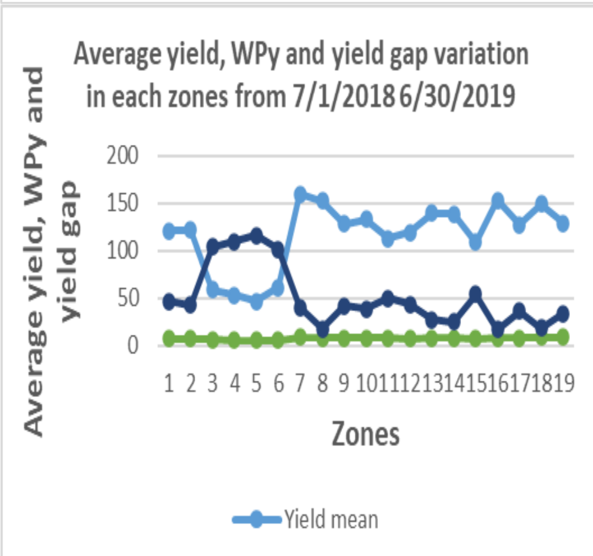
Average yield, WPy and yield gap variation in each zones from 7/1/2018 6/30/2019
Average yield, WPy and yield gap
200
150
100
50
0
1 2 3 4 5 6 7 8 9 10111213141516171819
Zones
Yield mean

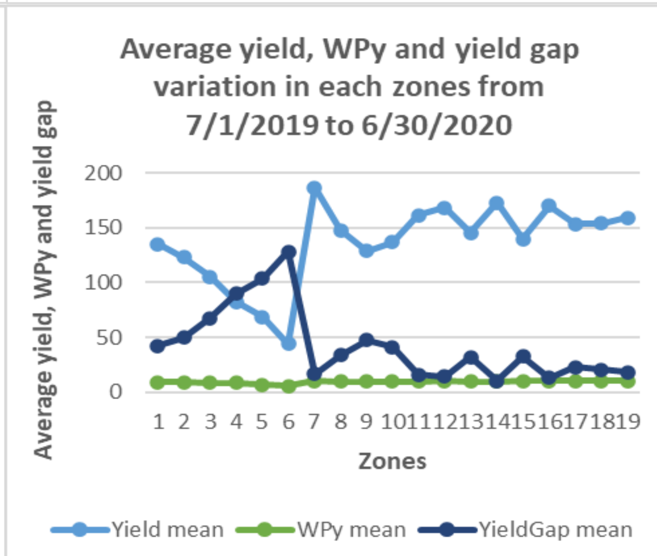
Average yield, WPy and yield gap variation in each zones from 7/1/2019 to 6/30/2020
Average yield, WPy and yield gap
200
150
100
50
0
1 2 3 4 5 6 7 8 9 10111213141516171819
Zones
Yield mean
WPy mean
YieldGap mean

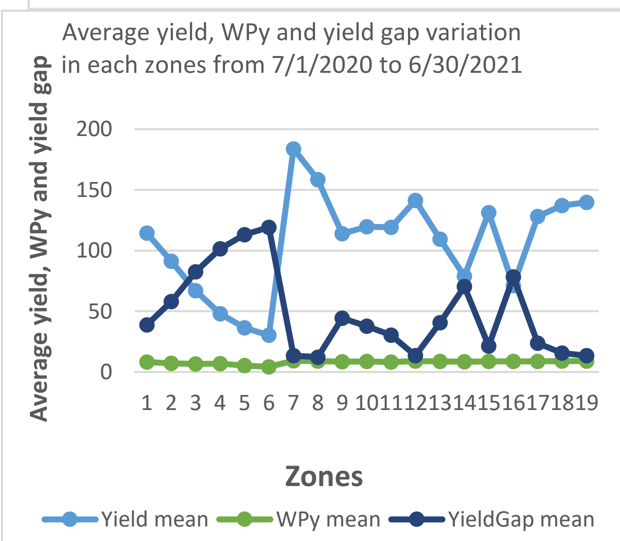
Average yield, WPy and yield gap variation in each zones from 7/1/2020 to 6/30/2021
Average yield, WPy and yield gap
200
150
100
50
0
1 2 3 4 5 6 7 8 9 10111213141516171819
Zones
Yield mean
WPy mean
YieldGap mean

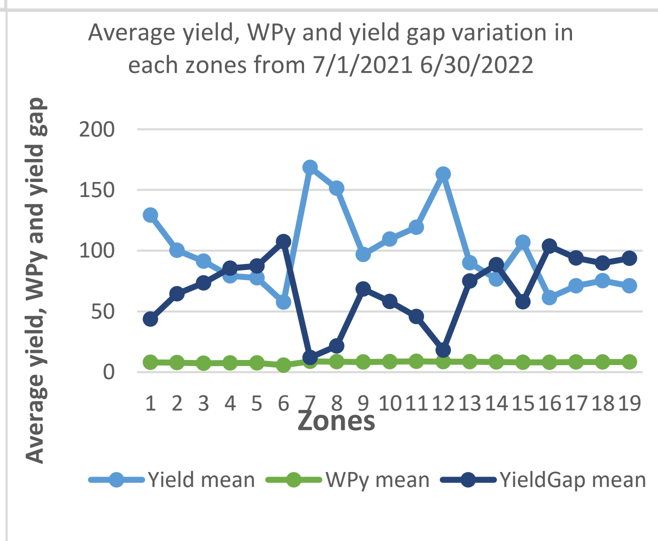
Average yield, WPy and yield gap variation in each zones from 7/1/2021 6/30/2022
Average yield, WPy and yield gap
200
150
100
50
0
1 2 3 4 5 6 7 8 9 10111213141516171819
Zones
Yield mean
WPy mean
YieldGap mean